



**COMPARISON OF A CONCEPTUAL MODEL AND OBJECTIVE INDICATORS
OF EXTRATROPICAL TRANSITION IN THE WESTERN NORTH PACIFIC**

THESIS

Gregory D. Fox, Captain, USAF

AFIT/GM/ENP/04-06

**DEPARTMENT OF THE AIR FORCE
AIR UNIVERSITY**

AIR FORCE INSTITUTE OF TECHNOLOGY

Wright-Patterson Air Force Base, Ohio

APPROVED FOR PUBLIC RELEASE; DISTRIBUTION UNLIMITED

The views expressed in this thesis are those of the author and do not reflect the official policy or position of the United States Air Force, Department of Defense, or the United States Government.

AFIT/GM/ENP/04-06

COMPARISON OF A CONCEPTUAL MODEL AND OBJECTIVE INDICATORS
OF EXTRATROPICAL TRANSITION IN THE WESTERN NORTH PACIFIC

THESIS

Presented to the Faculty

Department of Engineering Physics

Graduate School of Engineering and Management

Air Force Institute of Technology

Air University

Air Education and Training Command

In Partial Fulfillment of the Requirements for the

Degree of Master of Science in Meteorology

Gregory D. Fox, BS

Captain, USAF

March 2004

APPROVED FOR PUBLIC RELEASE; DISTRIBUTION UNLIMITED

COMPARISON OF A CONCEPTUAL MODEL AND OBJECTIVE INDICATORS
OF EXTRATROPICAL TRANSITION IN THE WESTERN NORTH PACIFIC

Gregory D. Fox, BS
Captain, USAF

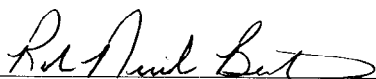
Approved:



Ronald P. Lowther (Chairman)

10 Mar 04

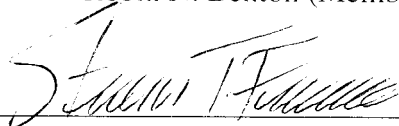
date



Robin N. Benton (Member)

10 Mar 04

date



Steven T. Fiorino (Member)

10 MAR 04

date



Michael K. Walters (Member)

10 MAR 04

date

Abstract

The primary purpose of this research is to provide guidance to forecasters from the Joint (Air Force/Navy) Typhoon Warning Center (JTWC) in Pearl Harbor to use in differentiating between the stages of extratropical transition (ET) of tropical cyclones (TCs). Not only is ET relevant to the Department of Defense, since JTWC stops providing TC warnings once they have undergone ET, but it is also applicable to the meteorological community since there currently “is no commonly accepted definition of ET” (Jones et al. 2003). This research compares the results of a conceptual model of ET using subjective satellite analysis with the results of objective indicators based on Navy Operational Global Atmospheric Prediction System (NOGAPS) model analyses. The ultimate goal is to find a way to reduce the negative impact of incorrect TC forecasting by providing tools which are more objective in defining stages of ET.

This work discusses the birth, growth, and death of TCs by describing what energy sources are necessary for their growth and dissipation. Recent studies provide a conceptual model of ET with definitions of two stages and ways to use satellite analysis to identify them (Klein et al. 2000). While this conceptual model was being analyzed with data from the western North Pacific Ocean, TCs were also being analyzed using data from the Atlantic Ocean (Hart and Evans 2001). The research from the Atlantic led to the exploitation of objective indicators in a hodograph-like display (Evans and Hart 2003).

This thesis statistically compares the results of the conceptual model on 12 TCs in the western North Pacific with the results of the objective indicators on the same 12 TCs. Additionally, three specific case study comparisons are performed: 1) a “classic” TC that had undergone ET (Typhoon David in September 1997), 2) a TC whose output from the two methods matched each other almost perfectly (Super Typhoon Joan in October 1997), and 3) a TC whose stages of ET were difficult to forecast using the conceptual model alone (Typhoon Halong in July 2002). The overall findings demonstrate that the objective indicators are easier to utilize, more definitive, and less subjective than the results achieved through the use of the conceptual model method. This study strongly encourages the use of objective indicators by JTWC forecasters (and others) in defining the beginning and end of ET. Additionally, this thesis provides recommendations for improvements in ET forecasting and a definition of ET for adoption by the American Meteorological Society and the World Meteorological Organization.

Acknowledgments

I would like to start by acknowledging my sponsor, the Joint Typhoon Warning Center, for their submission of such an interesting topic: extratropical transition. More importantly, however, I would like to express sincere appreciation to my advisor, Lt Col Ronald P. Lowther, for his guidance and support throughout the course of this thesis endeavor; his insight and experience were more than appreciated.

Special thanks goes to Dr. Pat A. Harr from the Naval Post-Graduate school for keeping me on track and providing excellent ideas for operational comparisons. Most importantly, however, I need (and want) to profoundly thank Dr. Robert E. Hart, currently at Florida State University, who not only provided me with output from his objective indicator program, which was essential to my research, but also took the time and energy to walk me through the process and provided in-depth answers to the numerous questions I asked of him.

Finally, I would not even be a graduate student at the Air Force Institute of Technology (possibly not even a member of the United States Air Force for that matter) if it were not for the everlasting love and support of my wife and children. They have been there during some of the roughest times and will now be there for some of the greatest times.

Gregory D. Fox

Table of Contents

| | Page |
|--|--------|
| Abstract | iv |
| Acknowledgments | vi |
| List of Figures | ix |
| List of Tables | xii |
| 1. Introduction | 1 |
| a) Background..... | 1 |
| b) Relevancy | 4 |
| c) Problem Statement..... | 5 |
| d) Research Objectives | 6 |
| d) Research Preview | 8 |
| 2. Literature Review | 11 |
| a) Tropical Cyclones..... | 11 |
| 1) Suitable Environmental Conditions..... | 12 |
| 2) Additional Criteria..... | 13 |
| b) Extratropical Transition..... | 14 |
| 1) The Transformation Stage | 16 |
| 2) Displaced Vortices..... | 17 |
| 3) The Reintensification Stage..... | 20 |
| 4) Operational Forecasting..... | 20 |
| 5) Midlatitude Circulation Contributions | 23 |
| 6) Objective Indicators..... | 23 |
| 3. Data and Methodology..... | 28 |
| a) Data..... | 28 |
| b) Methodology..... | 31 |
| 1) Cyclone Phase Analysis | 31 |
| 2) Cyclone Thermal Symmetry Parameter | 32 |
| 3) Cyclone Thermal Wind Parameter | 34 |
| 4) Cyclone Phase Diagrams | 35 |
| 5) Statistical Analysis | 41 |
| 4. Results and Analysis | 42 |

| | |
|--|----|
| a) Results..... | 42 |
| b) Statistical Analysis | 47 |
| 1) Sign Test..... | 47 |
| 2) Wilcoxon Signed Rank Test..... | 48 |
| c) Operational Comparison..... | 51 |
| 1) Typhoon David..... | 51 |
| 2) Super Typhoon Joan..... | 59 |
| 3) Super Typhoon Halong..... | 65 |
| 5. Conclusions and Recommendations | 73 |
| a) Conclusions..... | 73 |
| b) Recommendations | 74 |
| Appendix A. Acronym Page | 76 |
| Appendix B. Conceptual Model Analysis of Typhoon Halong..... | 77 |
| Bibliography | 81 |
| Vita..... | 84 |

List of Figures

| Figure | Page |
|---|------|
| 1. Best track of Typhoon David..... | 2 |
| 2. Best track of Hurricane Lili | 2 |
| 3. Tracks of ETTCs from 1970-1999 in a) western North Pacific and in b) North Atlantic | 3 |
| 4. Total number of TCs and ETTCs during 1970-1999 in a) the Atlantic and b) the western North Pacific..... | 4 |
| 5. Locations of tropical cyclone origin | 11 |
| 6. Graphic illustration of CISK..... | 13 |
| 7. Schematic of ET evolution in western North Pacific | 16 |
| 8. IR imagery of Super Typhoon Violet and Typhoon Opal showing steps of transformation stage..... | 17 |
| 9. Conceptual model of ET transformation..... | 18 |
| 10. Comparison of four COAMPS simulations | 19 |
| 11. Comparisons of midlatitude circulation and TC contributions..... | 21 |
| 12. Typical Atlantic 500 hPa flow patterns for ET | 22 |
| 13. Tracks of TCs encountering a) northwest and b) northeast midlatitude circulations..... | 24 |
| 14. Cyclone phase space for Hurricane Floyd with a) AVN and b) NOGAPS analyses..... | 26 |
| 15. Thermal wind cyclone phase space for Hurricane Floyd with NOGAPS analyses..... | 27 |
| 16. NOGAPS surface pressure analysis of Typhoon David | 28 |

| | |
|---|----|
| 17. 900-600 hPa thickness examples of a) a symmetrical (nonfrontal) TC and b) an asymmetrical (frontal) extratropical cyclone | 33 |
| 18. Examples of a) a warm-core TC and b) a cold-core extratropical cyclone | 35 |
| 19. Examples of a) \mathbf{B} vs $-V_T^L$ phase space and b) $-V_T^L$ vs $-V_T^U$ phase space with summary of general locations of conventional TCs | 36 |
| 20. Cyclone phase space for Hurricane Erin with AVN and NOGAPS analyses | 38 |
| 21. Both cyclone phase space diagrams for Hurricane Floyd with NOGAPS analyses | 39 |
| 22. Phase space diagrams of Typhoon Stella..... | 43 |
| 23. Phase space diagrams of Typhoon Ginger..... | 45 |
| 24. Comparison of step 1 of Typhoon David..... | 52 |
| 25. Comparison of step 2 of Typhoon David..... | 54 |
| 26. Comparison of step 3 of Typhoon David..... | 56 |
| 27. Reintensification stage of Typhoon David | 58 |
| 28. Comparison of step 1 of Typhoon Joan | 59 |
| 29. Comparison of step 2 of Typhoon Joan | 62 |
| 30. Comparison of step 3 of Typhoon Joan | 63 |
| 31. High-resolution IR satellite image of Typhoon Halong on 15 July 2002..... | 65 |
| 32. Comparison of step 1 of Typhoon Halong..... | 66 |
| 33. Comparison of step 2 of Typhoon Halong..... | 68 |
| 34. High-resolution IR satellite image of Typhoon Halong on 13 July 2002..... | 69 |
| 35. High-resolution IR satellite image of Typhoon Halong on 16 July 2002..... | 70 |

| | |
|--|----|
| 36. Comparison of step 3 of Typhoon Halong..... | 71 |
| B1. a) SSM/I satellite image of Typhoon Halong at 0000 UTC on 13 July 2002 and b) high-resolution IR satellite imagery at the same time | 77 |
| B2. High-resolution IR satellite image of Typhoon Halong at 1200 UTC on 13 July 2002..... | 77 |
| B3. High-resolution IR satellite image of Typhoon Halong at 0000 UTC on 14 July 2002..... | 78 |
| B4. High-resolution IR satellite image of Typhoon Halong at 1200 UTC on 14 July 2002..... | 78 |
| B5. a) High-resolution IR satellite image of Typhoon Halong at 0000 UTC on 15 July 2002 and b) visible satellite imagery at the same time | 79 |
| B6. High-resolution IR satellite image of Typhoon Halong at 1200 UTC on 15 July 2002..... | 79 |
| B7. High-resolution IR satellite image of Typhoon Halong at 0000 UTC on 16 July 2002..... | 80 |
| B8. High-resolution IR satellite image of Typhoon Halong at 1200 UTC on 16 July 2002..... | 80 |

List of Tables

| Table | Page |
|---|------|
| 1. NOGAPS tendencies..... | 30 |
| 2. Strengths and weaknesses of Hart's OIs..... | 40 |
| 3. Comparison data from Klein's conceptual model and Hart's objective indicators | 46 |
| 4. Sign test statistics | 48 |
| 5. Sign test frequencies | 48 |
| 6. Example of Wilcoxon signed rank test for end time SLP comparisons | 49 |
| 7. Wilcoxon signed rank tests frequencies..... | 50 |
| 8. Wilcoxon signed rank tests results..... | 50 |
| 9. Wilcoxon signed rank tests statistics | 50 |

COMPARISON OF A CONCEPTUAL MODEL AND OBJECTIVE INDICATORS OF EXTRATROPICAL TRANSITION IN THE WESTERN NORTH PACIFIC

1. Introduction

a. Background

Each year, billions of dollars of damage and countless deaths are the destructive results of tropical cyclones (TCs) in the Pacific Ocean basin. Consequently, the Joint Typhoon Warning Center (JTWC), based in Pearl Harbor, requested guidance for military forecasters to use in differentiating between the different phases of extratropical transition (ET) of tropical cyclones. This research was requested by JTWC, through the U.S. Pacific Command, and was ranked as one of the highest priority research needs by the U.S. Air Force Director of Weather, Deputy Chief of Staff for Air and Space Operations, and U.S. Air Force Deputy to the National Oceanic and Atmospheric Administration.

Currently, “there is no commonly accepted definition of ET” in the scientific literature (Jones et al. 2003). However, ET is generally thought to occur when a TC encounters a synoptic disturbance in the mid-latitudes and changes from a warm-core vortex to a cold-core vortex. Fig. 1, from the Global Tropical Cyclone Climatic Atlas (GTCCA), illustrates the best track of Typhoon David in September 1997 (note that the green dots annotate where the storm has transitioned extratropically).

JTWC defines a system as extratropical when it has lost the tropical characteristics of a migratory, barotropic, warm-core vortex (Wakeham 2001). TCs that have undergone ET (ETTCs), like Hurricane Lili in October 1996 (best track portrayed in Fig. 2), may re-intensify and bring strong (even gale force) winds and heavy rain to the

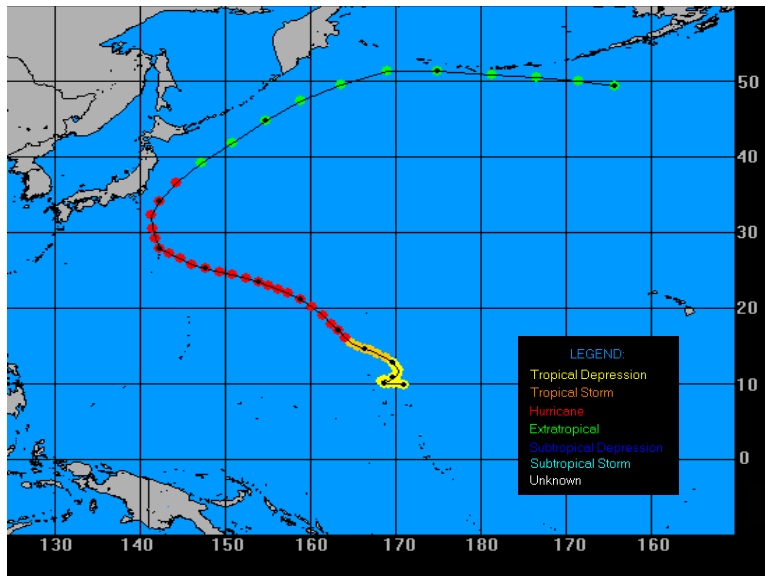


FIG. 1. Best track of Typhoon David (GTCCA 2003).

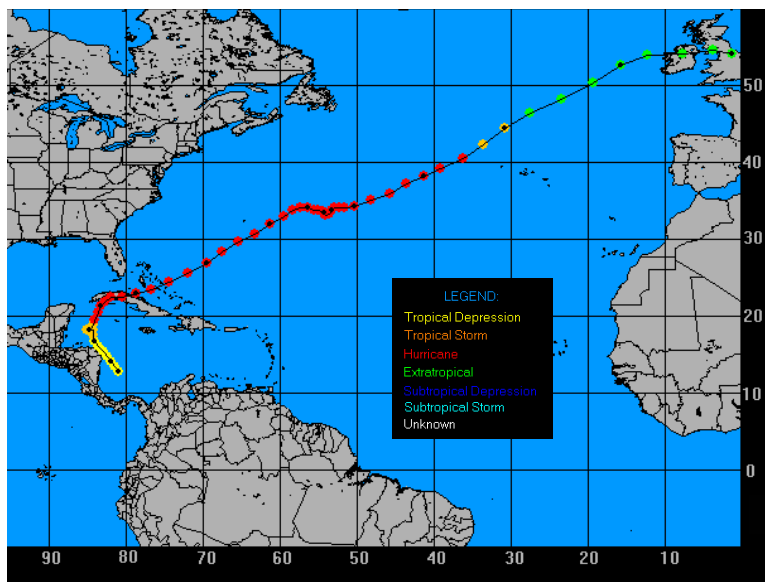


FIG. 2. Best track of Hurricane Lili (GTCCA 2003).

eastern side of ocean basins (Browning et al. 1998). Another reason to better understand ET is that ETTCs often increase in forward translation speed shortly after transition making accurate forecasts difficult (Jones et al. 2003).

Fig. 3 illustrates that a much larger number of ETTCs occurred in the western North Pacific basin (from 1970 to 1999) than in the North Atlantic basin. However, comparing the shaded bars (number of ETTCs) with the open bars (number of TCs) in Fig. 4 reveals that the North Atlantic basin contains only a slightly larger percentage of ETTCs than the western North Pacific basin (Jones et al. 2003).

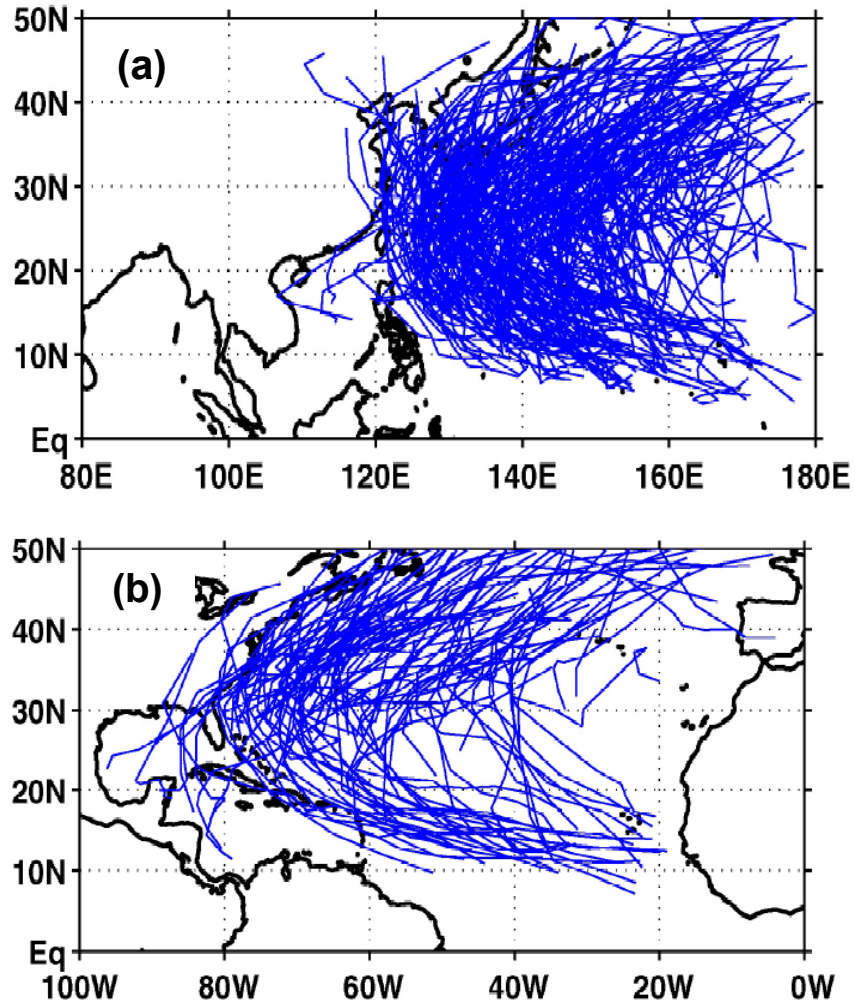


FIG. 3. Tracks of ETTCs from 1970-1999 in a) western North Pacific basin and in b) North Atlantic basin (Jones et al. 2003).

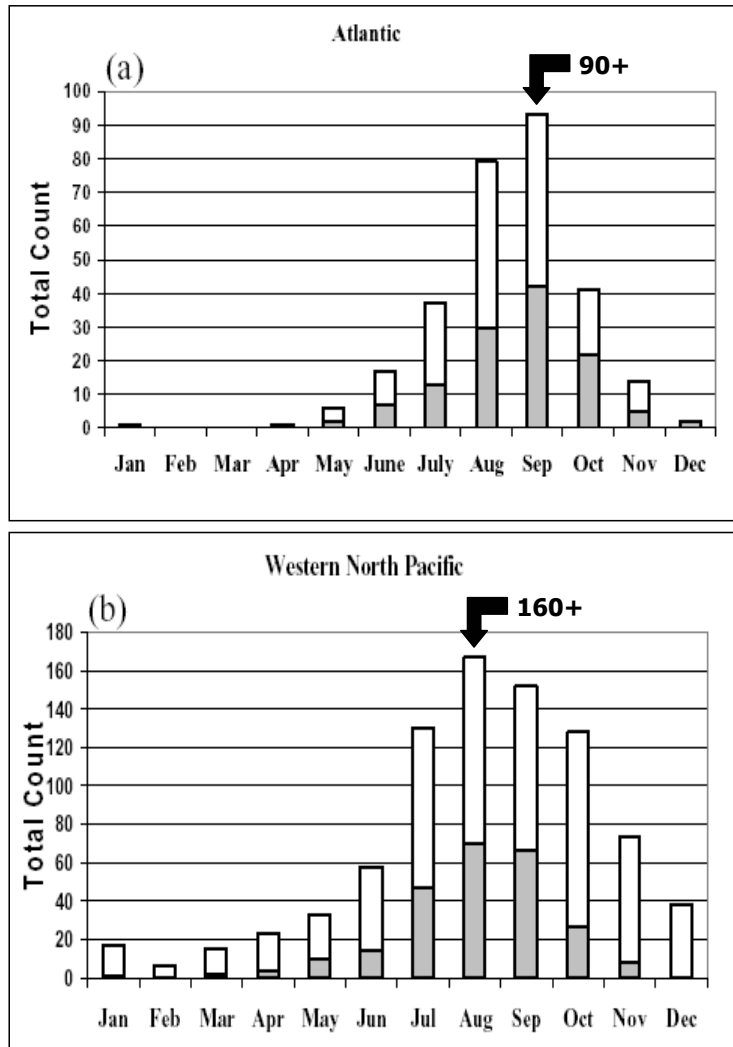


FIG. 4. Total number of TCs (open bars) and ETTCs (shaded bars) during 1970-1999 in a) the Atlantic and b) the western North Pacific (adapted from Jones et al. 2003).

b. Relevancy

The relevancy of this thesis research is twofold; first, from a Department of Defense (DoD) perspective, JTWC is very interested in ETTCs since once ET has occurred, JTWC stops providing TC warnings and then “hands off” the forecast responsibility of TC tracking to the Naval Pacific Meteorological Oceanographic Center (NAVPACMETOCEN) WEST (for Navy operational tracking) and to the 20th

Operational Weather Squadron (OWS) (for Air Force operational tracking). JTWC forecasters have been inconsistent (and even reluctant) to classify TCs as having undergone ET for a variety of reasons (S. Vilpors 2003, personal communication). A major reason for this inconsistency (and even reluctance) is that there has never been a clear definition of ET. In the 1970s, ETTCs were categorized as “complex” when they formed on a front, “compound” when they merged with mid-latitude systems, and “dissipaters” when they dissipated (Wakeham 2001). In the mid 1990s, ETTCs were categorized as “captured” when they were caught in pre-cold frontal poleward flow (analogous to complex) and “cradled” when they transitioned poleward in a pattern featuring easterly flow (Wakeham 2001). A clear and concise definition of ET is needed to help JTWC know when to hand the TC forecasting, tracking, and warning responsibilities over to the other operational forecast centers. During a busy tropical storm season, this “hand off” would allow JTWC to use their valuable resources more wisely, as opposed to needlessly tracking TCs for which they are no longer responsible.

The second realm of relevancy of this research is scientific in nature. As stated previously, “there is no commonly accepted definition of ET” (Jones et al. 2003). In fact, the World Meteorological Organization (WMO) has no published definition of ET and ET isn’t listed in the latest edition of the Glossary of Meteorology published by the American Meteorological Society (Glickman 2000). Therefore, this work aims to establish a clear definition of ET and to recommend its adoption by the American Meteorology Society and the WMO.

c. Problem Statement

More than 25 articles were written about ET in the last five years exemplifying the increased interest of the meteorological community (Jones et al. 2003). The First

International Workshop on the ET of TCs took place in Germany in 1999 and was hosted by the University of Munich with the support of the WMO Commission on Atmospheric Science and the U.S. Office of Naval Research (WMO 1998). Then, in 2002, ET was one of the major topics at the Fifth WMO International Workshop on Tropical Cyclones (ITWC-V) held in Australia (WMO 2002). Most recently, a second International Workshop on ET was held in Nova Scotia in November 2003.

Even though the meteorological community has yet to agree on a common definition of ET, there are two leading “trains of thought” when it comes to defining its stages. Klein et al. (2000) developed a conceptual model of ET where satellite imagery is used to define the transformation and reintensification stages. More recently, Hart (2003a) created objective indicators (OIs) which utilize definitions of the beginning and end of ET using model output. Since aerial reconnaissance of TCs is not utilized in the Pacific theater of operations, JTWC must rely on one of these two methods. This research compares the results of these two theories and describes their strengths and weaknesses, thereby providing guidance for JTWC forecasters to use in differentiating between the stages of ET.

d. Research Objectives

The primary goal of this research compares the results of a conceptual model of ET with the results of Hart’s OIs in the analysis of TCs in the western North Pacific. The specific tasks necessary to achieve this goal are to:

1. Select a suitable baseline for ETTC analysis comparison. The analysis of 30 ETTCs (from 1994 – 1998) by Klein et al. (2000) makes an appropriate baseline comparison; however, the data (described in the next task) has only been archived since 1997 leaving data available for a 12-storm comparison.

2. Collect Navy Operational Global Atmospheric Prediction System (NOGAPS) $1^{\circ} \times 1^{\circ}$ global GRIdded Binary (GRIB) data for 0000 and 1200 UTC times for the entire track of each of the selected storms from the Fleet Numerical Meteorology and Oceanography Detachment (FNMOC) through the Air Force Combat Climatology Center (AFCCC) in Asheville, North Carolina.
3. Execute the OI program written by Hart (2003a) to process the NOGAPS data for each storm. Using the numerical and graphical output, calculate the beginning, end, and duration of ET for each of the storms (as well as the sea level pressures [SLPs] at each of those times).
4. Statistically analyze the output of each of the two ET theories. More precisely, use the sign test and the Wilcoxon signed-rank test to compare the beginning, end, and duration of ET for each of the storms (as well as the SLPs at the beginning and end of ET).
5. Perform a case study of a “classic” ETTC (Hurricane David) as defined by Klein et al. (2000) by comparing an analysis using their conceptual model with an analysis provided by Hart’s (2003a) OI program. Describe the similarities and differences between the two theories in addition to pointing out their strengths and weaknesses.
6. If the conceptual model of a “classic” ETTC, as defined by Klein et al. (2000), doesn’t compare well with the analysis provided by Hart’s (2003a) OI program, analyze a TC that does indeed match. Then, describe the strengths and weaknesses of the two theories for this TC and any others that may be like it.
7. Perform a case study of a TC for whom the stages of ET were difficult to forecast by comparing the analysis of the conceptual model proposed by Klein et al. (2000) with the analysis provided by Hart’s (2003a) OI program. Typhoon Halong “. . . was a small storm that did not seem to go through transformation as

- it maintained a nearly circular cloud pattern the entire time it passed along the eastern coast of Japan (P. A. Harr 2003, personal communication).” Describe the similarities and differences between the two theories in addition to pointing out their strengths and weaknesses for such a TC.
8. Present the results of the research by providing JTWC forecasters with guidance. Recommend how both theories may be used to effectively differentiate between the beginning and end of the ET of TCs in the western North Pacific and present reasons for JTWC to use one theory over the other.

e. Research Preview

Chapter 2 provides a brief background of TCs, the environmental conditions required for their development, and the theories behind how a cluster of thunderstorms can spin up into a cyclone of typhoon strength. Chapter 2 continues by providing definitions employed by Klein et al. (2000) for the transformation and reintensification stages of ET as well as discussing the three steps of the transformation stage evident in satellite imagery. These steps correspond with changes in SLP and provide an average timeline for transformation and reintensification. After studying 30 cases in the western North Pacific (of which 12 were used as the baseline for comparison in the research section of this thesis), Klein et al. (2000) proposed a conceptual model of ET using satellite analyses. In the meantime, Hart and Evans (2001) conducted an in-depth climatological study of 61 cases in the Atlantic. Klein et al. (2002) continued their research and created a simple three-by-three matrix to show the results of different levels of midlatitude circulation and TC remnant contributions. Harr and Elsberry (2000a,b) found that midlatitude circulation not only affects the timing of ET, but also affects the

tracks of TCs. Combining this information with the aforementioned conceptual model provides forecasters with tools to better predict the track and intensity of TCs. Recent research (Evans and Hart 2003) supplied objective tools which are used on 12 of the 30 tropical storms analyzed by Klein et al. (2000).

Chapter 3 describes NOGAPS data, its GRIB output, its tendencies, and how it's used in Hart's (2003a) OI program. The graphical output from the OI program is called a phase space diagram and is explained in detail. Each quadrant of the diagram represents a different type of tropical storm and the movement between these quadrants can be used to define the beginning and end of ET. Examples of the phase space diagrams for "classic" and "not-so-classic" ETTCs are included illustrating strengths and weaknesses of the OI program. The last part of the chapter explains the use of statistical analyses to compare the output of Hart's (2003a) OI program with the output from Klein et al.'s (2000) conceptual model.

Chapter 4 starts out by focusing on the results of Hart's OI program and by describing how the author overcame a few small obstacles in their analysis. Next, two nonparametric statistical tests were selected for comparison and their procedures explained. The results of the two tests were compiled and clarified with a statement of possible equalities declared. The last part of chapter 4 compared the results of the two theories operationally for three specifically selected ETTCs. In other words, the author juxtaposed satellite imagery of the steps of transformation, as defined by the conceptual model of Klein et al. (2000), with Hart's (2003b) phase space diagrams of the same times for each of the three ETTCs.

Chapter 5 presents conclusions derived from the statistical analyses and the operational comparisons. Recommendations for JTWC forecasters and meteorologists around the world are provided, while future research possibilities are discussed and

encouraged. Moreover, a recommended definition of ET is made to the American Meteorology Society for inclusion in the next edition of their Glossary of Meteorology.

2. Literature Review

a. Tropical Cyclones

Burpee (1986) describes a TC as “a nearly circular, warm-core vortex that extends throughout the depth of the troposphere and has a typical horizontal scale of a few hundred kilometers.” Ramage (1995) expands this definition by describing the warm-core direct atmospheric circulation as warm air rising and cold air sinking. One of the energy sources required to initiate TC genesis is supplied by sensible and latent heat from warm ocean surface temperatures found in the tropics. Fig. 5 displays the locations around the world which are, correspondingly, favorable for the birth of TCs.

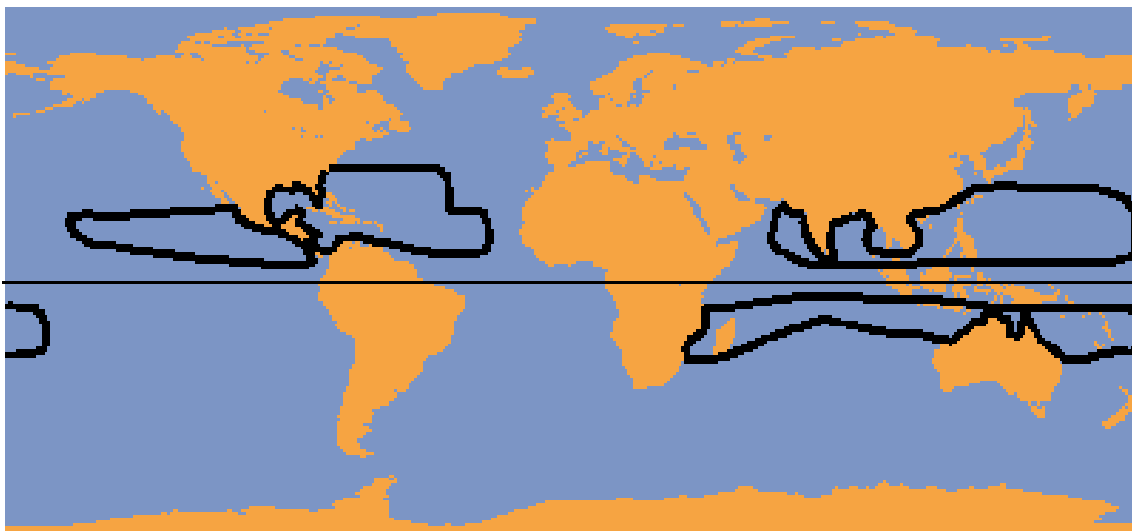


FIG. 5. Locations of tropical cyclone origin (UIUC 2003).

Approximately 80 TCs with maximum sustained winds greater than or equal to 20 m s^{-1} occur annually around the globe (Gray 1979). Rauber et al. (2002) state that the majority of TCs forms in the easterly trade winds and, as a result, starts moving westward.

However, the Coriolis force eventually causes them to move poleward through a right-directed force in the northern hemisphere and a left-directed force in the southern hemisphere.

1) SUITABLE ENVIRONMENTAL CONDITIONS

Before a TC can develop, a cluster of thunderstorms must be present. Rauber et al. (2002) describe three ways to trigger initial development of these thunderstorms through low-level convergence: 1) the Intertropical Convergence Zone (ITCZ), 2) low-pressure troughs and high-pressure ridges to the north and south of lower tropospheric easterly waves found in the trade winds, and 3) remnants of mid-latitude cold fronts that penetrate into tropical latitudes.

Rauber et al. (2002) also discuss four environmental conditions that are required to turn a cluster of thunderstorms into a TC: 1) sea surface temperature greater than or equal to 27°C (81°F), 2) a sufficiently deep layer of warm surface water, usually a minimum of 60 meters (approximately 200 feet), 3) weak vertical wind shear, and 4) the thunderstorm cluster needs to be at least five degrees away from the equator, either north or south. Ramage (1995) adds two extra conditions which must be met before a TC can form which are: 5) a pre-existing disturbance like an active cyclone formation in a summertime surface trough and 6) an upper-tropospheric outflow provided by climatologically divergent upper-tropospheric easterlies overlying the monsoon trough. Ramage further asserts that the Tropical Upper Tropospheric Trough (TUTT) is a major source region of TC genesis, especially when TCs form north of 20° North latitude.

2) ADDITIONAL CRITERIA

TCs aren't guaranteed to form even if all required environmental conditions exist. The authors of the Hurricanes Online Meteorology Guide (UIUC 2003) support the theory of Convective Instability of the Second Kind (CISK). CISK is considered a positive feedback mechanism which means that once the pattern starts, the outcomes enhance the original process and the cycle repeats itself over and over again. Fig. 6 depicts this process, starting with step 1 (surface air flowing into the low pressure area of an immature tropical depression creating convergence which forces air to rise and cool).

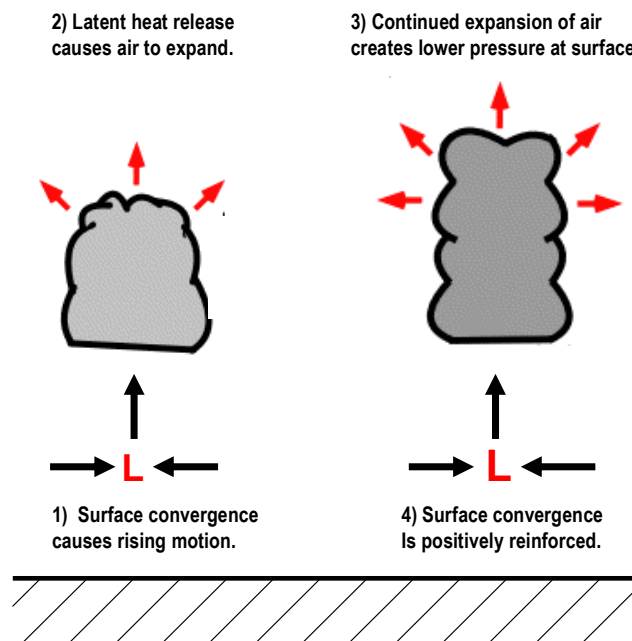


FIG. 6. Graphic illustration of CISK (adapted from UIUC 2003).

Moisture then condenses releasing latent heat into the atmosphere which provides energy to sustain the burgeoning storm. As the rising warm air expands in the cooler atmosphere, the surface pressure decreases which, consequently, increases the pressure

gradient causing more air to spiral into the core starting the whole process over again.

In contrast, Rauber et al. (2002) prefer the theory called Wind Induced Surface Heat Exchange (WISHE) which “occurs between the heat and moisture transfer from the ocean surface and the development of the vortex.” WISHE is also considered a positive feedback mechanism which starts as thunderstorm clusters intensify by extracting sensible heat, latent heat, and moisture from the ocean as winds blow across the surface. Then, as outflow from opposing thunderstorms converges at the tropopause, the resulting descending air warms adiabatically causing divergence in the column and lower pressure at the surface. This low surface pressure increases surface winds thereby escalating the transfer of heat and moisture from the ocean to the atmosphere starting the process all over again as heat and moisture are then transferred to the troposphere by ascending air in the developing eyewall strengthening the storm even more.

b. Extratropical Transition

Klein et al. (2000) state that “ET begins with commencement of the transformation stage and concludes when the reintensification stage is completed.” The transformation stage begins when satellite imagery conveys an asymmetric appearance of clouds. The widespread decrease of deep convection in the western quadrant of TCs is the typical cause of the asymmetry. The start of ET usually occurs when the outermost edge of the TC circulation is approaching a midlatitude baroclinic zone (cold front) on the northwestern side. The transformation stage is defined as complete when both satellite imagery and numerical weather prediction analyses show that the tropical storm

now displays the characteristics of a baroclinic cyclone in which the center of the storm is overcome by cold, descending air. Finally, Klein et al. (2000) finish off their descriptions by stating that the “reintensification stage is defined to begin at the synoptic time when the transformed storm has achieved its highest central SLP at or after the completion of transformation.” The reintensification stage is concluded when the storm’s deepest SLP holds steady or fills in the next analysis. Klein et al. (2000) created Fig. 7 to illustrate the timeline of events during ET in the western North Pacific based on 30 TC cases from 1 June through 31 October during the years 1994-98. Note that 4 of the 30 storms had little to no re-intensification, 15 of the 30 storms had moderate re-intensification, and only 11 of the 30 storms had deep re-intensification (of which 6 were rapid deepeners).

Whereas Klein et al. (2000) conducted their research using data from the western North Pacific, Hart and Evans (2001) accomplished an in-depth climatological study of Atlantic TCs evaluating more than twice the amount analyzed by Klein et al. (2000). They found that 46% of Atlantic TCs transitioned extratropically and that the likelihood of ET increases toward the second half of the TC season. They also established that even though TCs which have undergone ET rarely regain their peak intensity, more than half (51%) reintensified to some degree. An additional finding of interest was that while more than 60% of reintensified cyclones originated south of 20° North latitude, 90% of ETTCs that didn’t reintensify originated north of 20° North latitude, most probably a result of TUTT interaction.

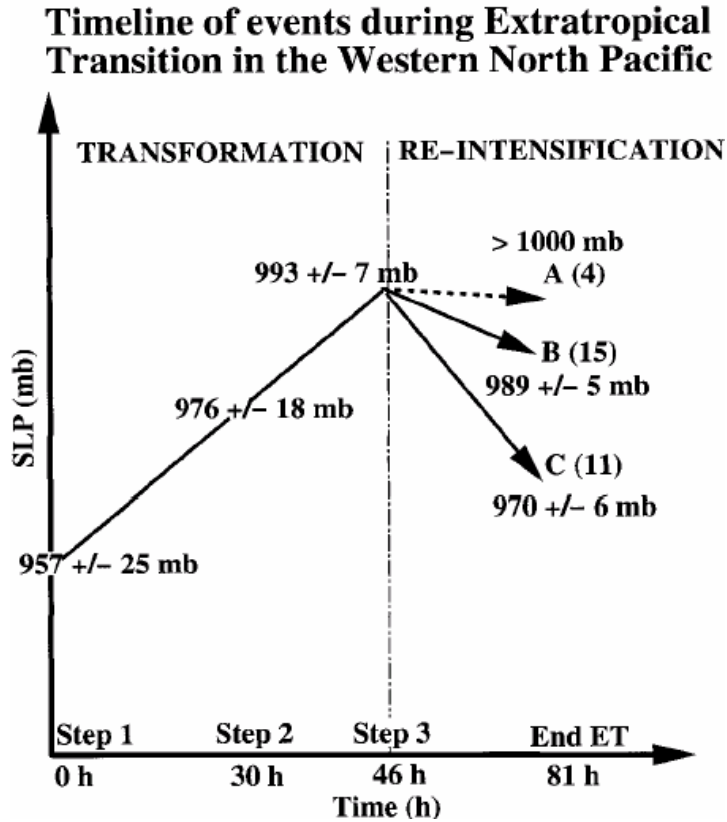


FIG. 7. Schematic of ET evolution in western North Pacific (Klein et al. 2000). The different levels of re-intensification are categorized as A) little to no re-intensification (SLP > 1000 hPa), B) moderate re-intensification (SLP between 980 and 999 hPa), and C) deep re-intensification (SLP < 980 hPa).

1) THE TRANSFORMATION STAGE

The three steps of the transformation stage depicted in Fig. 7 correspond to three distinct phases discernible in infrared (IR) imagery (Fig. 8). Step one (Figs. 8a and 8d) shows a marked decrease of cloudiness in the western quadrant which is represented by the asymmetric appearance of the clouds. The southern quadrant also appears less cloudy as dry slots begin to appear between rainbands. Step 2 (Figs. 8b and 8e) is made evident by the lack of deep convection in the southern quadrant and a reduction of deep convection in the eastern quadrant. Step 3 (Figs. 8c and 8f) is marked by a decay of the

eyewall as deep convection erodes west of the circulation center. After analyzing the 30 ET case studies in the western North Pacific, Klein et al. (2000) proposed a conceptual model of the transformation stage (Fig. 9).

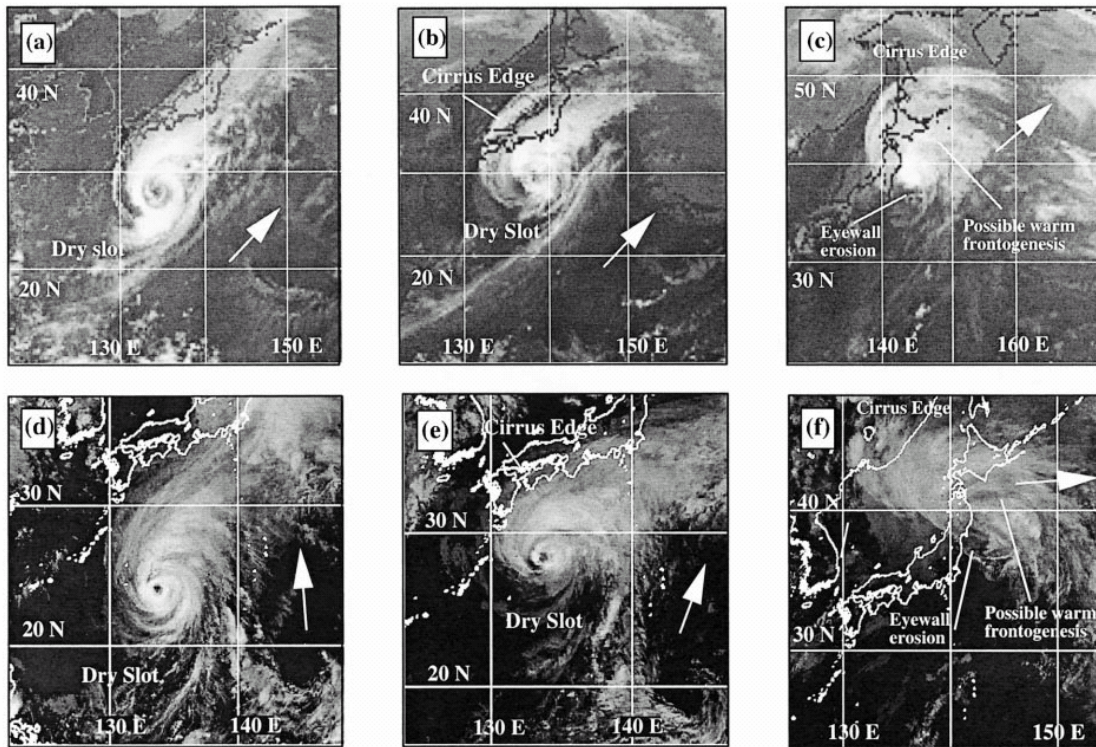


FIG. 8. IR imagery of Super Typhoon Violet (a,b,c) and Typhoon Opal (d,e,f) showing step 1 (a,d), step 2 (b,e) and step 3(c,f) of the transformation stage (Klein et al. 2000).

2) DISPLACED VORTICES

Klein et al. (2002) next used Coupled Ocean-Atmospheric Mesoscale Prediction System (COAMPS; Hodur 1997) to modify the model environment and compare: 1) a

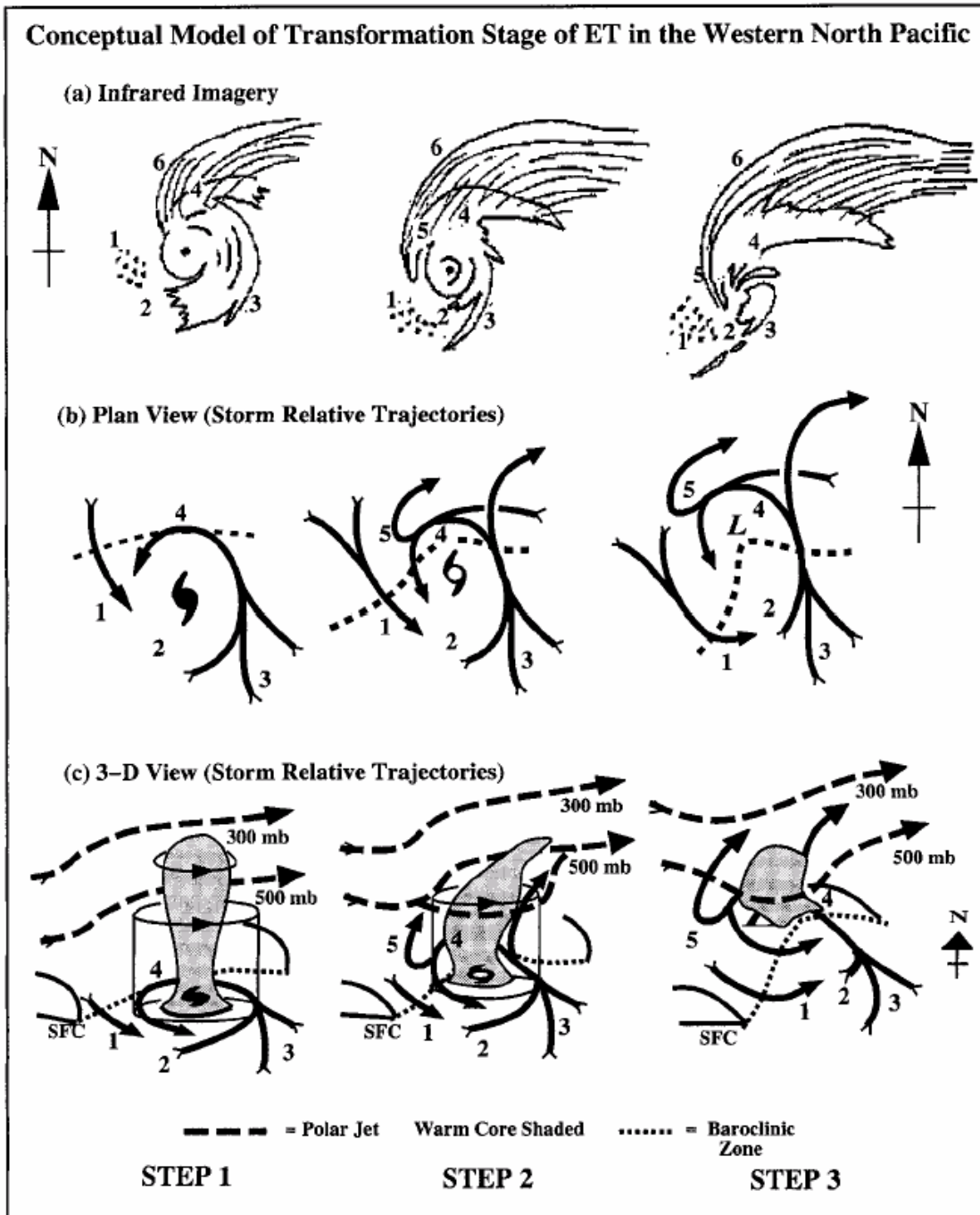


FIG. 9. Conceptual model of ET transformation (Klein et al. 2000). Areas labeled in the Fig. are as follows: 1) equatorward flow of cool, dry air as evidenced by open cell cumulus, 2) dry slot decreasing TC convection in western and southern quadrants, 3) warm, moist air flowing poleward maintaining asymmetric appearance of clouds, 4) warm moist inflow over tilted isentropic surfaces, 5) ascending air creating wrap-around clouds, and 6) a sharp cloud edge of a cirrus shield which is evident if system is confluent with the polar jet.

control TC, 2) a simulation that has had its TC remnants removed (NOTC), 3) vortices that have been displaced to the northeast, and 4) vortices that have been displaced to the southwest as portrayed in Fig. 10.

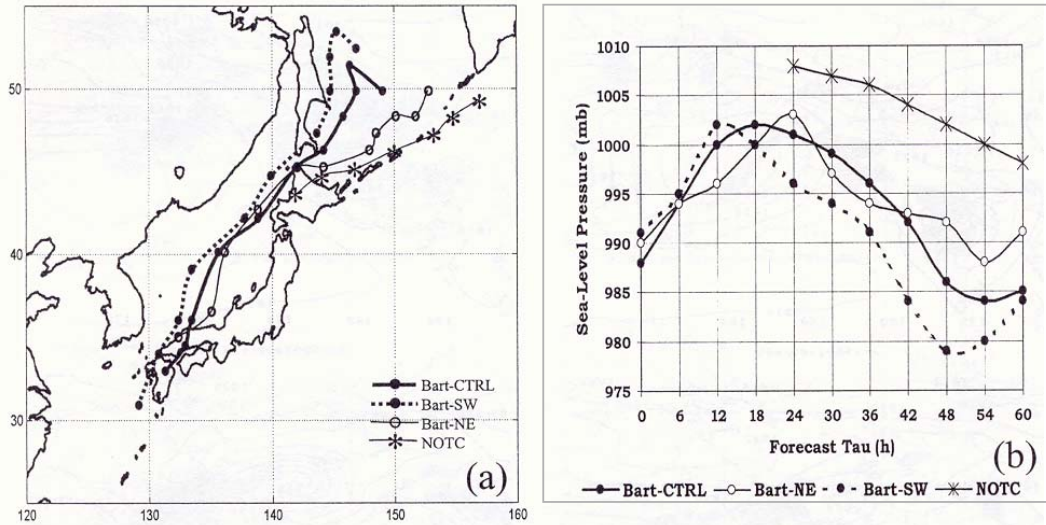


FIG. 10. Comparison of four COAMPS simulations (Klein et al. 2002).

The COAMPS model showed that extratropical cyclogenesis (ETC) occurred in the NOTC simulation implying that midlatitude contributions must have been favorable for ETC with or without a TC being present. Displacing the vortex to the southwest caused reintensification to start earlier and the SLP to deepen further than any of the other simulations. In contrast, displacing the vortex to the northeast caused reintensification to start later and the SLP to deepen less. The model runs revealed dynamic forcing downstream of the original vortex where a totally separate extratropical cyclone was forecasted to form. Reintensification, therefore, may be due to the vortex moving into development regions classified as containing at least one of the following three forcing mechanisms: 1) upper-level positive vorticity advection greater than $20 \times$

10^{-10} s^{-2} , 2) a dipole low-level temperature advection greater than $\pm 10 \times 10^{-5} \text{ K s}^{-1}$, or 3) upper-level divergence greater than $3 \times 10^{-5} \text{ s}^{-1}$.

3) THE REINTENSIFICATION STAGE

Klein et al. (2002) continued their research and typified the reintensification stage as being similar to type-B extratropical cyclogenesis (as proposed by Petterssen and Smebye 1971). Klein et al. further proposed that when the poleward-moving TC remnants interacted with a translating and evolving midlatitude circulation, mid- and upper-tropospheric dynamic support would be provided. This interaction, then, would encourage Petterssen-Smebye type-B cyclogenesis (which occurs when an upper level system moves over a baroclinic zone) and would, consequently, affect the magnitude of the reintensification stage. Subsequently, they created a simple three-by-three matrix to illustrate the effects of various levels of midlatitude circulation and TC contributions (Fig. 11). The location and strength of the TC contributions play an important role in deciding whether the TC will reintensify or decay as depicted in Fig. 11. Note that minor to significant TC contributions and neutral to favorable midlatitude contributions are required to achieve deep or rapid reintensification.

4) OPERATIONAL FORECASTING

Harr and Elsberry (2000b) believe that “it should be possible for a forecaster to

anticipate both the track and the intensity of ET based on the pattern into which the TC is translating as it completes the transformation.” If forecasters focus on step 2 of the transformation stage (see Fig. 9), they should be able to anticipate the open wave and streamline pattern in 500 hPa isoheights thereby enhancing their track and intensity forecasts.

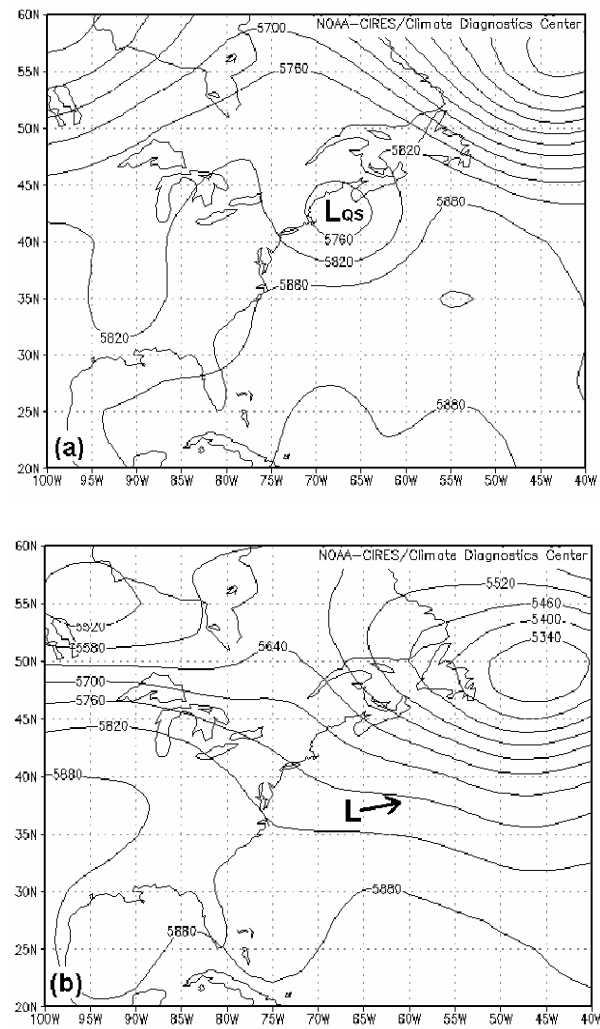
| Re-intensification Stage of ET | | | |
|--------------------------------|-------------|---------------------------|--------------------------------------|
| | | Midlatitude Contributions | |
| | | Unfavorable | Favorable |
| TC Contributions | Significant | Little or | Deep and/or Rapid Re-intensification |
| | Minor | | Moderate |
| | None | Decayers | Re-intensification |

FIG. 11. Comparisons of midlatitude circulation and TC contributions (Klein et al. 2002). The contributions are described as: Favorable – in a “NOTC” simulation, a development region is forecast, and significant extratropical cyclogenesis (ETC) occurs without a transitioning TC. Neutral – in a “NOTC” simulation, a weak or no development region is forecast, but weak ETC is predicted. Unfavorable – in a “NOTC” simulation, anticyclogenesis occurs in the transitioning TC domain. Significant – the TC remnants interact optimally with a midlatitude development region to maximize ETC. Minor – the TC interacts with a midlatitude development region in a less optimal manner such that less than maximum ETC occurs. None – the TC does not interact with a development region and no ETC occurs.

At the 25th American Meteorological Society Hurricane Conference, Fogarty (2002) presented schematics for three different 500 hPa flow patterns which could help forecasters make this observation (Fig. 12). Fig. 12a illustrates a typical flow pattern for TCs which dissipate as they move over land or colder SSTs (note the approaching ridge). Fig. 12b is representative of the zonal flow produced by a northeast pattern (low pressure

to the northeast of the TC). TCs encountering the northwest pattern illustrated in Fig.

12c



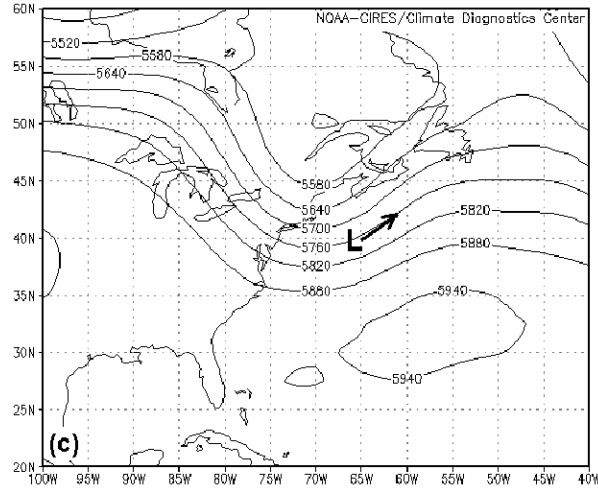


FIG. 12. Typical Atlantic 500hPa flow patterns for ET (Fogarty 2002). The “L” designates location of TC with the arrow indicating TC movement.

(low pressure to the northwest of the TC) often re-intensify as they interact with the approaching short-wave trough. Fogarty (2002) continued by implying that forecasters need only determine if any troughs are going to interact with the TC and, if so, advect the storm into the 500 hPa flow. His data provide evidence that “storms tend to move at 75% (50%) of the 500 hPa geostrophic wind during the initial (latter) stage of *extratropical* transition” (*word in italics added*).

5) MIDLATITUDE CIRCULATION CONTRIBUTIONS

Harr and Elsberry (2000a) ascertained that warm frontogenesis dominated the beginning of the transformation stage as a result of warm advection on the east side of the dying TC and of a deformation field revealed by its poleward movement. Harr and Elsberry (2000b) continued their research and found that when TCs transition into northwestern midlatitude circulation patterns, they tend to move poleward. However, when the TCs transition into a northeastern midlatitude circulation pattern, they enter a

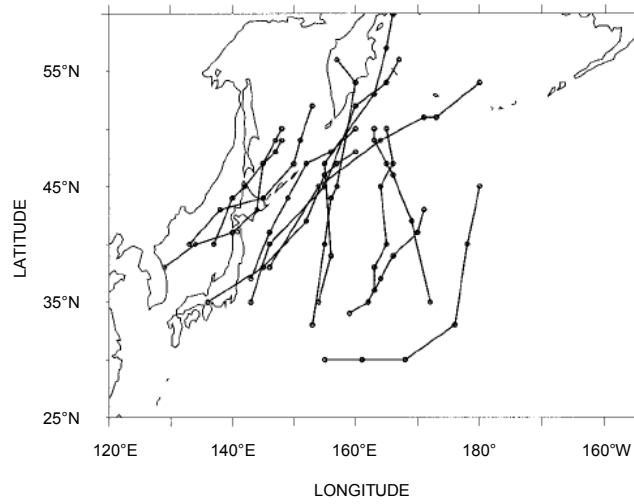
zonal flow created by the midlatitude circulation to the northwest and a subtropical ridge to the southeast as depicted in Fig. 13.

6) OBJECTIVE INDICATORS

In contrast to subjective satellite interpretation, Evans and Hart (2003) recently proposed objective indicators of the ET lifecycle. Scrutinizing 61 Atlantic TCs from 1979-1993, they derived the following equation to describe storm symmetry

$$B = h[(\overline{Z_{600} - Z_{900}})_R - (\overline{Z_{600} - Z_{900}})_L] \text{ m}, \quad (1)$$

a) Northwest Circulation/Poleward Flow



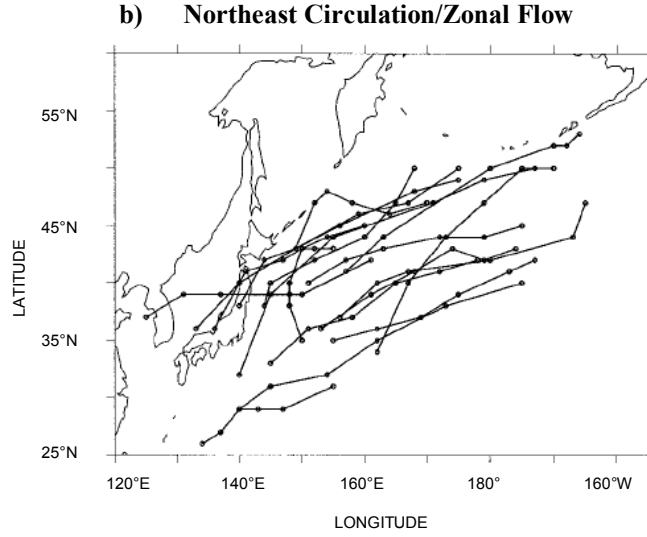


FIG. 13. Tracks of TCs encountering a) northwest and b) northeast midlatitude circulations (adapted from Harr and Elsberry 2000b).

where Z is the isobaric height, h indicates the hemisphere (1 for Northern Hemisphere and -1 for Southern Hemisphere), and R and L designate the right and left asymmetry of the thickness field. The cyclone is “perfectly” symmetrical when $B = 0$ m and Evans and Hart (2003) established $B > 10$ m as the onset of ET. Unlike the definition of ET completion provided by Klein et al. (2000) which requires the storms to reintensify, Evans and Hart (2003) define ET completion as the point when the warm-core vortex converts into a cold-core vortex. The following equation was derived to express the thermal wind measure of the cyclone in the lower troposphere

$$\left. \frac{\partial(Z_{MAX} - Z_{MIN})}{\partial \ln p} \right|_{900hPa}^{600hPa} = -V_T^L, \quad (2)$$

where $-V_T^L > 0$ implies a warm-core system and ET completion occurs when $-V_T^L$ first becomes negative. Finally, Hart (2003a) created a hodograph-like display called a cyclone phase space which exhibits both the symmetric objective indicator, using Eq. (1), and the lower tropospheric thermal wind objective indicator, using Eq. (2), at the same time (Fig. 14). Note the horizontal bar which highlights where $B > 10$ m and represents the point in time where the storm becomes asymmetric, thereby defining the beginning of ET. Now note the zero line on the abscissa separating the warm- and cold-cores; this demarcation makes it easier to see when the storm changes from warm- to cold-core defining completion of ET.

In order to demonstrate differences between the upper and lower thermal wind relationship, Hart (2003a) changed Eq. (2) so it would express the thermal wind measure of the cyclone of the upper troposphere:

$$\frac{\partial(Z_{MAX} - Z_{MIN})}{\partial \ln p} \bigg|_{600hPa}^{300hPa} = -V_T^U, \quad (3)$$

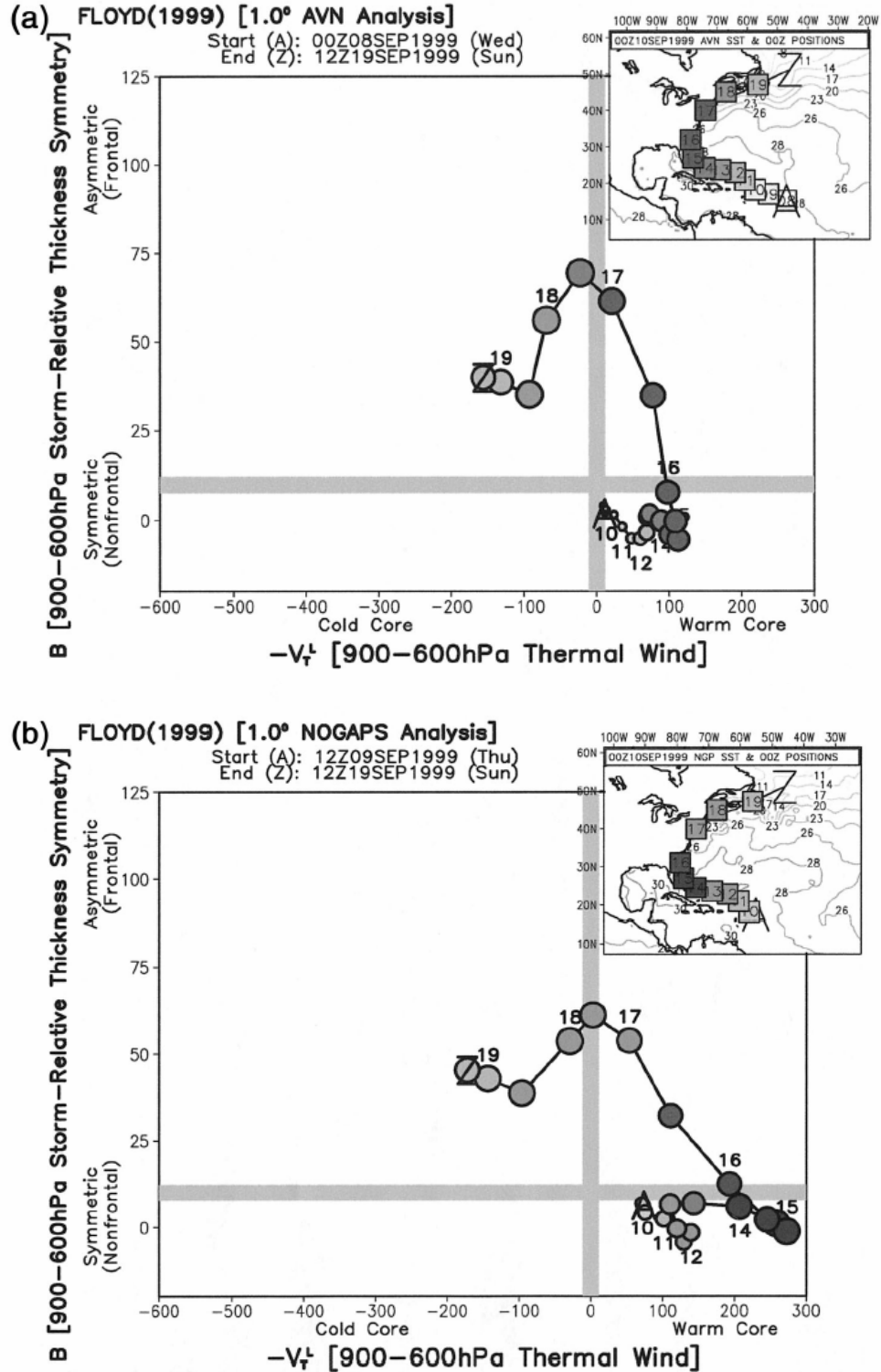


FIG. 14. Cyclone phase space for Hurricane Floyd with a) AVN and b) NOGAPS analyses (Evans and Hart 2003). The numbers above the circle are the days of the month at 0000 UTC and the inset provides the corresponding location of the TC.

An additional cyclone phase space diagram was then created (Fig. 15) to compare the upper and lower thermal wind relation terms supplied by Eqs. (2) and (3). This new phase space diagram helps analyze the thermal wind characteristics throughout the entire troposphere.

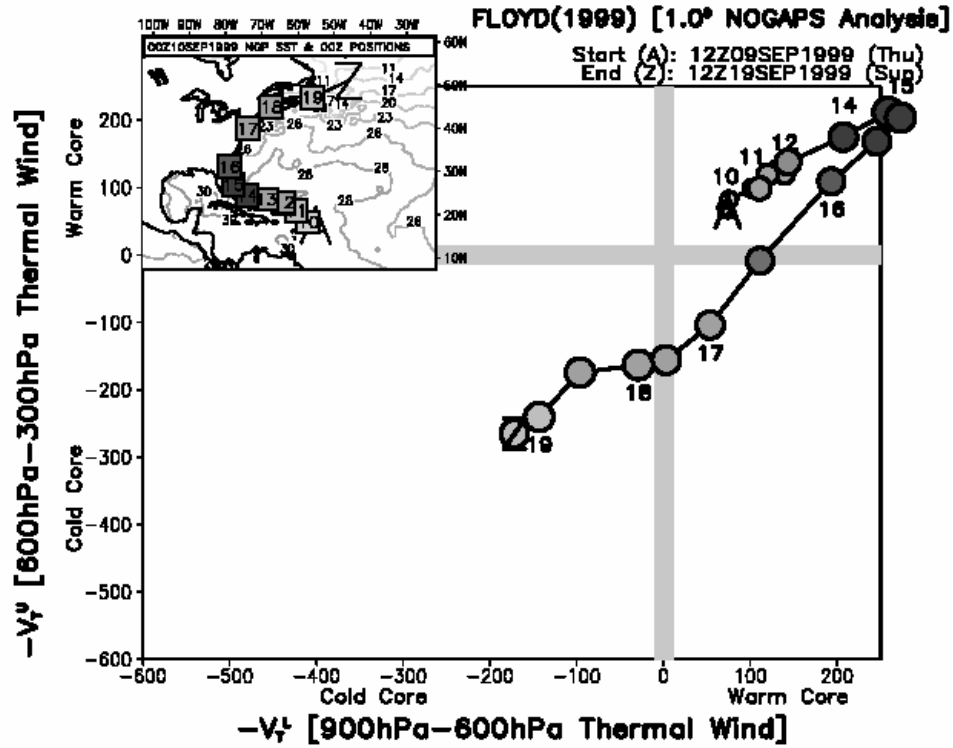


FIG. 15. Thermal wind cyclone phase space for Hurricane Floyd with NOGAPS analyses (Jones et al. 2003). The numbers above the circle are the days of the month at 0000 UTC and the inset provides the corresponding location of the TC.

3. Data and Methodology

a. Data

The data used in this research come from the NOGAPS model originating at the FNMOD and archived through AFCCC in Asheville, North Carolina. NOGAPS is a global, spectral, numerical weather prediction model which is similar in design and function to the operational models being run at other large forecast centers (Rosmond 1992). Fig. 16 is an example of a NOGAPS surface pressure analysis of Typhoon David.

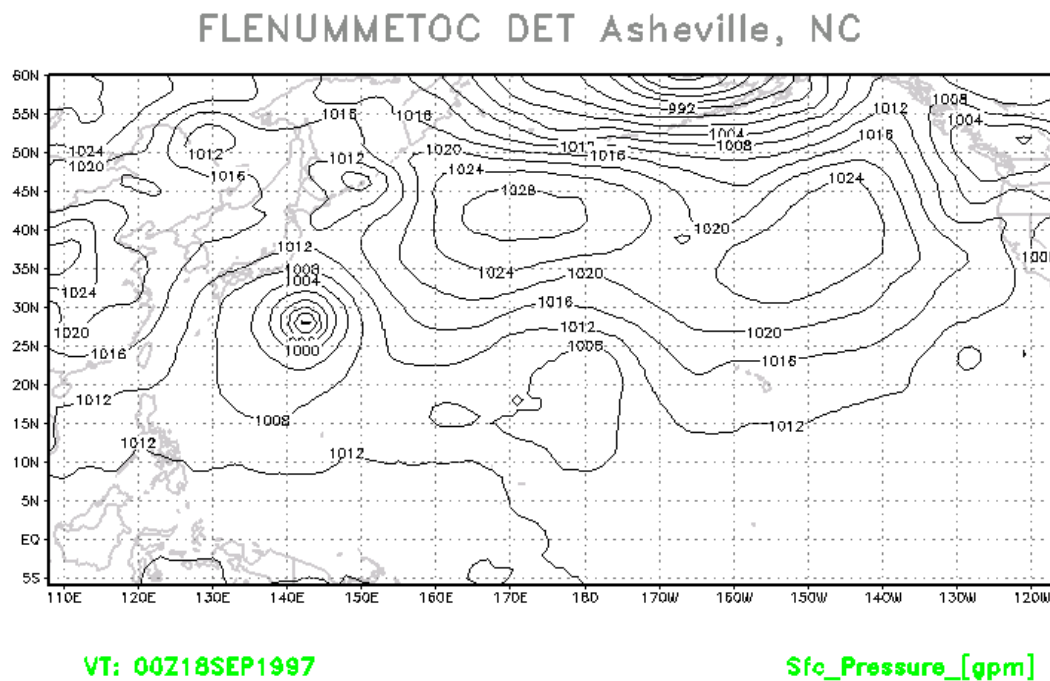


FIG. 16. NOGAPS surface pressure analysis of Typhoon David (FNMOD 2003).

Staudenmaier (1997) explains that NOGAPS uses optimal interpolation analysis and nonlinear normal model initialization. These techniques make it possible to perform four-dimensional data-assimilation schemes with the addition of unconventional data

sources like surface wind speeds from Special Sensor Microwave/Imager (SSM/I) data and precipitable water estimates. In 1993, the Navy purchased a CRAY computer, added a new set of radiation parameterizations, increased the horizontal resolution of the model to T159, and called this new version NOGAPS 3.4 (which is the version used for data in this research from 1997-1998).

Staudenmaier (1997) continues by describing that the equations used for NOGAPS are in spherical coordinates and a hybrid vertical coordinate like those used in the European Centre for Medium-Range Weather Forecasts (ECMWF) model. The 18 levels of the vertical coordinates are represented by a variation of the sigma coordinate and parameterizations for things like gravity-wave drag, vertical diffusion, and radiation are included in the model. To summarize, Staudenmaier (1997) pointed out 16 tendencies (compiled in Table 1) which are similar to tendencies of other global numerical models.

The output of the NOGAPS model is in GRIB data format which is the standard for the WMO due to its efficiency in quickly exchanging, and easily storing, gridded data fields within the international meteorological community. GRIB files are much more compact because they have a couple of packing/compression algorithms. One of these algorithms is the simple first difference: instead of storing raw values, a minimum value is sought which then becomes the reference value, from which, all other data points are subtracted, with the resulting smaller residuals being stored - since all residuals are positive, that saves even more space. Another major advantage of GRIB files is that they are self describing; each record stores information like time, variable, level, etc. As a result, GRIB is extremely useful for archiving because “each record is completely self-

identified as to content, each GRIB entity is logically a single chunk of related meteorological information, and each can be considered and manipulated as a blob” (Stackpole 1989).

TABLE 1. NOGAPS tendencies (Staudenmaier 1997).
Tendencies that pertain specifically to this study are highlighted in bold.

| |
|---|
| 1. Developing surface low pressure systems tend to develop slower in the model than in reality. |
| 2. Low-pressure systems north of the polar jet tend to deepen too much, while lows developing south of the polar jet are typically too weak and slow to deepen. |
| 3. Surface low-pressure systems over land have a tendency to be slightly too deep. |
| 4. The formation of upper-level cutoff lows is well forecasted by the model, although minimally weak throughout their life-cycle. |
| 5. Complex lows are usually merged into one elongated low-pressure system. |
| 6. Extratropical lows associated with former tropical cyclones are significantly underforecast, slow to re-deepen, and slow to move. |
| 7. Upper-level shortwave troughs embedded in either zonal flow or a broad trough are poorly forecast and difficult to follow. |
| 8. Upper-level lows north of the polar jet are too deep. |
| 9. Western ocean high pressure cells and eastward ridging off the east coast of continents are slightly weak, and slightly slow to move offshore. |
| 10. Mid-ocean high pressure cells are typically 1-2 mb too weak. |
| 11. Ridging into the west coast of continents tends to be too strong. |
| 12. The subtropical jet tends to be weaker than reality and slightly poleward of its real position. |
| 13. The forecast has a tendency to become more zonal toward the end of the integration. |
| 14. There tends to be an over prediction of the upper-level tropical easterlies. |
| 15. The bogusing technique used on Pacific typhoons has improved their storm track immensely, so that the NOGAPS-predicted typhoon tracks have been considered the best guidance available by the JTWC (<i>then in Guam</i>) (Rosmond 1992). |
| 16. The model tends to over-produce precipitation after day four. |

R. E. Hart (2003 personal communication) wrote his OI program using the Grid Analysis and Display System (GrADS) which takes the GRIB input and decodes it to return a fixed or floating point array of the numeric values either in the grid point array or sequential array of observations (along with appropriate descriptors). GrADS is an interactive desktop tool that provides easy access, manipulation, and visualization of earth science data. It uses a four-dimensional data environment (longitude, latitude, vertical level, and time) and has a programmable interface (scripting language) which allows for sophisticated analysis and display applications (Doty 1995).

b. Methodology

The following sections describe the different types of output from Hart's objective indicator program, how and why they were created, and how they can best be employed. The last section discusses how statistics were used to compare Hart's output with results from Klein et al. (2000).

1) CYCLONE PHASE ANALYSIS

Hart (2003a) created a phase space which, in order to successfully portray ET, required parameters that describe the strength of the warm-core structure within a tropical cyclone and the cold-core structure within an extratropical cyclone. This phase space also had to describe the stages of cold-core extratropical development (from formation, through intensification and occlusion, and then to decay) all at the same time. Moreover,

the parameters would have to take into account the tilted nature of extratropical cyclones while also accounting for the vertically stacked nature of tropical cyclones. After examining parameters like potential vorticity, Q vectors, and equivalent potential temperature; Hart (2003a) chose two simple, yet basic, ways to measure the structure of cyclones: thermal wind and thermal asymmetry. From these, he derived the following three parameters (calculated exclusively from three-dimensional height field data described in chapter 2) to illustrate cyclone structure: \mathbf{B} describes the lower-tropospheric thermal asymmetry, $-V_T^L$ describes the lower-tropospheric thermal wind (cold- vs. warm-core), and $-V_T^U$ describes the upper-tropospheric thermal wind (cold- vs. warm-core). All three parameters are necessary to synthesize model diagnostics with conventional fields and direct observations (surface observations, rawinsondes, and satellite imagery). Furthermore, the parameters can be evaluated using only the three-dimensional NOGAPS GRIB output (along with the mean SLP field to track the cyclone).

2) CYCLONE THERMAL SYMMETRY PARAMETER

Cyclones can be separated into two idealized categories: tropical and extratropical. TCs are usually symmetric (or nonfrontal), while extratropical cyclones are usually asymmetric (or frontal) and are associated with a time-varying horizontal temperature gradient. Fig. 17 provides examples of a symmetrical TC and an asymmetrical extratropical cyclone (the circle denotes the 500 km radius). The thermal symmetry parameter, \mathbf{B} , as defined by Eq. (1), expresses the asymmetry of the storm-

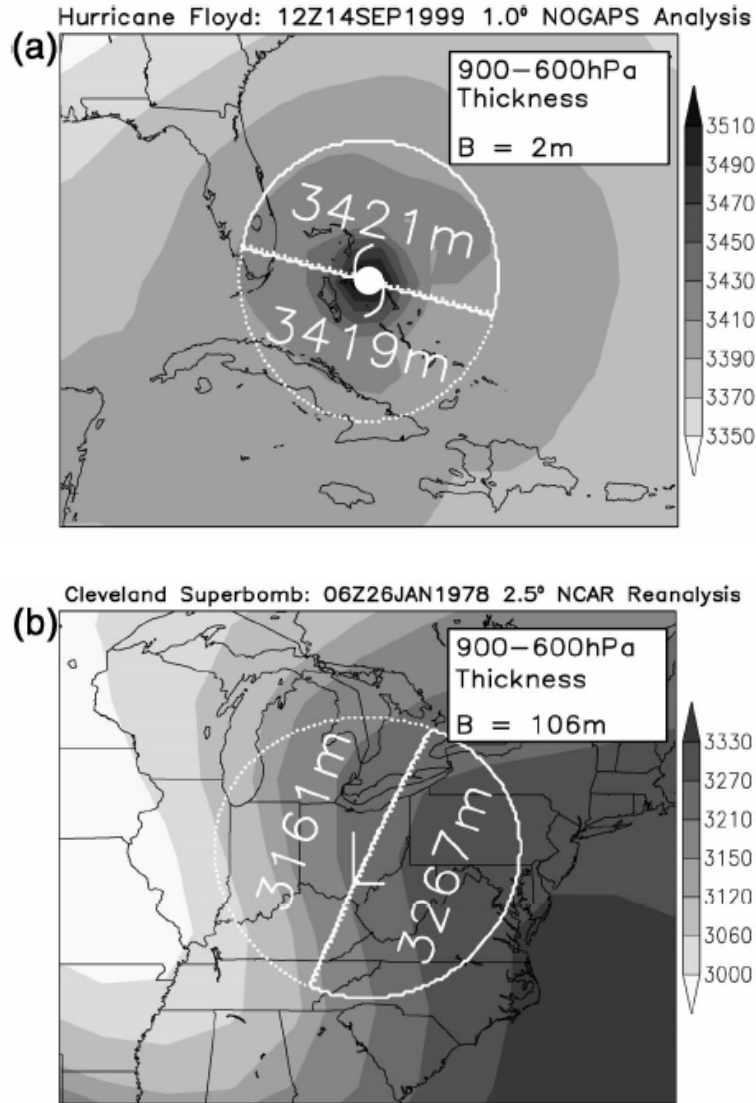


FIG. 17. 900-600 hPa thickness examples of a) a symmetrical (nonfrontal) TC and b) an asymmetrical (frontal) extratropical cyclone (Hart 2003a).

motion-relative 900-600 hPa thickness across the cyclone (within that 500 km radius) and can be used to differentiate between stages of frontal evolution. Instead of just measuring a range of temperatures across the cyclone circulation, B measures the gradient of the mean-layer temperature perpendicular to the motion of the storm. Positive values of B agree with the thermal wind relationship between the temperature

gradient and the vertical shear of the thermal wind indicating cold air on the left of the cyclone track (in the Northern Hemisphere). Thermally direct circulations (positive B values) can, therefore, be distinguished from those which are thermally indirect (negative B values). Moreover, positive values of B agree with warm advection downstream of the cyclone as expressed by the quasigeostrophic theory (positive vorticity advection increasing with height indicates rising air downstream of storm motion).

3) CYCLONE THERMAL WIND PARAMETER

The cold- versus warm-core parameters are nothing more than the vertical derivatives of the maximum geopotential height gradients (in the lower and upper troposphere) within a 500 km radius of the cyclone's center (Jones et al. 2003). Assuming thermal wind balance, Eqs. (2) and (3) can be used to represent the vertical structure of the cyclone's height perturbation (amplitude) to help distinguish between tropical and extratropical systems. Cyclone structures with larger amplitudes at the top of the layer than at the bottom are considered cold-core. The inverse is also true with the larger amplitude at the bottom of the layer indicating a warm-core structure. Fig. 18 provides examples of a warm-core tropical cyclone and a cold-core extratropical cyclone. Both upper and lower $-V_T$ parameters must be positive (with lower $-V_T$ having a greater magnitude) to indicate a warm-core TC. Similarly, both upper and lower $-V_T$ parameters must be negative (with upper $-V_T$ having a greater magnitude) to indicate a cold-core extratropical cyclone. Transitioning (or hybrid) cyclones can have thermal wind parameters with opposite signs.

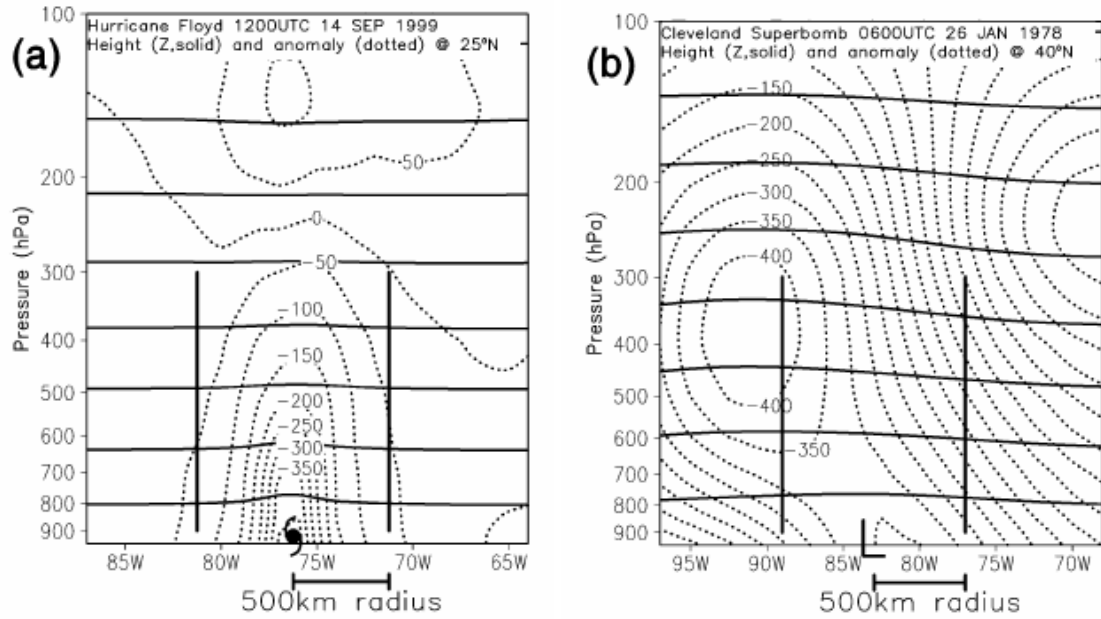


FIG. 18. Example of a) a warm-core TC and b) a cold-core extratropical cyclone (Hart 2003a).

4) CYCLONE PHASE DIAGRAMS

A cyclone phase space can be imagined in three-dimensional space, but it's difficult to project that image in print. As a result, Hart (2003a) uses two cross sections through the 3-D cube (B vs $-V_T^L$ and $-V_T^L$ vs $-V_T^U$) to illustrate the cyclone's characteristics (as depicted in Fig. 19). Research has shown that the quadrants contain the TC types depicted in Fig. 19, but these boundaries aren't necessarily exact and TCs could show up in the wrong quadrant. Nevertheless, "substantial insight into the structural changes during cyclone development at various phases within its life cycle can be evaluated based upon the location and movement within the diagram" (Hart 2003a).

Fig. 20 provides a colorful example of the full life cycle of a TC with the different

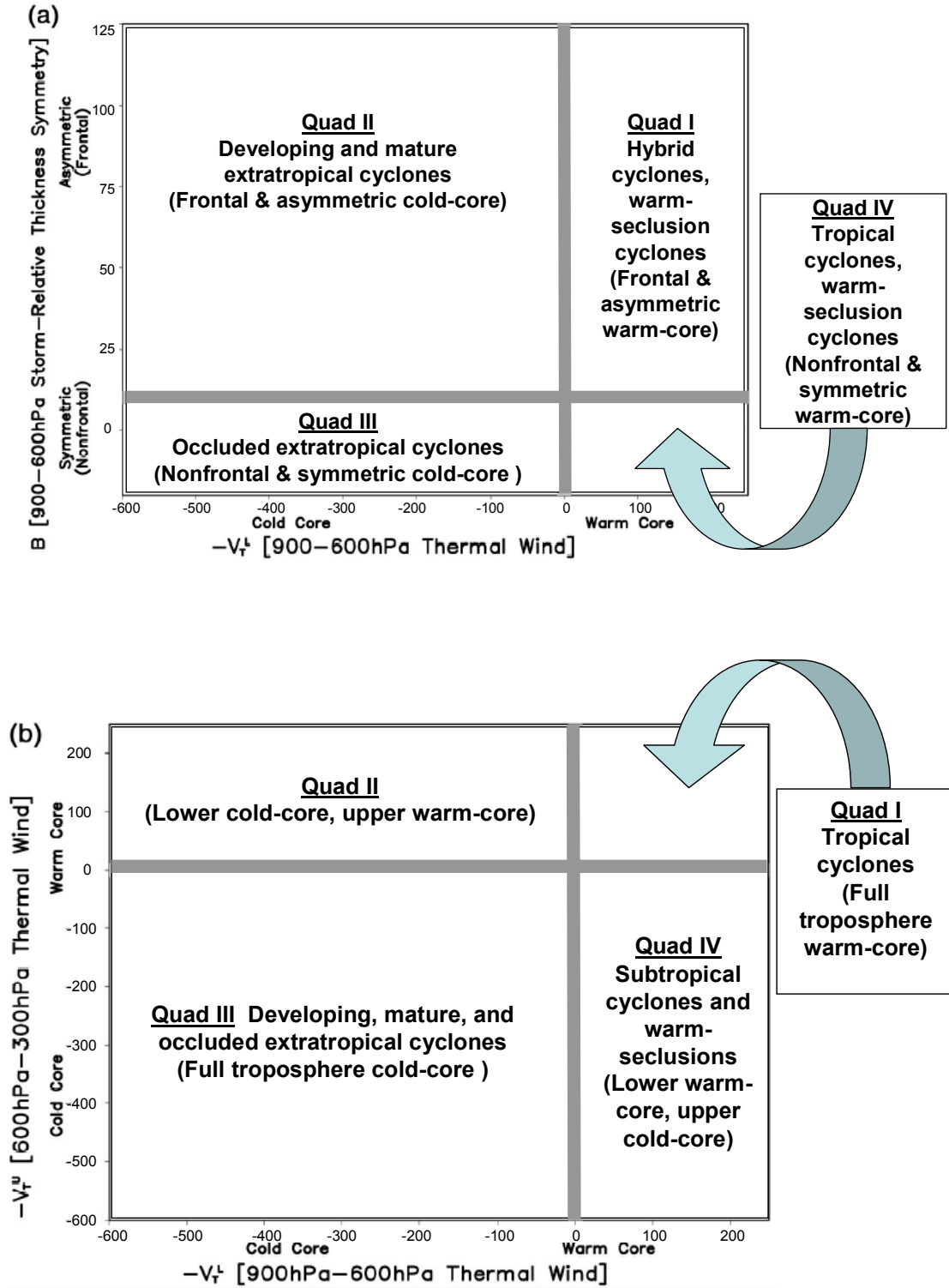


FIG. 19. Examples of a) B vs $-V_T^L$ phase space and b) $-V_T^L$ vs $-V_T^U$ phase space with summary of general locations of conventional TCs (adapted from Hart 2003).

model types being used for analysis labeled along the top. The start of the cyclone (as defined by the available dataset within its geographic boundaries) is labeled ‘A’ and the end is labeled ‘Z’. During the phase evolution, the 00Z times are labeled with the two-digit date. The coloring of the lines and markers indicates the TC’s intensity (minimum central pressure in hPa) with black being the weakest (>1015 hPa) and pink being the most intense (<950 hPa). The size of the marker represents the mean radius of the 925 hPa gale force wind field (in kilometers). The corresponding model analysis is shown in the upper right inset with the two-digit 0000 UTC times marking the location of the lowest SLPs for those dates (Hart 2003b).

Fig. 20 also provides a representative example of the life cycle of intense TCs as they transition extratropically (see Hurricane Floyd depicted in Fig. 21a for a similar example). Both storms start out in quad IV as warm-core cyclones before becoming strong hybrid cyclones and remaining in quad I for at least a day. Then, they intensify slightly once they become cold-core and move into quad II. The reader should be forewarned, however, that even though this trajectory may be the best-documented path of ET, the majority of transition cases researched have not complied with this path. For the “classic” case of ET, TCs must be located in such a way that the approaching trough (which is amplifying) withstands the shear which is inherent in this environment and which would eventually tear apart the TC. The strong warm-core characteristics actually augment the baroclinicity in the ET redevelopment phase of the storm’s evolution (Evans and Hart 2003). Fig. 21 presents an example of the life cycle of the “conventional” ET of TCs using both phase space diagrams at the same time. Focusing on the thermal wind

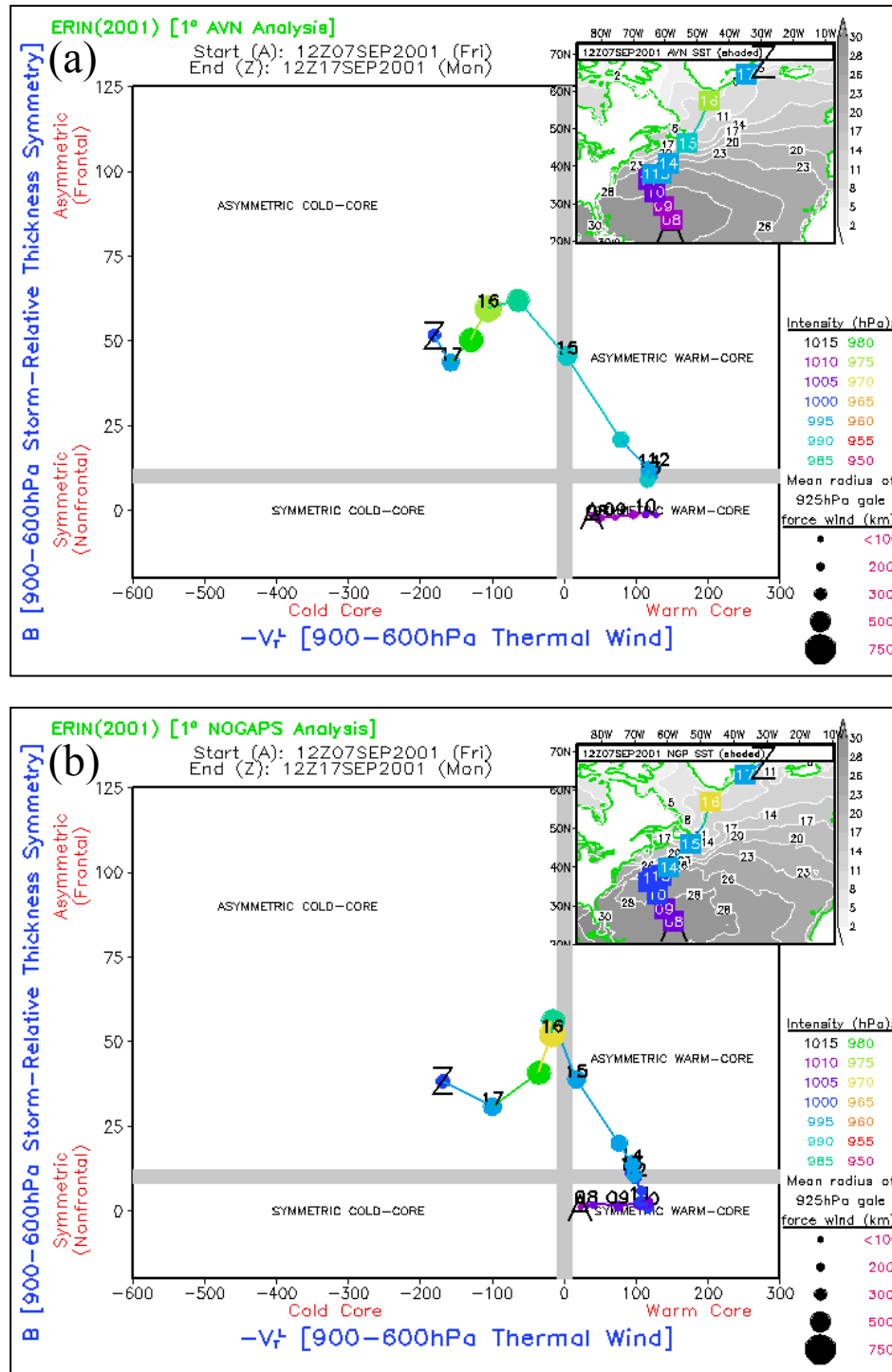


FIG. 20. Cyclone phase space for Hurricane Erin with a) AVN and b) NOGAPS analyses (Evans and Hart 2003).

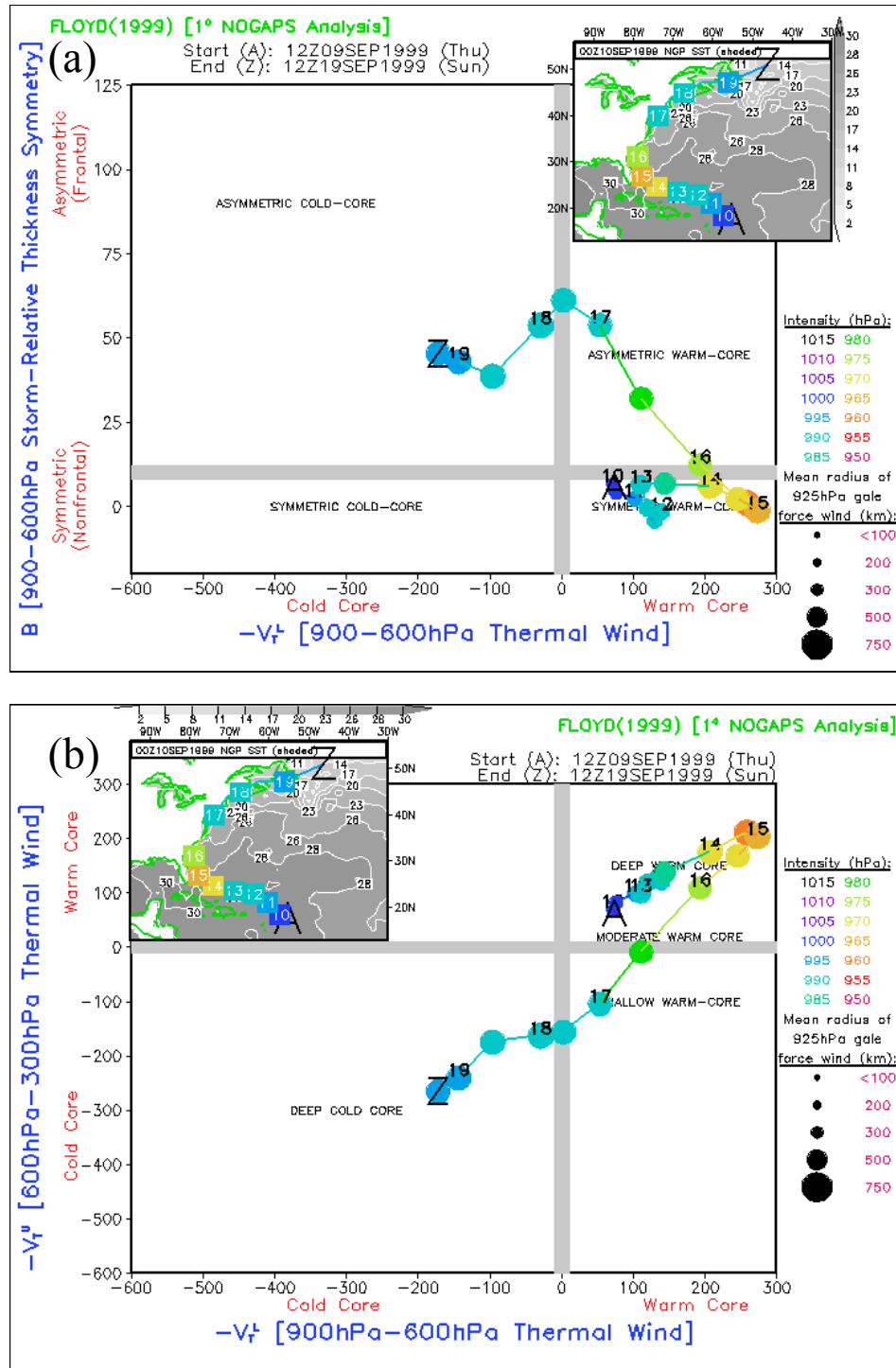


FIG. 21. Both cyclone phase space diagrams for Hurricane Floyd with NOGAPS analyses (Hart 2003b).

cyclone phase space (Fig. 21b), Hurricane Floyd started out (in quad I) as a warm-core tropical storm (throughout the entire troposphere) before hybridizing (lower warm-core and upper cold-core) and staying in quad IV for more than a day (as is typical of “conventional” ETTCs). Then, Hurricane Floyd became a cold-core system extending throughout the entire troposphere as it intensified (and moved into quad III) before dissipating.

In summary, the two cyclone phase space diagrams created by Hart’s OI program are extremely helpful in analyzing the ET of TCs (as well as analyzing “normal” cyclones). They also provide repeatable diagnoses to operationally compare model analysis with satellite analysis (Evans and Hart 2003). However, there are some drawbacks to be concerned with; Hart (2003b) points out some of the strengths and weaknesses of using the cyclone phase spaces as objective indicators of ET (Table 2).

TABLE 2. Strengths and weaknesses of Hart’s OIs (Hart 2003b).

| STRENGTHS | WEAKNESSES |
|---|--|
| Understanding the phase of cyclones gives a broader, yet insightful, perspective on the overwhelming distribution of all cyclones and there is a great continuum of cyclone types with a significant fraction of them having characteristics of both tropical and extratropical cyclones. | Tracking errors, while unusual given the tracking method complexity described in (<i>Hart 2003a</i>) section 2, will lead to phase diagnostics (especially for parameter B) that may not be representative of the actual cyclone. |
| The phase of a cyclone (warm- vs cold-core, in particular) is related to its intensity, size, forecast uncertainty, and ultimately the threat it poses to us. The diagnostics shown here give an indication of whether a cyclone that is developing within the models is a pure warm-core development, or hybrid development. | The phase analyses ... are derived completely from model analyses and forecasts. They will not and cannot represent the complete or true structure of the observed cyclone. The phase diagrams are only as accurate as the model analyses and forecasts from which they are derived. |

5) STATISTICAL ANALYSIS

While Hart's OIs can be extremely helpful in defining the stages of ET, it's essential to compare their output with other data to determine their similarity and/or applicability. The only other definitive ET theory for the western North Pacific at the present time is the conceptual model proposed by Klein et al. (2000). By using Hart's OI program to analyze 12 of the 30 storms that Klein et al. studied (from 1997-1998), this study provided data which could be easily compared with results from Klein et al. (2000). These data were then analyzed using two different statistical tests: 1) a sign test for matched pairs and 2) a Wilcoxon signed-rank test for matched pairs. These tests don't require the assumption of normality (which can't be proven) and were beneficial in validating the hypotheses that their means are equal (thereby implying similarity).

4. Results and Analysis

a. Results

The first problem encountered with analyzing Hart's phase space diagrams was trying to pinpoint the exact start-time of ET; explicitly, when **B** (thermal symmetry parameter) exceeded 10 m. The author of this thesis started out by using the numerical output (as opposed to the graphical phase space diagrams) because that seemed the more accurate way of analysis. On the other hand, Evans and Hart (2003) defined the onset of ET when **B** > 10 m using the phase space diagrams (not the numerical output). Unfortunately, using the phase diagrams alone can lead to ambiguity since there are times when the marker is directly over the **B** > 10 m line. Fig. 22a provides an example of this ambiguity; the circle representing 1200 UTC 15 September lies squarely on the demarcation between the quadrants (in actuality, the numerical output for **B** at this time is -1.1 m). This seemingly incongruous placement of the circle can be explained by the 24 hour running mean smoother applied to the OI data by R. E. Hart (2003, personal communication). The following equation for the 1200 UTC value is an example of the 24 hour running mean smoother used to combat the sometimes noisy raw NOGAPS data:

$$1200UTCvalue = (0000UTCvalue + 1200UTCvalue + 0000UTCvalue) / 3 \quad (4)$$

As a result of this smoothing, the plotted values could be off by 12 hours. Then again, since this study is using 12 hour increments for analysis, 12 hours of difference can be considered negligible. At any rate, Fig. 22b displays the marker clearly in quadrant I

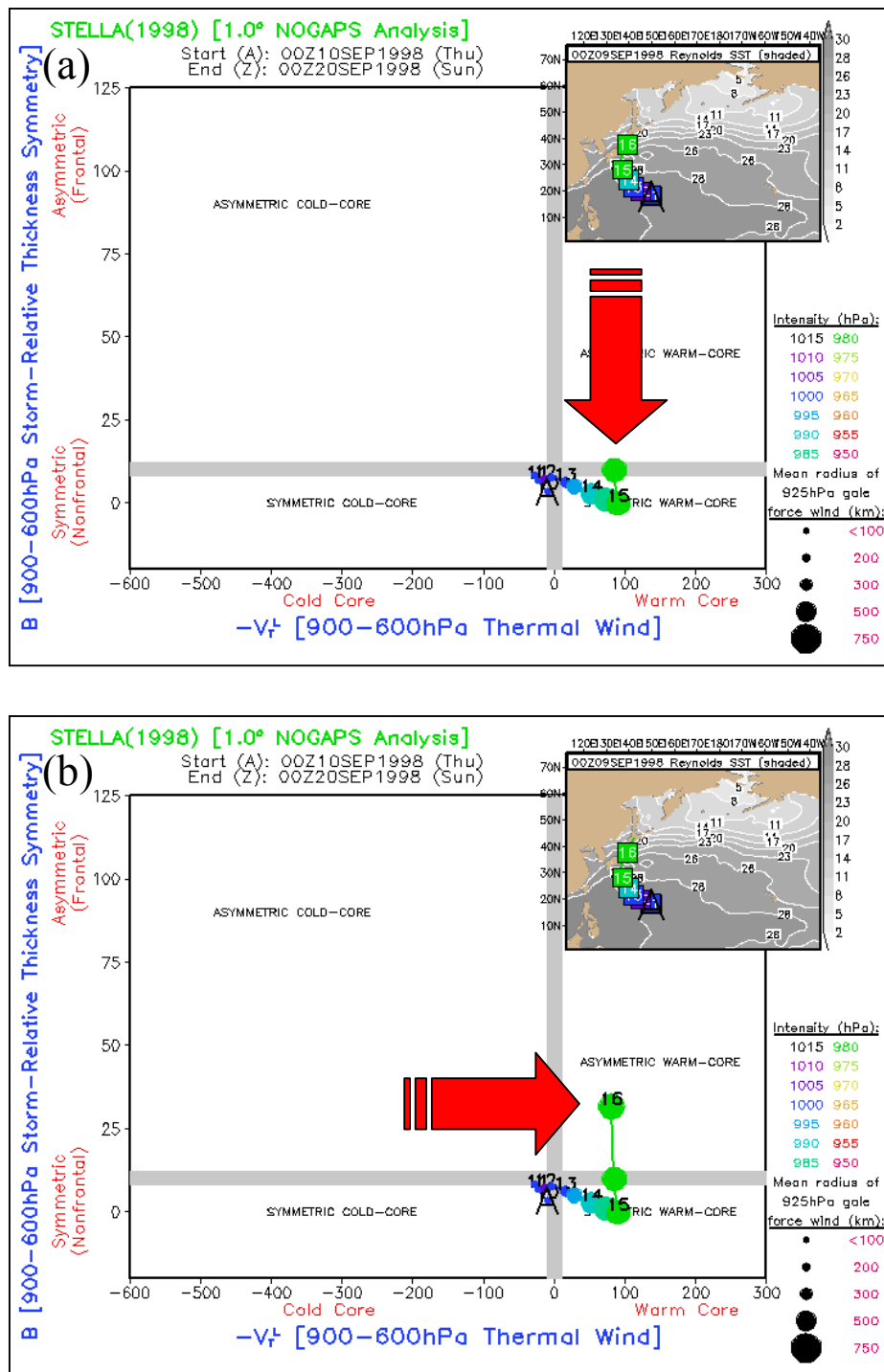


FIG. 22. Phase space diagrams of Typhoon Stella (Hart 2003b).

indicating that ET has begun. Ergo, in concurrence with Hart (2003a), the start of ET for this study is declared as the time when the center of the circle (marker) is in quadrant I of the \mathbf{B} vs $-V_T^L$ phase space diagram.

Another hindrance to the pinpointing of the onset of ET was missing data; either the data weren't archived or there were incomplete data in the vertical. Since there were only a few cases with just one or two analyses missing, the phase space calculations weren't significantly impacted. However, there were more than 72 consecutive hours of data missing from Typhoon Yule (August 1997) which made it impossible to produce an accurate phase space diagram (dropping the number of storms available for comparison from 13 to 12). There were also instances when consecutive missing analyses occurred during a dramatic shift in storm motion causing calculated \mathbf{B} values to be slightly different from reality. For example, Typhoon Ginger has five consecutive analyses missing between 1200 UTC 26 September (Fig. 23a) and 1200 UTC 29 September (Fig. 23b) making it difficult to declare the exact time of the initiation of ET.

The ambiguity of ET start-time being noted, the start-time SLPs created by Hart's OIs were, regrettably, much larger than those provided by Klein et al. (2000). The larger SLPs are a result of Hart's OI output being based on the $1^\circ \times 1^\circ$ NOGAPS data which tends to analyze tropical cyclones weaker than reality (R. E. Hart 2003, personal communication). For example; when a 950 hPa TC (in reality) is placed on a 1° grid resolution, it will generally have a minimum SLP around 970 or 980 hPa. As a side note, the reason the end-time SLPs are in better agreement is because operational analyses can calculate size and intensity better once TCs have weakened and grown in size, as is the

case at the end of ET.

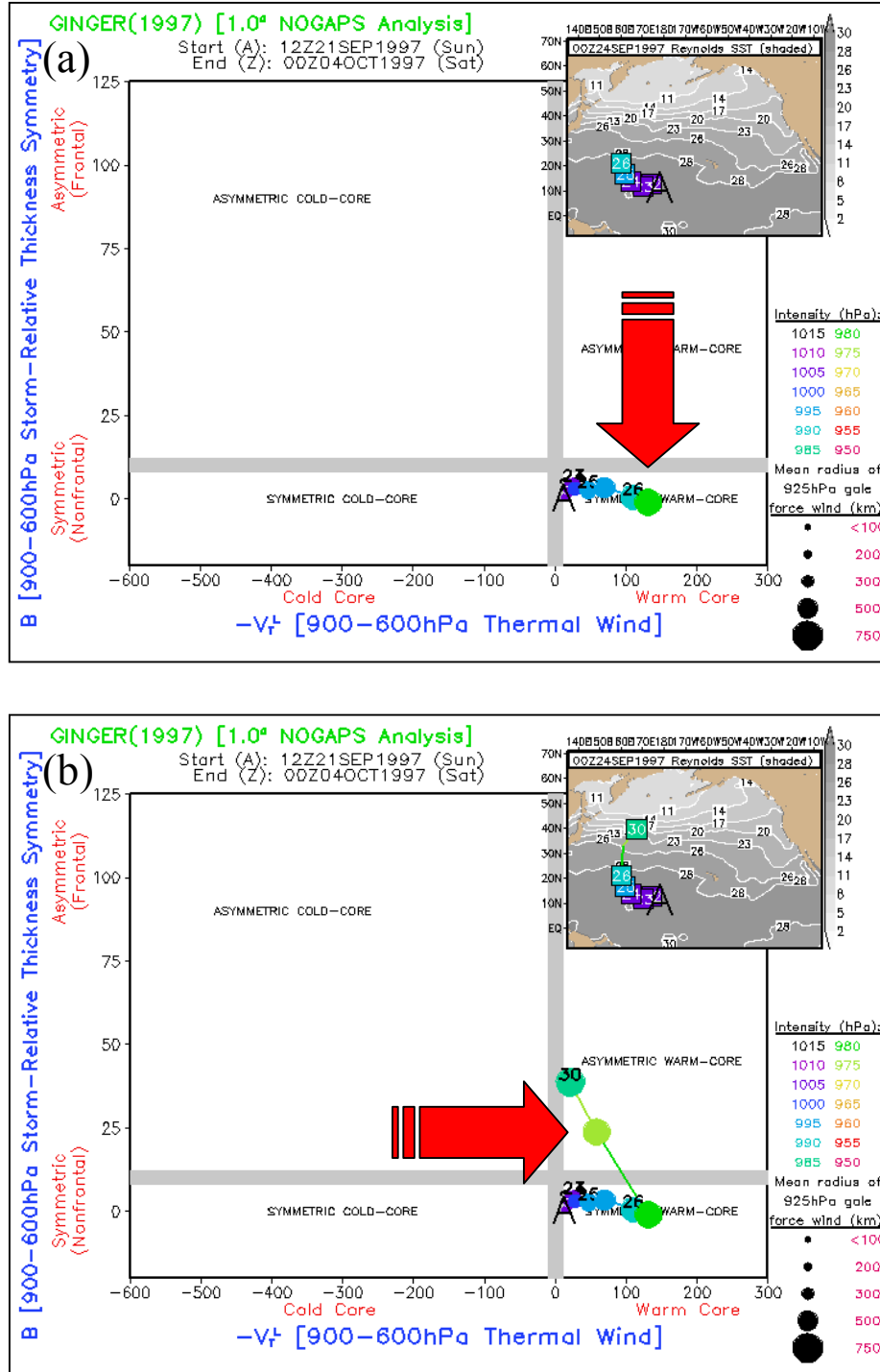


FIG. 23. Phase space diagrams of Typhoon Ginger (Hart 2003b).

In contrast, the start-time SLPs supplied by Klein et al. (2000) were taken directly from JTWC's individual tropical storm folders. Being unable to track down this information, JTWC informed the author about the Atkinson and Holliday (1977) method used in calculating minimum SLPs via maximum sustained wind speeds. Concordantly, Table 3 contains a max wind column for Hart's OIs which was used to reanalyze the start-time SLPs employing the Atkinson and Holliday method; this new data improved the statistical results dramatically.

TABLE 3. Comparison data from Klein's Conceptual Model and Hart's Objective Indicators.

| TC name | Klein's Conceptual Model | | | | Hart's Objective Indicators | | | | |
|---------|--------------------------|--------------|------------|-------------|-----------------------------|----------|--------------|------------|-------------|
| | ET start time | SLP at start | SLP at end | length (hr) | ET start time | max wind | SLP at start | SLP at end | length (hr) |
| Nestor | 00Z 06/13/97 | 938 | 996 | 36 | 12Z 06/13/97 | 80 | 963 | 994 | 36 |
| Opal | 12Z 06/18/97 | 954 | 990 | 48 | 12Z 06/20/97 | 55 | 984 | 993 | 36 |
| Peter | 00Z 06/27/97 | 976 | 986 | 48 | 00Z 06/28/97 | 55 | 984 | 985 | 12 |
| Tina | 12Z 08/07/97 | 980 | 996 | 60 | 12Z 08/09/97 | 40 | 994 | 991 | 0 |
| Bing | 12Z 09/03/97 | 949 | 993 | 36 | 00Z 09/01/97 | 125 | 916 | 993 | 96 |
| David | 00Z 09/18/97 | 976 | 988 | 36 | 00Z 09/19/97 | 65 | 976 | 988 | 12 |
| Ginger | 00Z 09/28/97 | 927 | 984 | 48 | 12Z 09/29/97 | 90 | 954 | 984 | 12 |
| Joan | 00Z 10/22/97 | 927 | 997 | 60 | 00Z 10/22/97 | 115 | 927 | 996 | 60 |
| Rex | 00Z 09/05/98 | 984 | 984 | 36 | 12Z 09/06/98 | 55 | 984 | 984 | 48 |
| Stella | 00Z 09/15/98 | 976 | 980 | 48 | 00Z 09/16/98 | 65 | 976 | 989 | 24 |
| Vicki | 00Z 09/21/98 | 954 | 1004 | 36 | 00Z 09/22/98 | 90 | 954 | 1003 | 24 |
| Zeb | 12Z 10/15/98 | 962 | 987 | 36 | 00Z 10/16/98 | 80 | 963 | 986 | 48 |

Finally, it's important to remember that this study compares output of operational analyses based on the resolution of $1^\circ \times 1^\circ$ NOGAPS data with satellite analyses that have a much higher resolution in time and space. As R. E. Hart (2003, personal communication) reminded the author, "NOGAPS analyses don't represent reality . . . only its approximation." Accordingly, there could be significant errors when comparing analyses with reality. These errors are only increased by the fact that this study uses 12 hour analysis time increments (instead of the now available six hour increments).

b. Statistical Analysis

Since FNMOD's archival database doesn't include NOGAPS $1^\circ \times 1^\circ$ data before 1997, there was only enough data to successfully create phase space diagrams for 12 of the 30 storms analyzed by Klein et al. (2000). With such a small number of samples, it was difficult to make statistical assumptions about the underlying distribution of the data. As a result, two nonparametric tests were used to compare the output from Klein et al.'s (2000) conceptual model with Hart's (2003a) objective indicators: 1) the sign test and 2) the Wilcoxon signed rank test. Each of these tests provides test statistics for values of n down to six samples for an alpha of 0.05 (Montgomery and Runger 2003) allowing the small amount of data to be sufficient for these statistical analyses.

1) SIGN TEST

The first statistical test applied was the sign test for matched pairs which uses the test hypotheses about the median of a continuous distribution. The observations are paired, the differences calculated, and then the differences are counted. Since the differences can only be positive or negative, all ties are thrown out and the resulting distribution is binomial. The null hypothesis (that the medians of each output are equal) should be rejected if the P-values were less than alpha (0.05), however, since the P-values are all greater than alpha (as shown in Table 4), the null hypothesis should not be rejected. Table 4 shows the test statistics for all three cases (SLP at start, SLP at end, and

ET duration) as well as the P-values, labeled as “Exact Sig. (2-tailed).” Table 5 shows the results of the sign test.

TABLE 4. Sign test statistics.

| | OI SLP at start - CM SLP at start | OI SLP at end - CM SLP at end | OI length (hr) - CM length (hr) |
|-----------------------|--------------------------------------|----------------------------------|------------------------------------|
| Exact Sig. (2-tailed) | 0.125 | 0.289 | 0.344 |

TABLE 5. Sign test frequencies.

| | | N |
|-----------------------------------|-------------|----|
| OI SLP at start - CM SLP at start | Negative | |
| | Differences | 1 |
| | Positive | |
| | Differences | 6 |
| | Ties | 5 |
| | Total | 12 |
| OI SLP at end - CM SLP at end | Negative | |
| | Differences | 6 |
| | Positive | |
| | Differences | 2 |
| | Ties | 4 |
| | Total | 12 |
| OI length (hr) - CM length (hr) | Negative | |
| | Differences | 7 |
| | Positive | |
| | Differences | 3 |
| | Ties | 2 |
| | Total | 12 |

2) WILCOXON SIGNED RANK TEST

The second statistical test applied was the Wilcoxon signed ranks test for matched pairs which uses the test hypotheses about the mean of a continuous distribution. The

observations are paired, the differences calculated, and then the differences are ranked (from smallest to largest) by absolute value. Differences of zero are thrown out and ties are assigned average ranks. The positive ranks are all added together and the absolute values of all the negative ranks are added together as shown in Table 6. W is the smaller of the two numbers (sum of positive ranks or sum of absolute value of negative ranks). For the two-sided alternative, the null hypothesis is that the mean of the differences is zero and should be rejected when W is less than W_{star} (found in Appendix Table VIII, Montgomery and Runger 2003).

TABLE 6. Example of Wilcoxon signed rank test for end time SLP comparisons.

| TC name | Klein's Conceptual Model | | Hart's Objective Indictors | | end | absolute | normal | signed | positive | negative |
|---------|--------------------------|------------|----------------------------|------------|------------|-----------|--------|--------|----------|----------|
| | ET start time | SLP at end | ET start time | SLP at end | difference | end value | rank | rank | rank | rank |
| Bing | 12Z 09/03/97 | 993 | 00Z 09/01/97 | 993 | 0 | 0 | 0 | 0 | 0 | 0 |
| David | 00Z 09/18/97 | 988 | 00Z 09/19/97 | 988 | 0 | 0 | 0 | 0 | 0 | 0 |
| Ginger | 00Z 09/28/97 | 984 | 12Z 09/29/97 | 984 | 0 | 0 | 0 | 0 | 0 | 0 |
| Rex | 00Z 09/05/98 | 984 | 12Z 09/06/98 | 984 | 0 | 0 | 0 | 0 | 0 | 0 |
| Joan | 00Z 10/22/97 | 997 | 00Z 10/22/97 | 996 | 1 | 1 | 2 | 2.5 | 2.5 | 0 |
| Peter | 00Z 06/27/97 | 986 | 00Z 06/28/97 | 985 | 1 | 1 | 1 | 2.5 | 2.5 | 0 |
| Vicki | 00Z 09/21/98 | 1004 | 00Z 09/22/98 | 1003 | 1 | 1 | 3 | 2.5 | 2.5 | 0 |
| Zeb | 12Z 10/15/98 | 987 | 00Z 10/16/98 | 986 | 1 | 1 | 4 | 2.5 | 2.5 | 0 |
| Nestor | 00Z 06/13/97 | 996 | 12Z 06/13/97 | 994 | 2 | 2 | 5 | 5 | 5 | 0 |
| Opal | 12Z 06/18/97 | 990 | 12Z 06/20/97 | 993 | -3 | 3 | 6 | -6 | 0 | -6 |
| Tina | 12Z 08/07/97 | 996 | 12Z 08/09/97 | 991 | 5 | 5 | 7 | 7 | 7 | 0 |
| Stella | 00Z 09/15/98 | 980 | 00Z 09/16/98 | 989 | -9 | 9 | 8 | -8 | 0 | -8 |
| Total | | | | | | | | | 22 | 14 |

Table 7 shows the results of the Wilcoxon signed ranks test and Table 8 takes the W computed earlier and compares it with W_{star} . In each and every case, W is not less than W_{star} , hence, the null hypothesis (that the mean of the differences is zero) could not be rejected. Table 9 provides the test statistics for all three cases (SLP at start, SLP at end, and ET duration) and also gives the P-values, labeled as “Asymp. Sig. (2-tailed)”. Since the P-values are all greater than alpha (0.05), the null hypothesis cannot be rejected

which implies that the means of the differences could be zero and the theories could be compatible! The Z information in the Table 9 is equivalent to normalizing the data distribution which allowed for easier computation of the P-values.

TABLE 7. Wilcoxon signed ranks test frequencies.

| | | N | Mean Rank | Sum of Ranks |
|-----------------------------------|----------------|----|-----------|--------------|
| OI SLP at start - CM SLP at start | Negative Ranks | 1 | 7 | 7 |
| | Positive Ranks | 6 | 3.5 | 21 |
| | Ties | 5 | | |
| | Total | 12 | | |
| OI SLP at end - CM SLP at end | Negative Ranks | 6 | 3.67 | 3.67 |
| | Positive Ranks | 2 | 7 | 7 |
| | Ties | 4 | | |
| | Total | 12 | | |
| OI length (hr) - CM length (hr) | Negative Ranks | 7 | 5.79 | 40.5 |
| | Positive Ranks | 3 | 4.83 | 14.5 |
| | Ties | 2 | | |
| | Total | 12 | | |

TABLE 8. Wilcoxon signed ranks test results.

| Difference | W | Wstar | Results |
|-----------------------------------|------|-------|-----------------------------------|
| CM SLP at start – OI SLP at start | 7 | 2 | $W > Wstar$: cannot reject H_0 |
| CM SLP at end – OI SLP at end | 14 | 3 | $W > Wstar$: cannot reject H_0 |
| CM length (hr) – OI length (hr) | 14.5 | 8 | $W > Wstar$: cannot reject H_0 |

TABLE 9. Wilcoxon signed ranks test statistics.

| | OI SLP at end - CM SLP at end | OI length (hr) - CM length (hr) | OI length (hr) - CM length (hr) |
|-----------------------|----------------------------------|------------------------------------|------------------------------------|
| Z | -1.183 | -0.567 | -1.336 |
| Exact Sig. (2-tailed) | 0.237 | 0.571 | 0.181 |

c. Operational Comparison

In view of the fact that neither of these statistical tests could disprove their null hypotheses, the outputs from the two methods of ET definition could, statistically, be considered not significantly different from equal! Hence, the following section examines the individual cases of a conventional ETTC whose outputs didn't match well, an ETTC whose outputs matched almost "perfectly," and an ETTC whose ET was difficult to forecast using the conceptual model alone.

1) TYPHOON DAVID

Typhoon David was extensively analyzed by Klein et al. (2000) and was, therefore, selected by the author as a "classic" case of ETTC for comparison with Hart's OI output. Fig. 24a is an IR satellite image from the Commonwealth of Australia's Bureau of Meteorology Geostationary Satellite Archive (C. of A. 2003) and depicts step 1 of the transformation stage (as defined by Klein et al. 2000) with the corresponding step of the conceptual model inset and defined on the right side. Note the asymmetric shape of the clouds caused by a decrease of deep convection in the western quadrant. There is also a dry slot forming in the southern quadrant. Figs. 24b and 24c display Hart's (2003b) phase space diagrams for the same zulu hour classifying the storm as still being symmetric and deep warm-core.

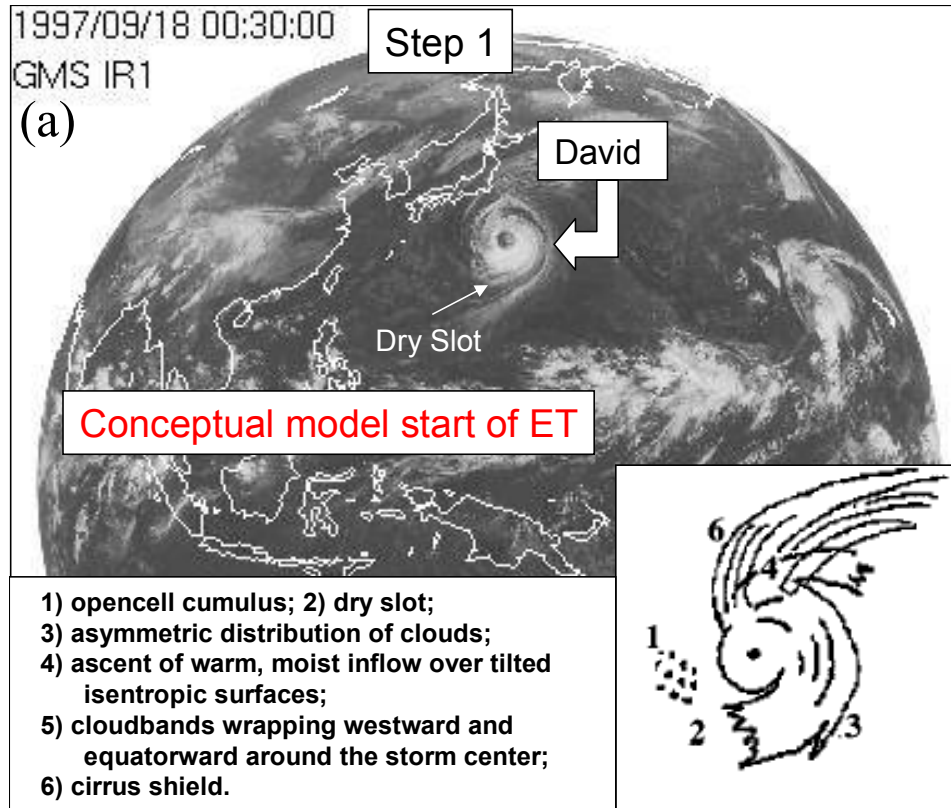


FIG. 24. Comparison of step 1 of Typhoon David. The IR image in a) is from C. of A. (2003) with part of the conceptual model of Klein et al. (2000) inset and described. The phase space diagrams b) and c) come from Hart's (2003b) webpage (the diagrams are shown on the next page with arrows added for clarification).

Fig. 25a shows the dry slot growing larger in the southern quadrant for the classification of step 2 of Typhoon David's transformation stage (as determined by Klein et al. 2000) with cloudbands wrapping equatorward on the western side. A cirrus edge is also visible indicating confluence with the polar jet. Fig. 25b displays Hart's phase space diagram which demonstrates the beginning of Typhoon David's transition into an extratropical cyclone when B exceeds 10 m by 0000 UTC 19 September. The cyclone's hybridization (having characteristics of both tropical and extratropical cyclones) is manifest in Fig. 25c as $-V_T^U$ first becomes negative.

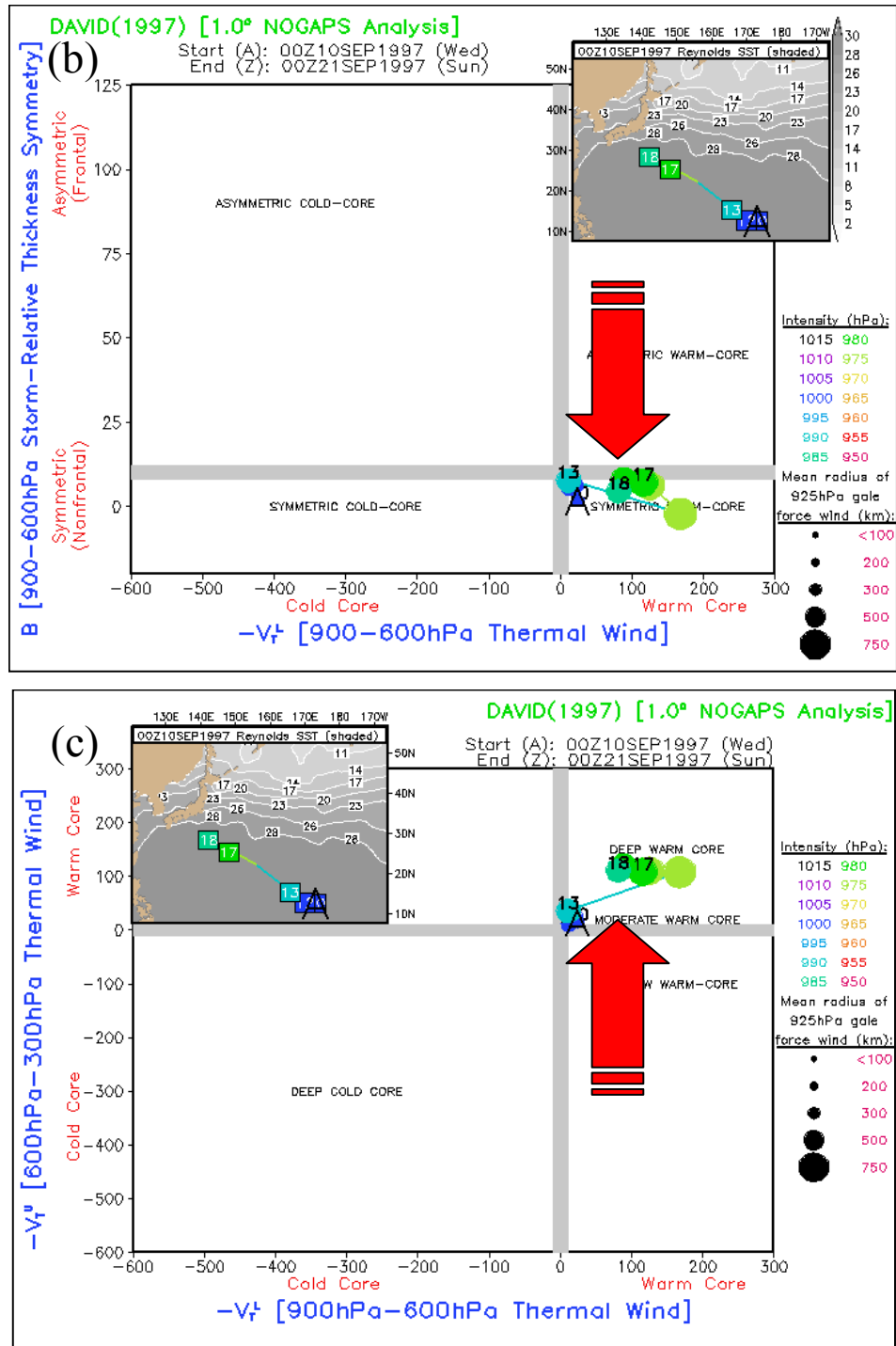


FIG. 24. Continued.

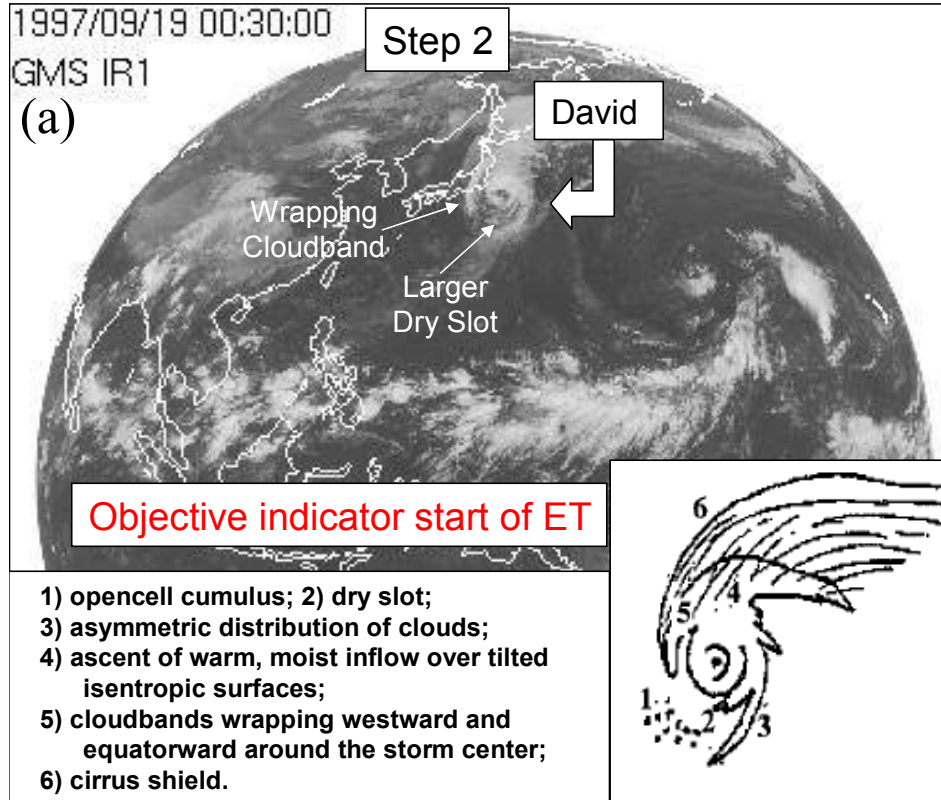


FIG. 25. Comparison of step 2 of Typhoon David. The IR image in a) is from C. of A. (2003) with part of the conceptual model of Klein et al. (2000) inset and described. The phase space diagrams b) and c) come from Hart's (2003b) webpage (the diagrams are shown on the next page with arrows added for clarification).

Both models agree that the end of transition time for Typhoon David is 1200 UTC 19 September as shown in Fig. 26. The third step of the transformation stage (which corresponds to Hart's definition of ET completion) is illustrated in Fig. 26a as the cyclone begins to look more frontal in nature with the eyewall eroding and the cirrus edge becoming sharper. Hart's OIs agree that ET has occurred; Figs. 26b and 26c illustrate that Typhoon David has converted to an asymmetric (and deep) cold-core system as $-V_r^L$ is negative in both phase space diagrams.

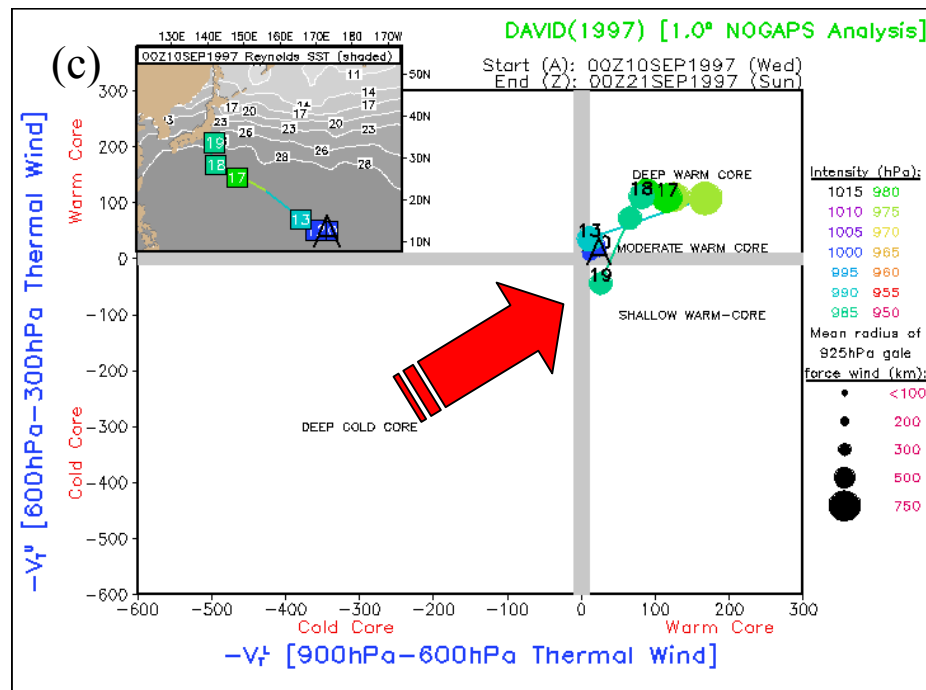
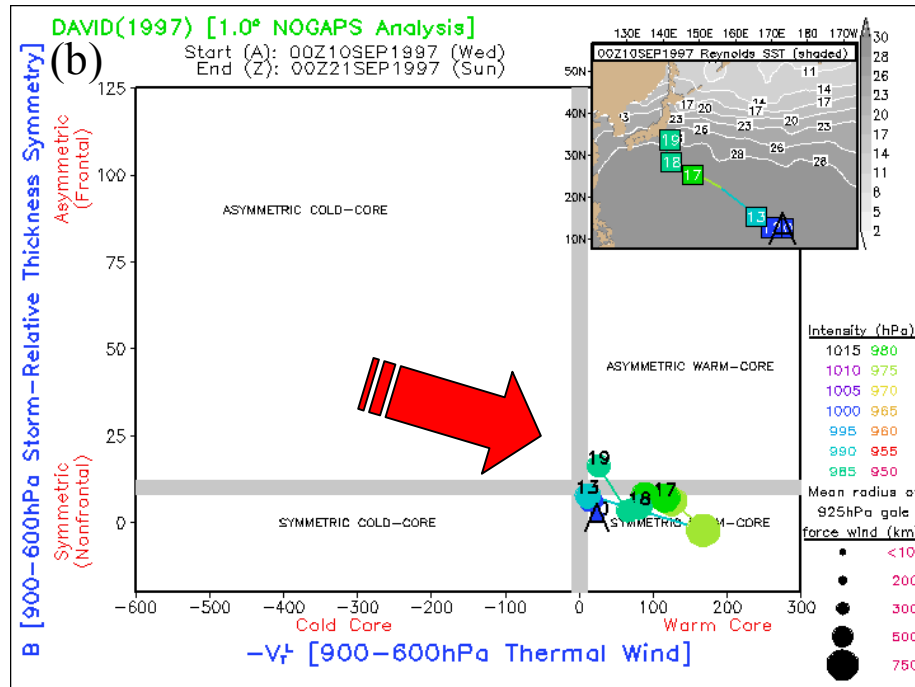


FIG. 25. Continued.

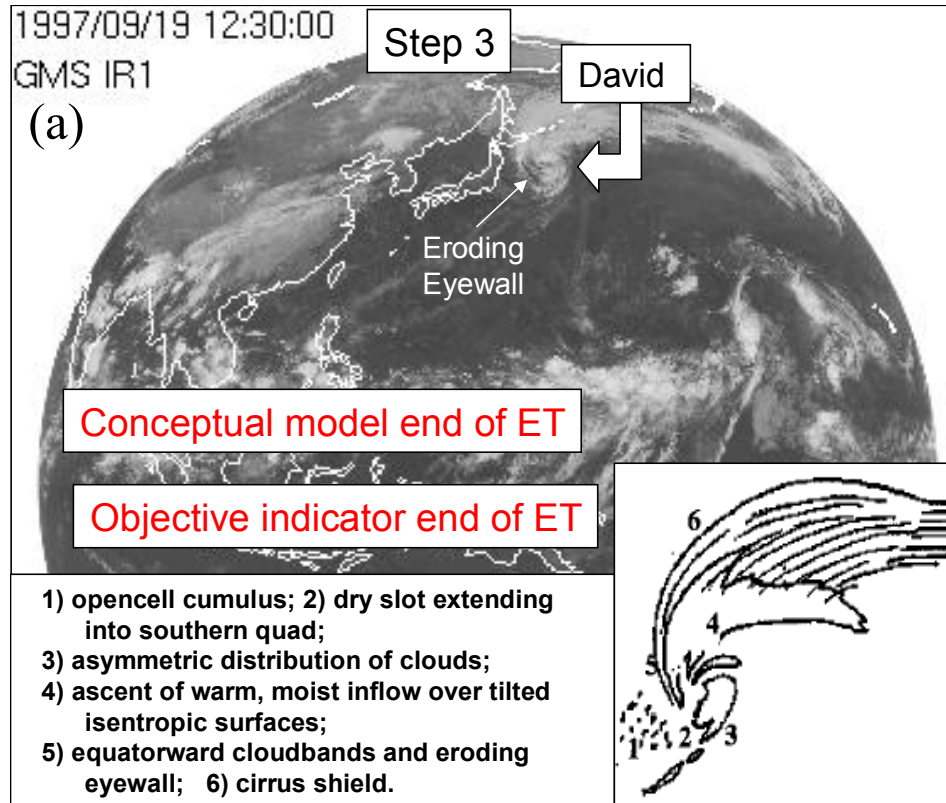


FIG. 26. Comparison of step 3 of Typhoon David. The IR image in a) is from C. of A. (2003) with part of the conceptual model of Klein et al. (2000) inset and described. The phase space diagrams b) and c) come from Hart's (2003b) webpage (the diagrams are shown on the next page with arrows added for clarification).

Even though the conceptual model and the OIs didn't produce the exact same results for Typhoon David, a number of interesting items were identified. First off, David followed the "conventional path" of ETTCs (described in section 3b) with the top-down transition (occurring in the upper troposphere first and then working downward later) typical of TCs interacting with approaching troughs. Second, the OIs did a great job illustrating the reintensification stage of Typhoon David (as discussed by Klein et al. 2000) in Figs. 27a and 27b. Finally, David differed from conventional ETTCs because it didn't stay in quadrant I of the \mathbf{B} vs $-V_T^L$ phase space diagram for more than 24 hours.

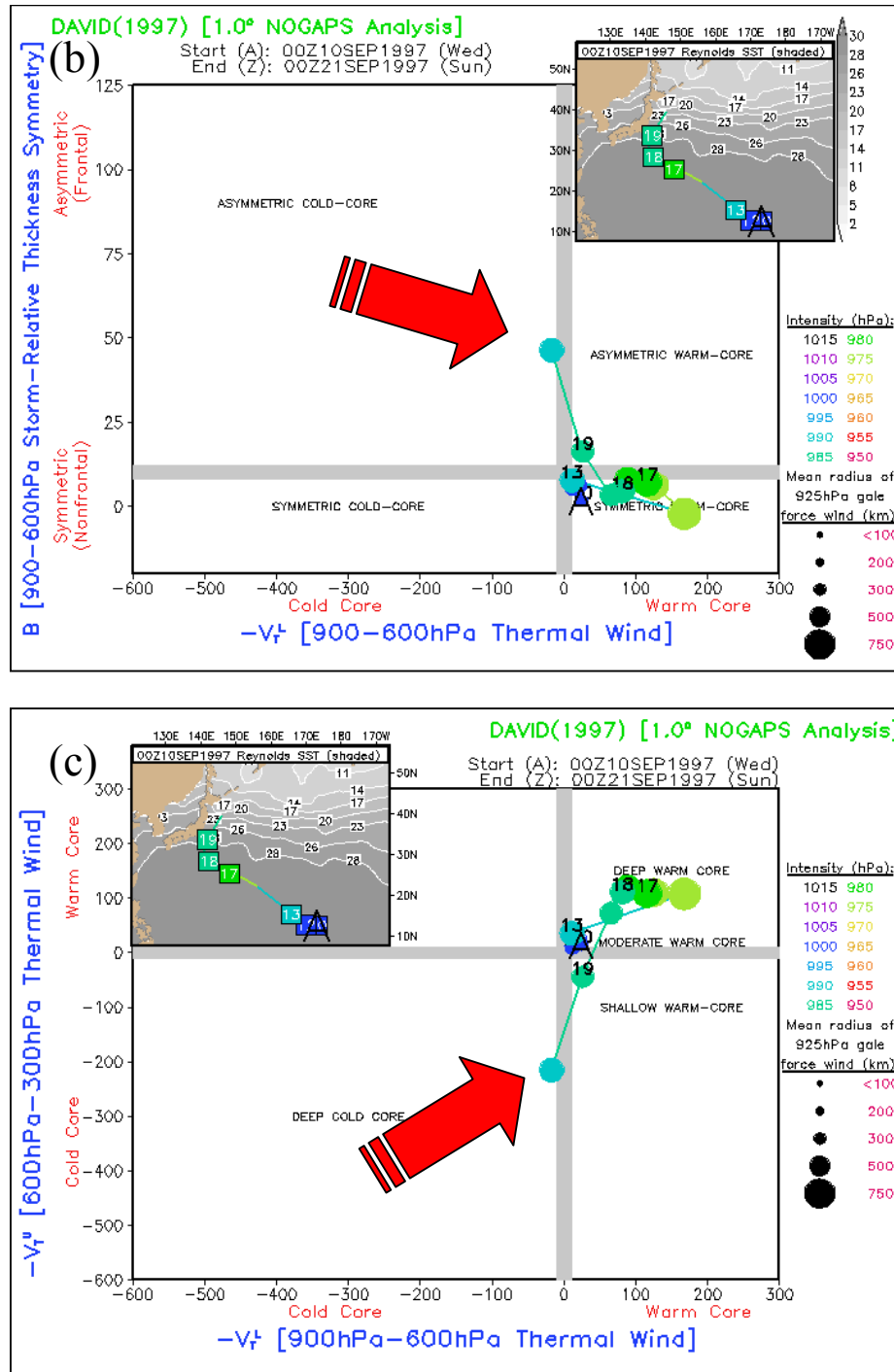


FIG. 26. Continued.

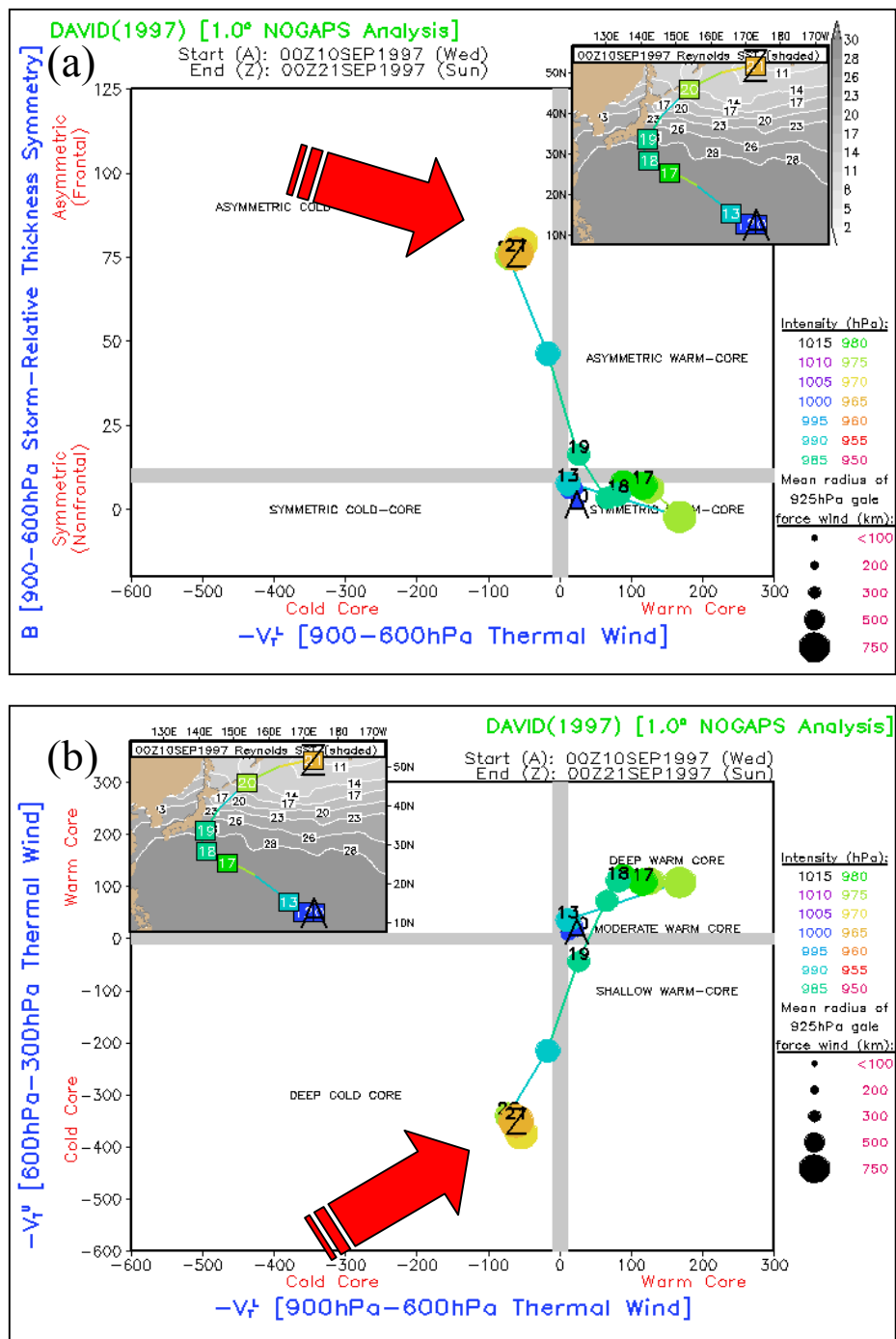


FIG. 27. Reintensification stage of Typhoon David. The phase space diagrams a) and b) come from Hart's (2003b) webpage (with arrows added for clarification).

2) SUPER TYPHOON JOAN

Since Hart's OI output didn't match the conceptual model of Typhoon David very well, the author selected one of the 12 storms that was a "perfect" match meaning that the output from both models was almost identical. More specifically, the analysis of Super Typhoon Joan provided the same ET start time, the same start time SLP, the same duration of ET, and similar end time SLPs for both theories (step 1 shown in Fig. 28). The IR satellite imagery of Joan at the start of ET (Fig. 28a) highlights the asymmetric

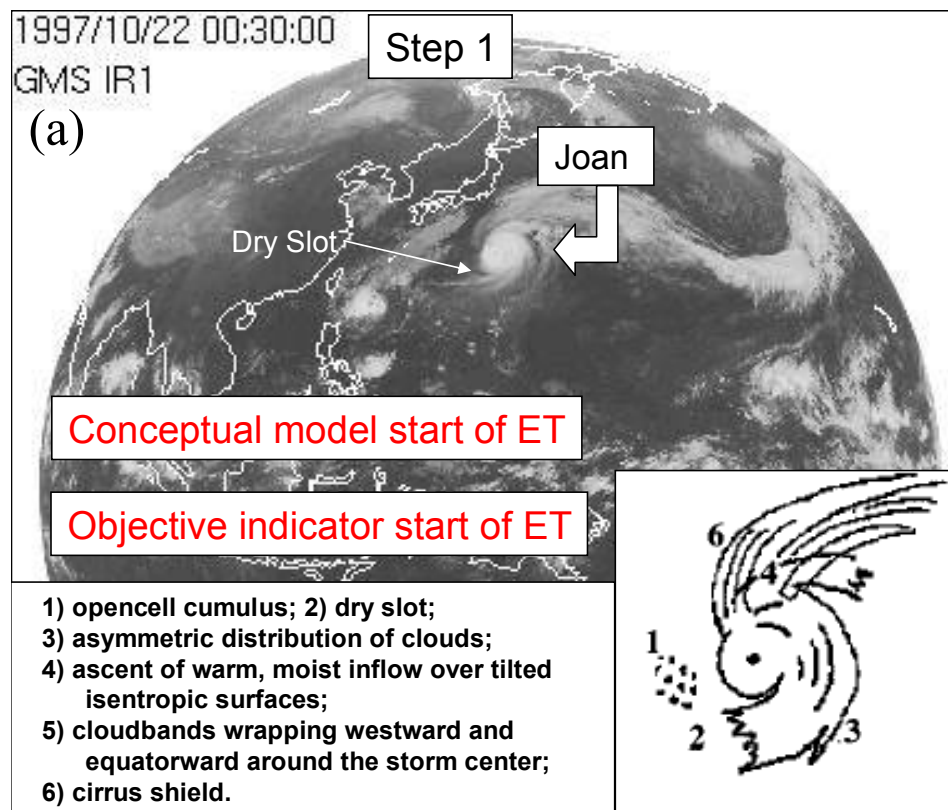


FIG. 28. Comparison of step 1 of Typhoon Joan. The IR image in a) is from C. of A. (2003) with part of the conceptual model of Klein et al. (2000) inset and described. The phase space diagrams b) and c) come from Hart's (2003b) webpage (the diagrams are shown on the next page with arrows added for clarification).

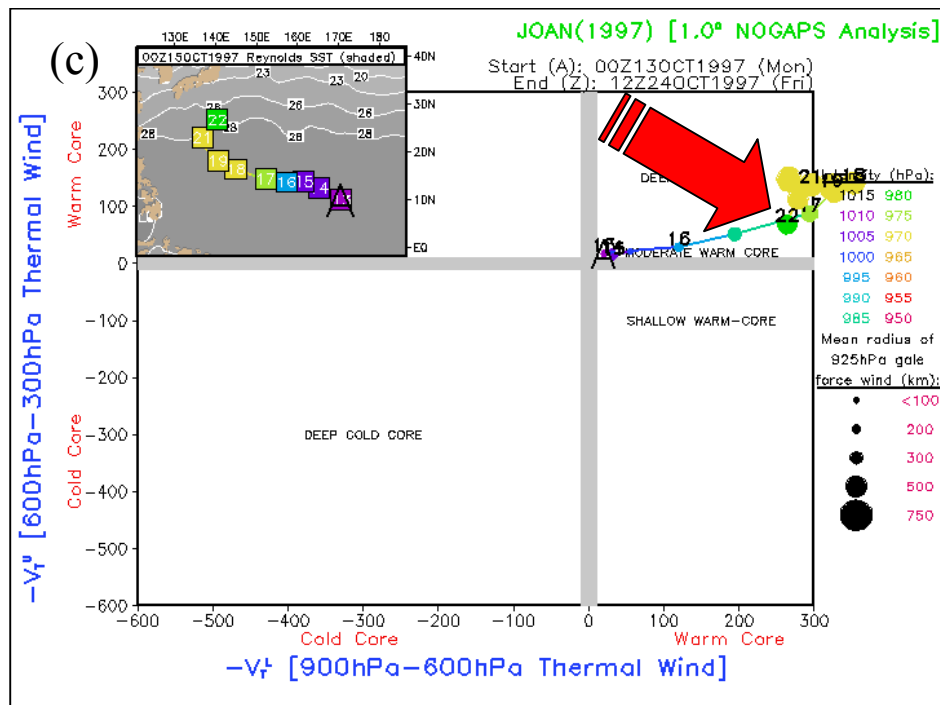
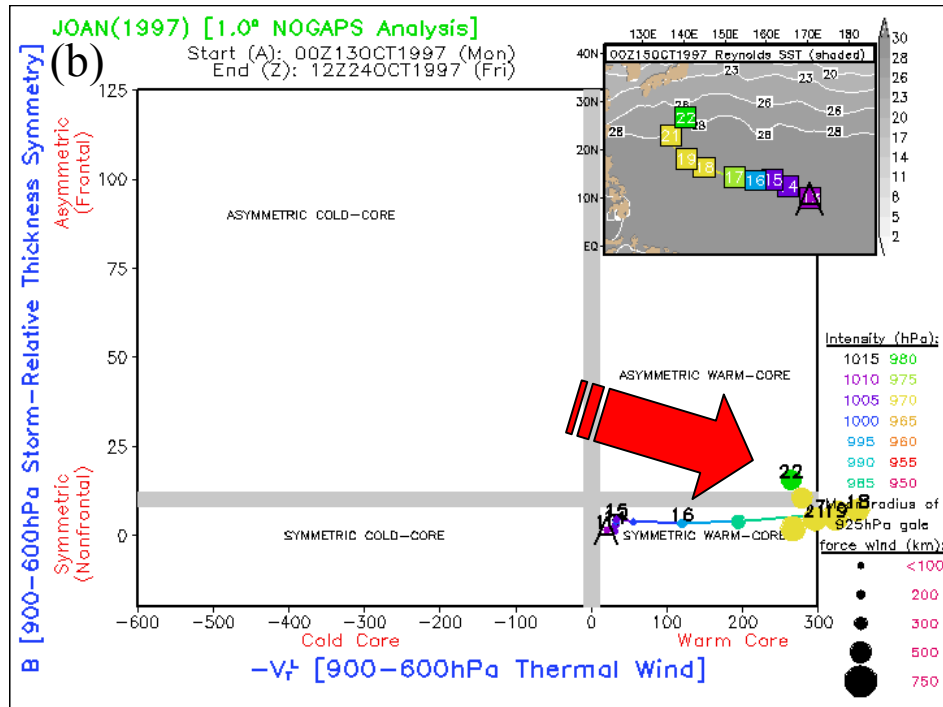


FIG. 28. Continued.

appearance of the clouds resulting from lack of convection in the western quadrant. Notice that even though ET has commenced in Fig. 28b, the TC is still considered a deep warm-core system (Fig. 28c) that hasn't yet started its top-down transition.

Since Klein et al. (2000) didn't specify step 2 for Typhoon Joan and since she was in quadrant I of the \mathbf{B} vs $-V_T^L$ phase space diagram for such a long time, the author designated a time near the middle of the 60 hour ET duration to portray step 2 (1230 UTC 23 October). Decreased cloudiness in Joan's southern quadrant and a sharper edge to her cirrus shield, represented in Fig. 29a, are evidence of her change to step 2 of the conceptual model. The accompanying phase space diagrams (Figs. 29b and 29c) correspond to the closest IR satellite image time and help substantiate Joan's slow transition.

Lastly, the agreement by both models on the end-time of ET is made apparent in Fig. 30 with a) exposing the third step of the conceptual model through satellite analysis, b) indicating the end of ET as $-V_T^L$ becomes negative, and c) indicating that the TC is now considered cold-core throughout the entire atmosphere (as $-V_T^L$ is also negative).

While the IR satellite imagery provided (Fig. 30a) doesn't agree very well with the features specified in the conceptual model, 1200 UTC 24 October was declared the end of ET by Klein et al. (2000). Notwithstanding the conceptual model disparities, Figs. 30b and 30c establish that Joan stayed in quadrant I of the \mathbf{B} vs $-V_T^L$ phase space for more than 48 hours making it a "more conventional" ETTC than Typhoon David.

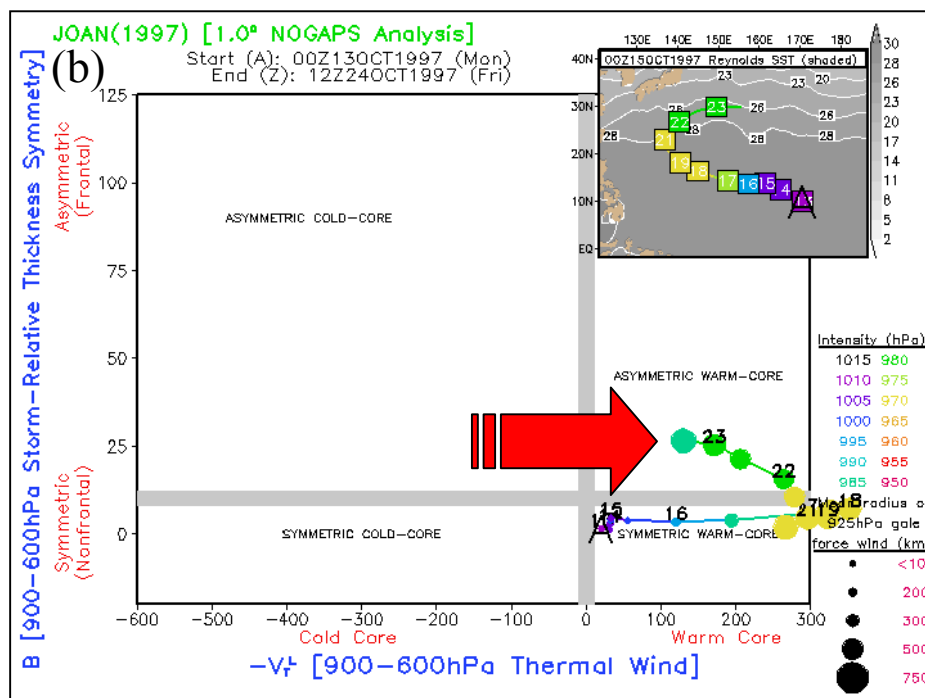
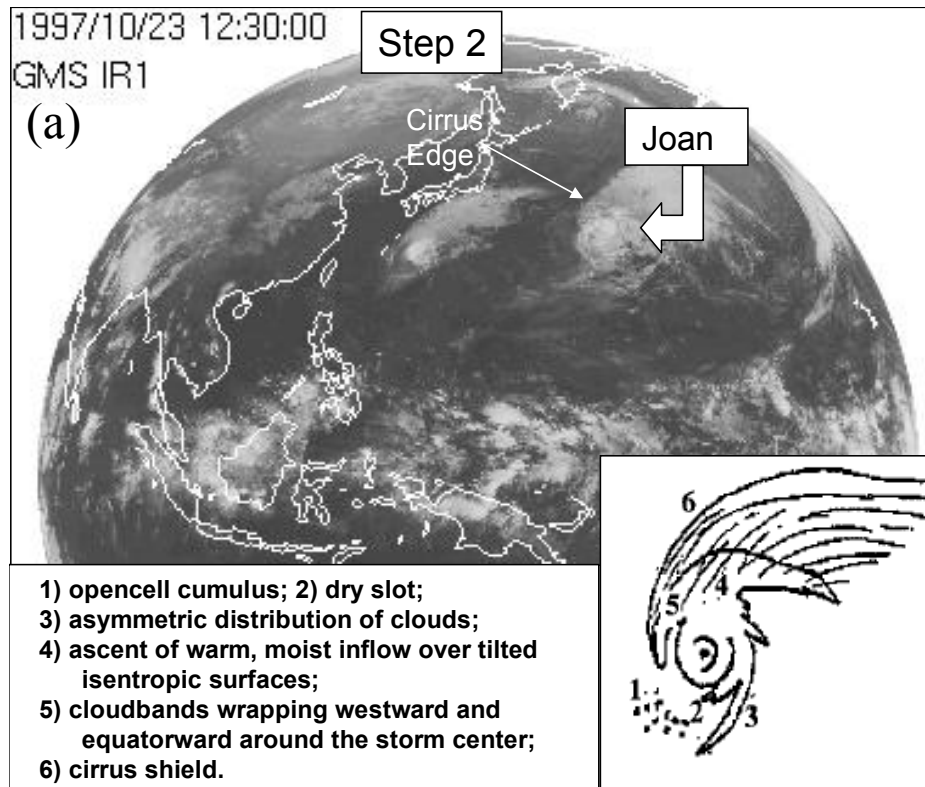


FIG. 29. Comparison of step 2 of Typhoon Joan. The IR image in a) is from C. of A. (2003) with part of the conceptual model of Klein et al. (2000) inset and described. The phase space diagram b) comes from Hart's (2003b) webpage (c is on next page with arrow added for clarification).

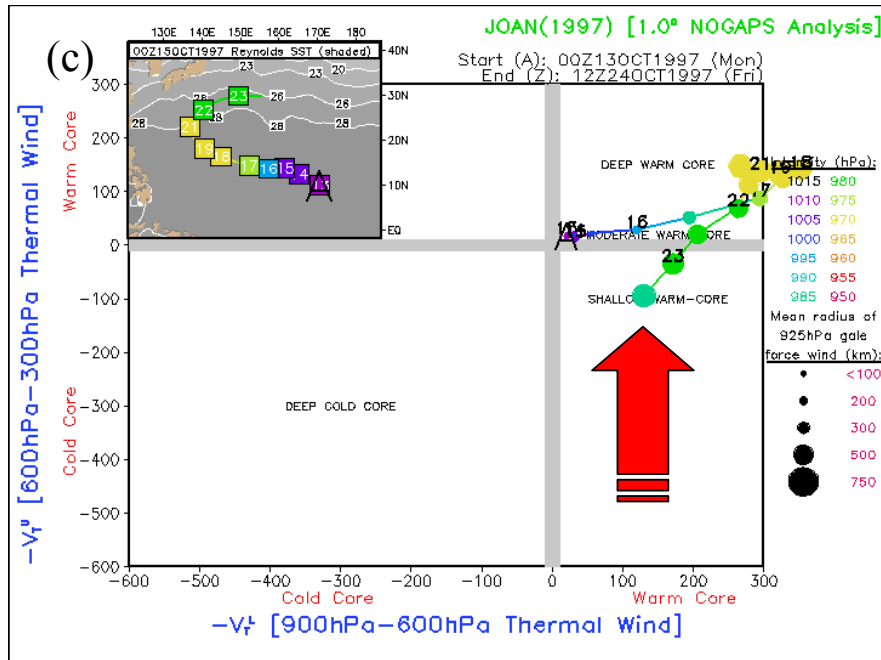


FIG. 29. Continued.

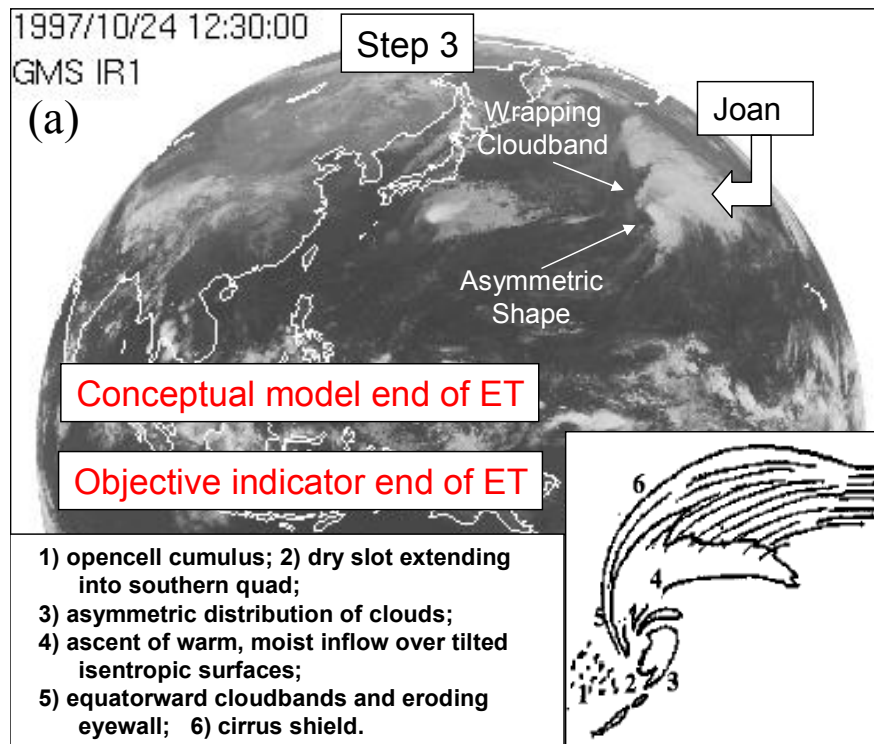


FIG. 30. Comparison of step 3 of Typhoon Joan. The IR image in a) is from C. of A. (2003) with part of the conceptual model of Klein et al. (2000) inset and described. The phase space diagrams b) and c) come from Hart's (2003b) webpage (the diagrams are shown on the next page with arrows added for clarification).

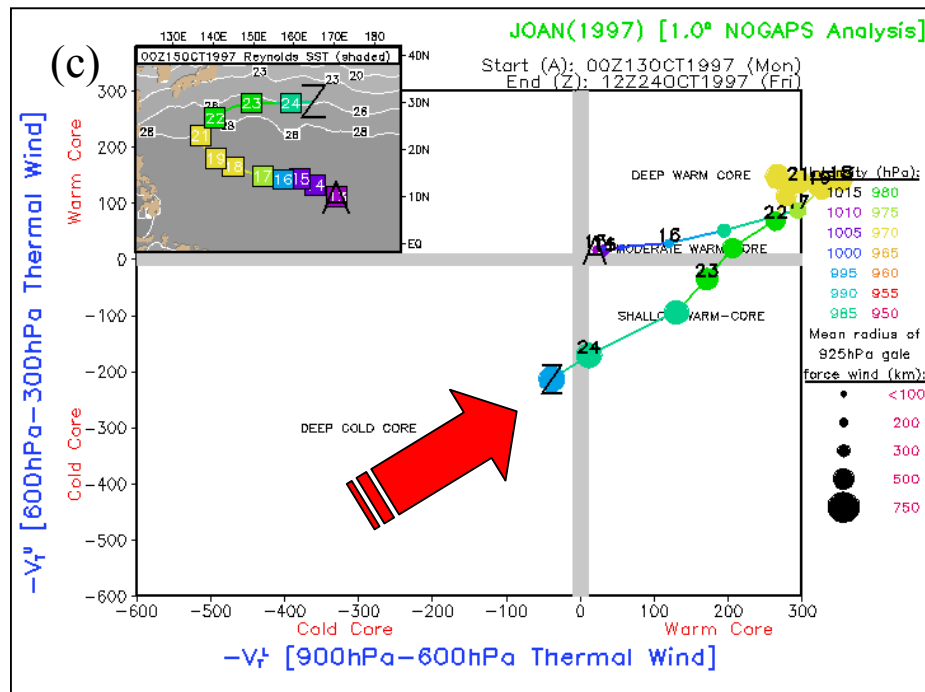
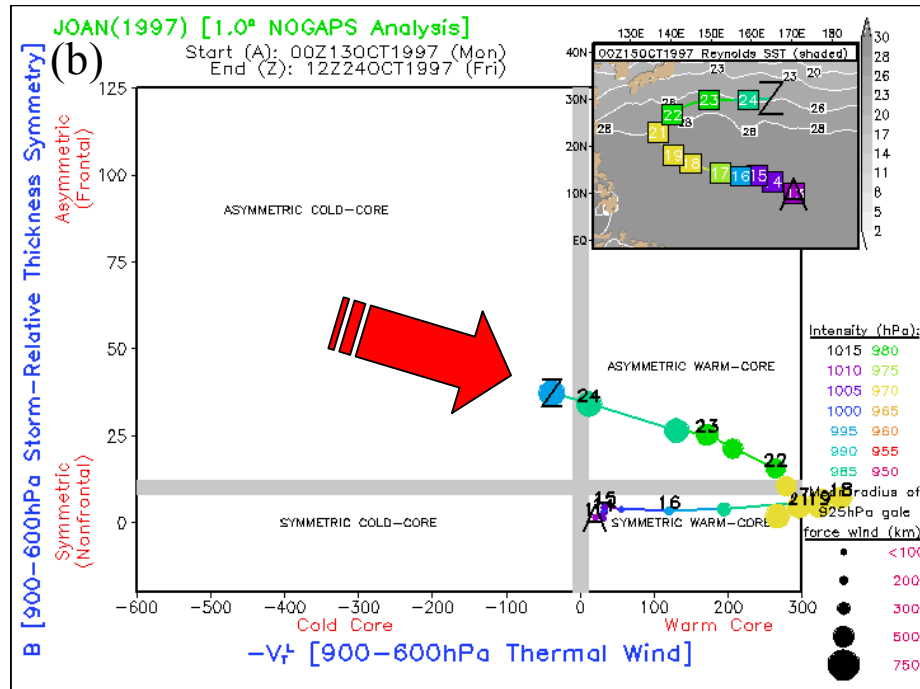


FIG. 30. Continued.

3) SUPER TYPHOON HALONG

The steps of ET of Typhoon Halong (July 2002) were difficult to forecast because the cloud shape stayed symmetrical throughout the majority of its life (P. Harr 2003, personal communication). Appendix B includes some of the high-resolution satellite data used by the author to analyze the three steps of ET using the conceptual model of Klein et al. (2000). From the author's analysis (part of which is shown in Fig. 31), ET was

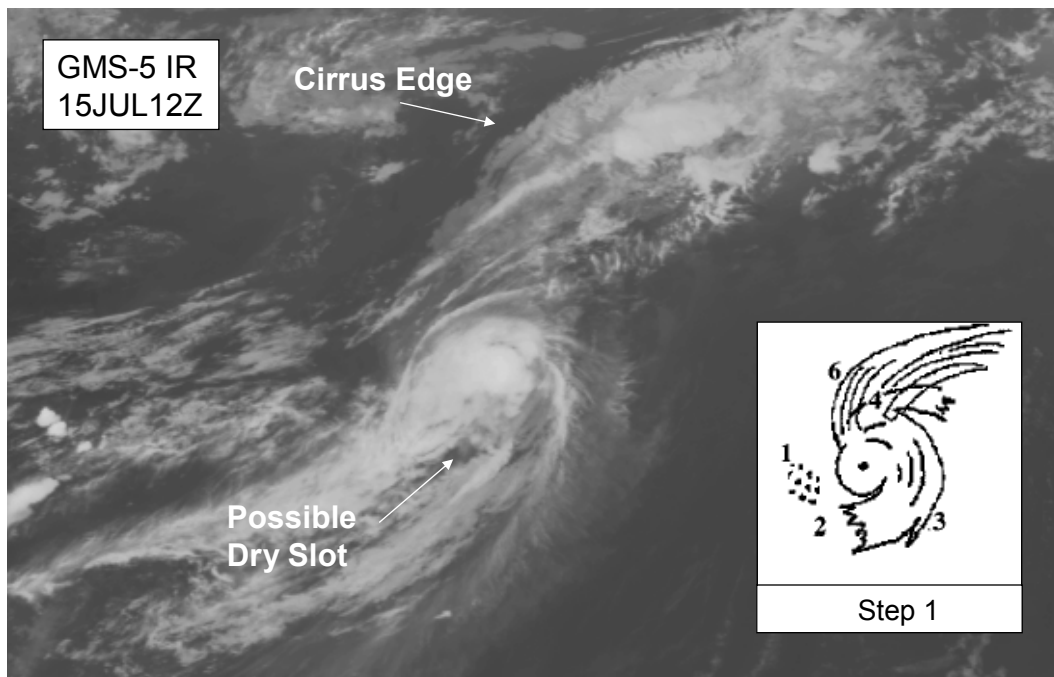


FIG. 31. High-resolution IR satellite image of Typhoon Halong on 15 July 2002 (UW-Madison 2003). Step 1 of the conceptual model of Klein et al. (2000) inset.

declared to commence at 1200 UTC 15 July 2002. Fig. 32a is a low-resolution IR satellite image of the same time showing Halong's location at the southern tip of Japan. Even though ET hasn't officially begun (Fig. 32b), the top down transition is beginning as the marker moves into quadrant IV (Fig. 32c).

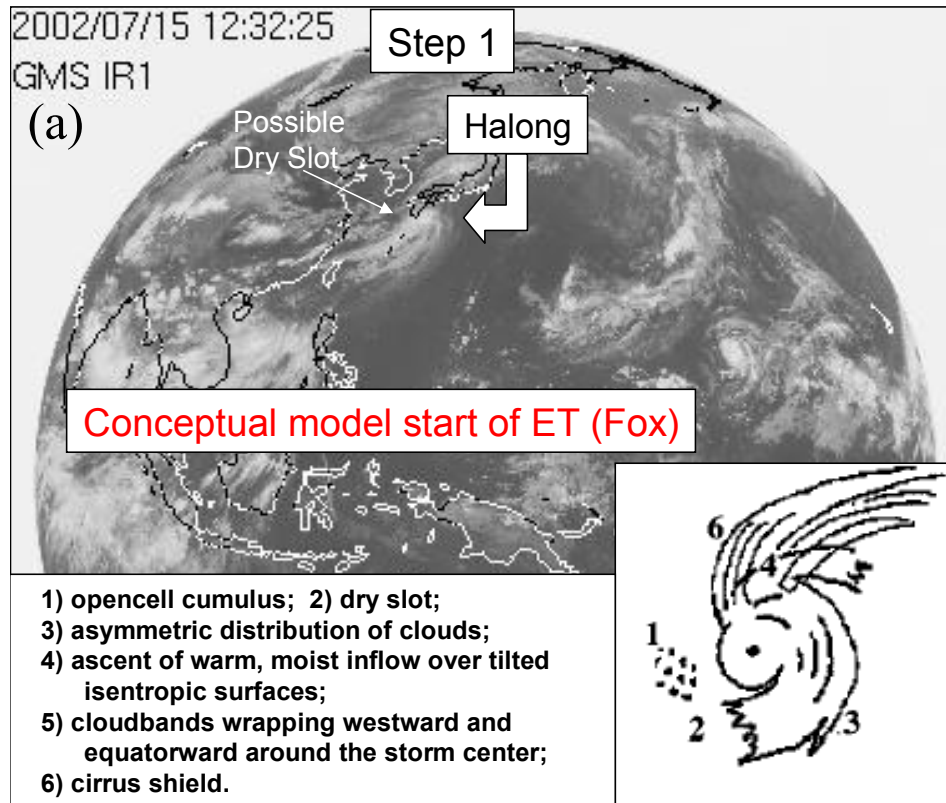


FIG. 32. Comparison of step 1 of Typhoon Halong. The IR image in a) is from C. of A. (2003) with part of the conceptual model of Klein et al. (2000) inset and described. The phase space diagrams b) and c) come from Hart's (2003b) webpage (the diagrams are shown on the next page with arrows added for clarification).

Step 2 of the conceptual model (as defined by the author and portrayed in Fig. 33a) corresponds with Hart's \mathbf{B} vs $-V_T^L$ phase space diagram (Fig. 33b) which shows that ET took less than 12 hours. As a result, ET was catalogued as having zero hours of duration making it difficult to forecast any steps of this quickly transitioning TC. Furthermore, forecasting the different steps of ET for Typhoon Halong using the conceptual model was made even more difficult because some of the early satellite imagery showed a tropical system that looked almost completely inverted (Fig. 34).

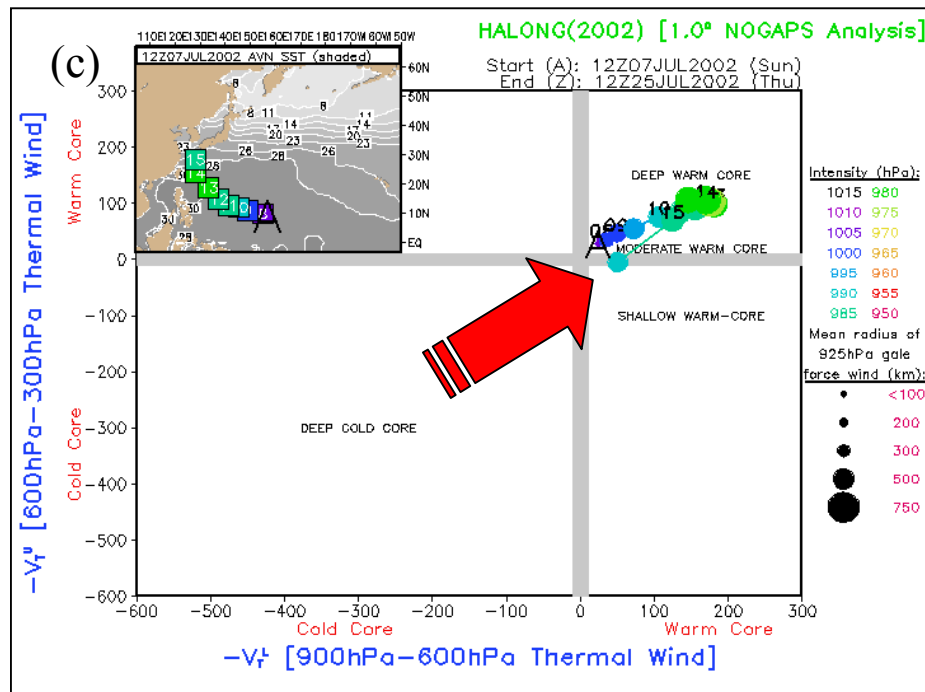
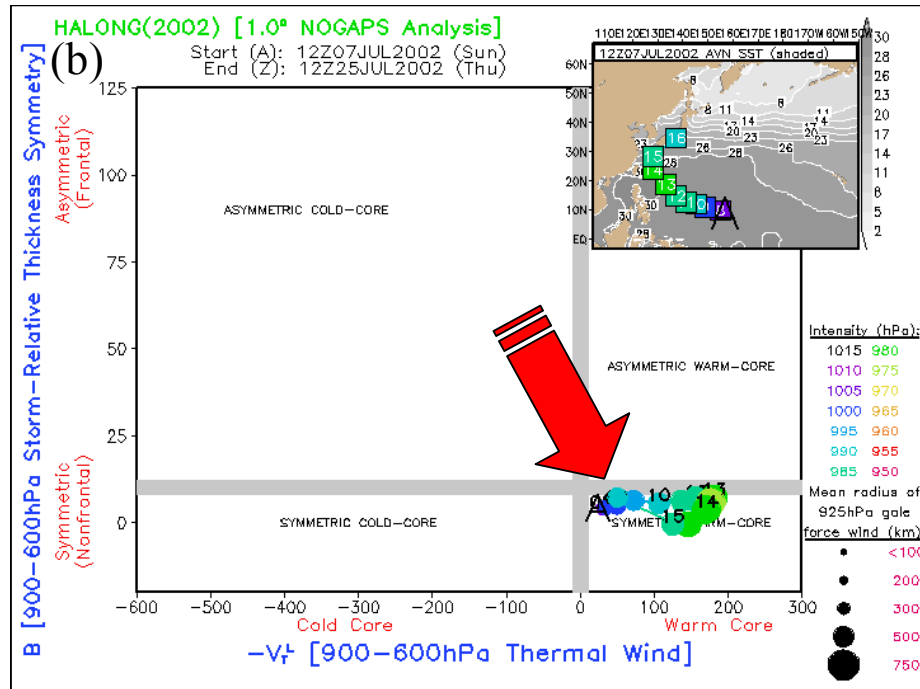


FIG. 32. Continued.

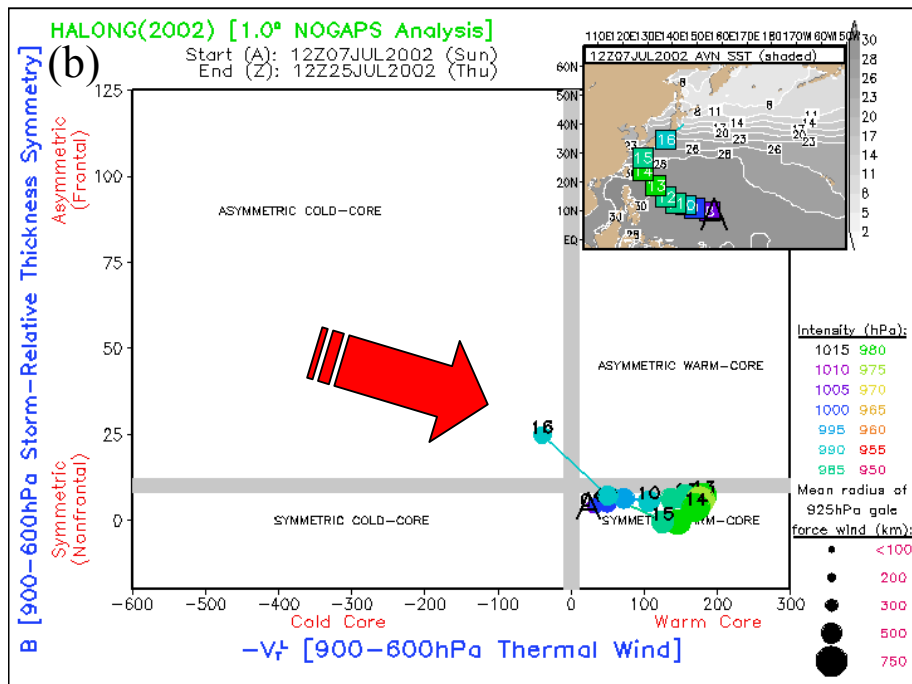
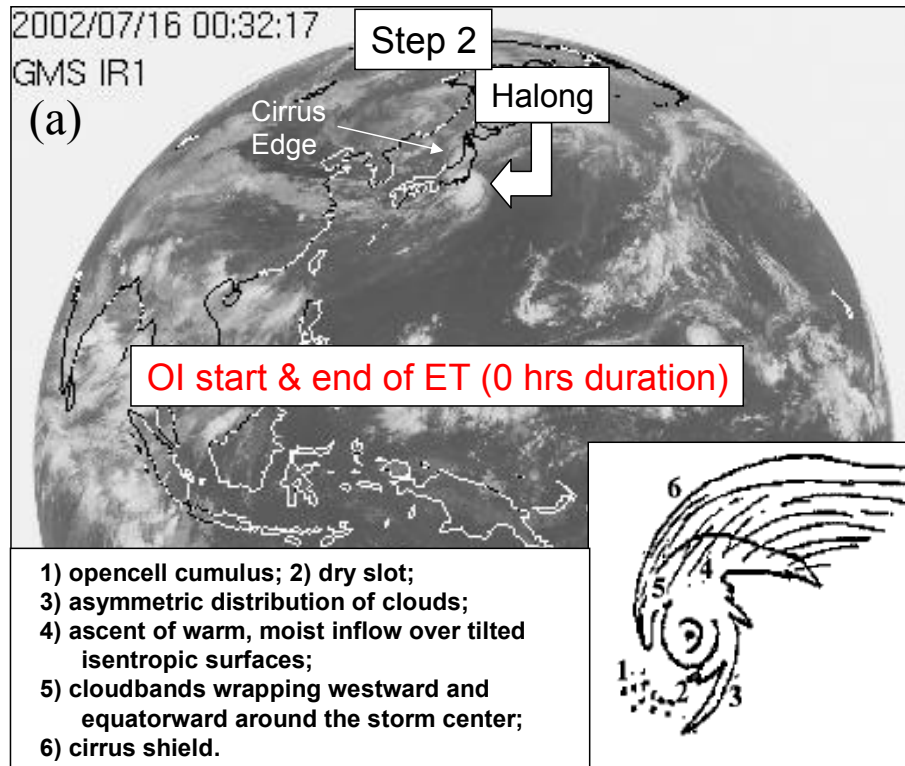
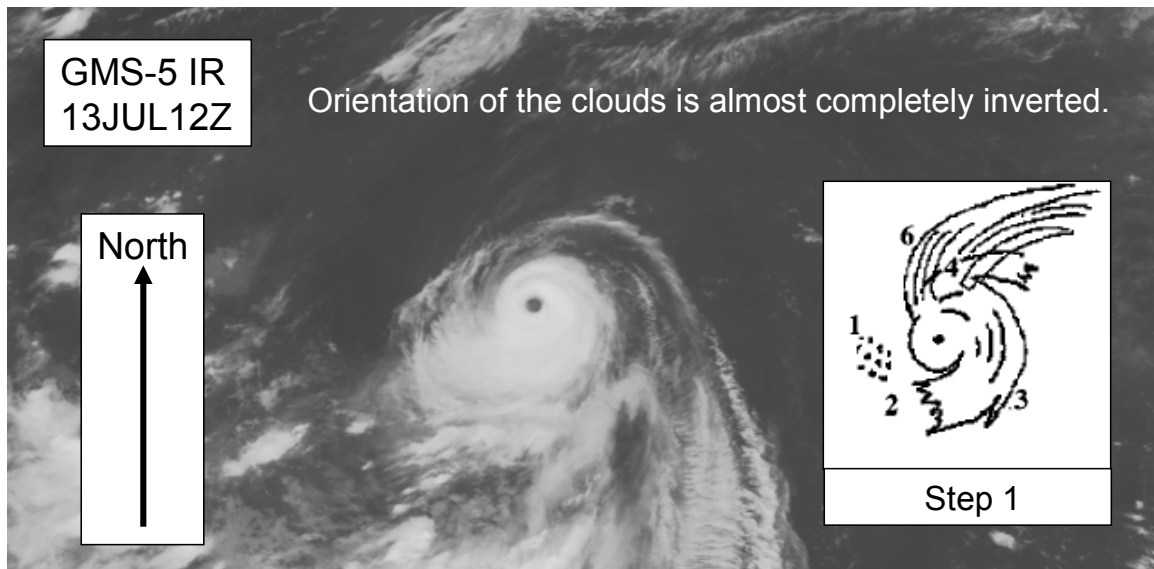
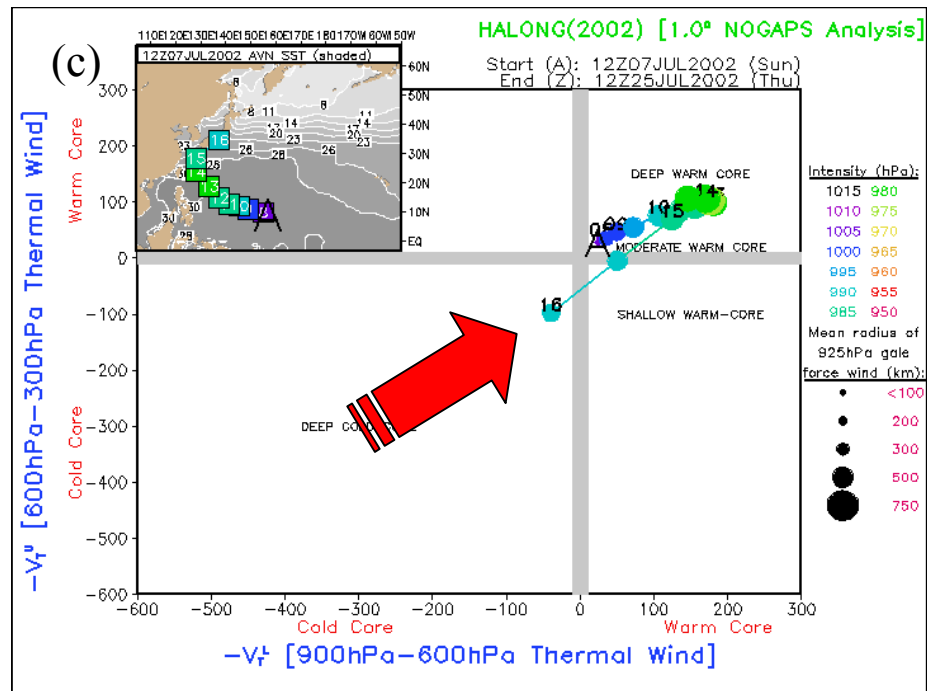


FIG. 33. Comparison of step 2 of Typhoon Halong. The IR image in a) is from C. of A. (2003) with part of the conceptual model of Klein et al. (2000) inset and described. The phase space diagram b) comes from Hart's (2003b) webpage (c is on next page with arrow for clarification).



The high-resolution IR satellite image (Fig. 35) provides indicators of the third step of the conceptual model; namely, the frontal appearance of the clouds, an increasingly large dry slot in the southern quadrant, and the obvious cirrus edge in the northern quadrant. In contrast, Halong's third step of transformation is barely visible in the low-resolution IR satellite image (Fig. 36a), while Hart's phase space diagrams of the same time frame (Figs. 36b and 36c) don't show much more than a weakening deep cold-core system.

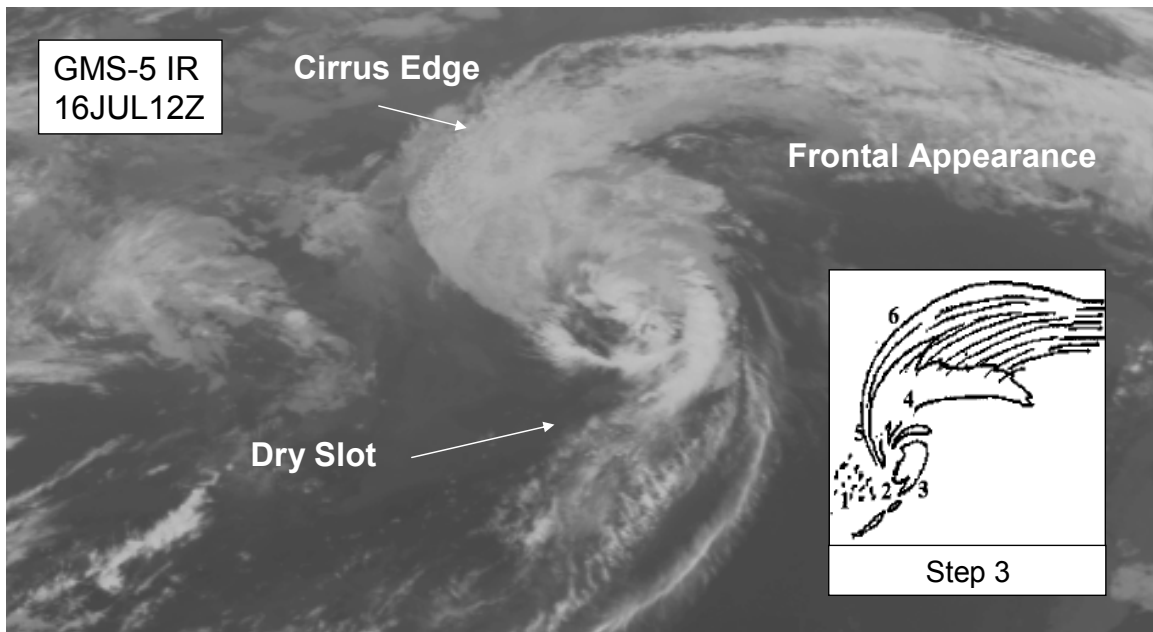


FIG. 35. High-resolution IR satellite image of Typhoon Halong on 16 July 2002 (UW-Madison 2003). Step 3 (inset) of the conceptual model of Klein et al. (2000).

Through the analysis of Typhoon Halong's ET, it's apparent that Hart's OIs provide a much easier, more specific, and certainly less subjective, method of defining the beginning and end of ET.

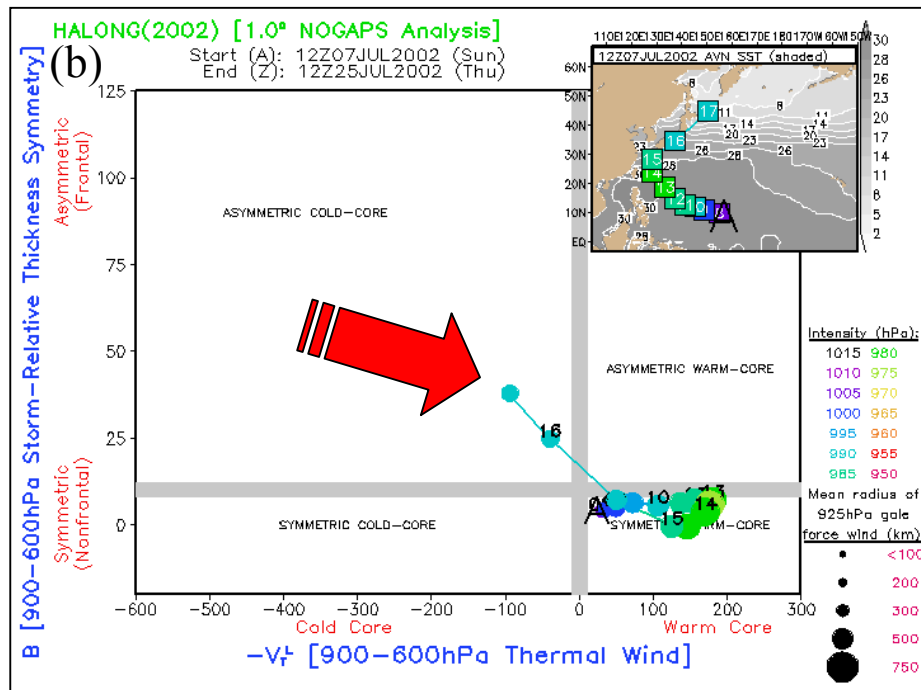
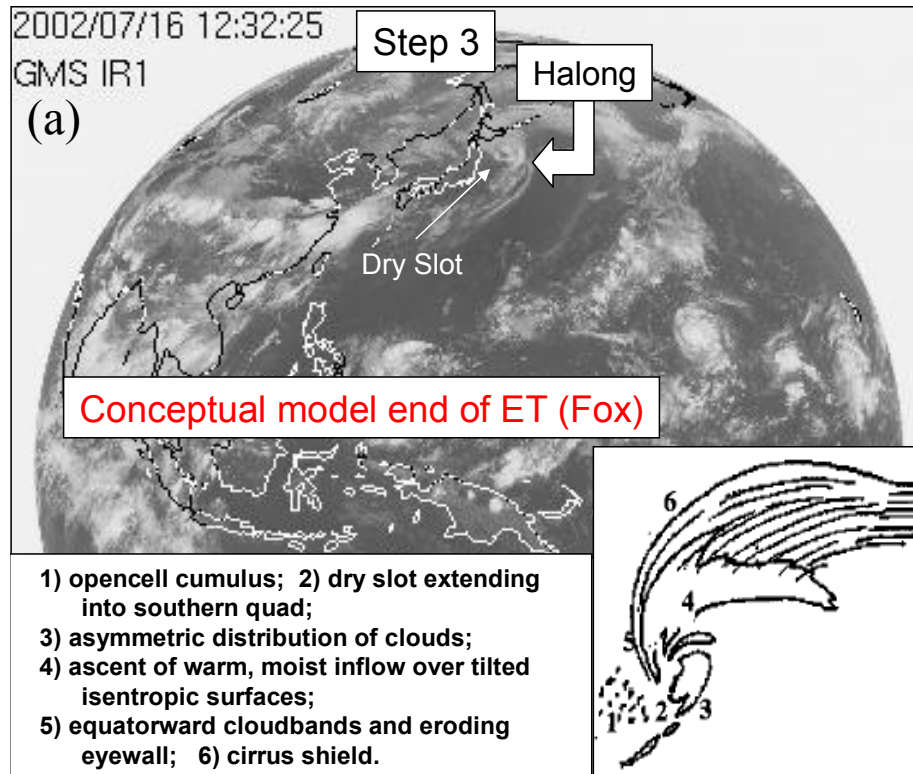


FIG. 36. Comparison of step 3 of Typhoon Halong. The IR image in a) is from C. of A. (2003) with part of the conceptual model of Klein et al. (2000) inset and described. The phase space diagram b) comes from Hart's (2003b) webpage (c is on next page with arrow for clarification).

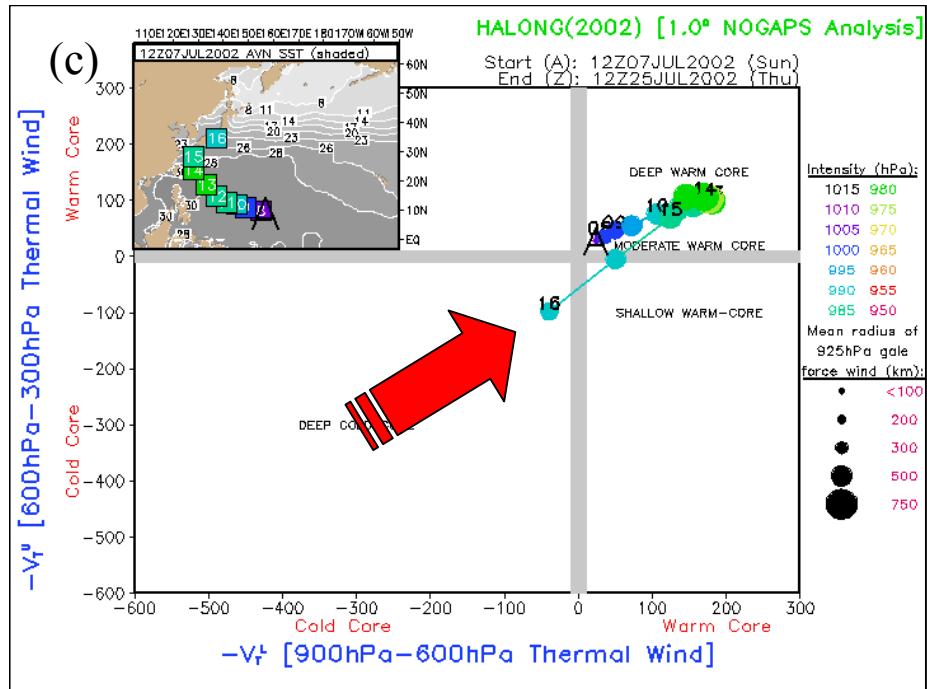


FIG. 36. Continued.

5. Conclusions and Recommendations

a. Conclusions

The primary purpose of this study is to provide guidance for JTWC forecasters to use in differentiating between the stages of ET. Hart (2003a) created OIs that define the beginning and end of ET which correspond well with definitions describing the beginning and end of the transformation stage of the conceptual model proposed by Klein et al. (2000). This research compares these definitions using data from 12 TCs in the western North Pacific. Hart's OIs, which discern the start and stop of ET, are also demonstrated providing a way to reduce the negative impacts of incorrect TC forecasting.

The objectives listed in the introduction were more than sufficient and extremely beneficial in comparing the results of the conceptual model with the results of Hart's OIs. Additionally, the statistical tests were successful in revealing that the two theories could be considered equal which alluded to the value of further research. The three case studies were useful in pointing out differences between the two theories allowing the author to suggest areas of strength and/or weakness in each of the theories.

The results provide evidence that the output from Hart's OI program corresponds well with the definition of the transformation stage of the conceptual model. Nevertheless, the OI results are much more objective than the satellite analysis required for the conceptual model. As a matter of fact, the author proposes that if one were to give five different forecasters the same satellite images and then ask them to individually define the beginning and end of ET using the conceptual model alone, they would not

agree on the same times. On the other hand, if one were to give the same five forecasters output from Hart's OI program and then ask them to define the beginning and end of ET, there would be little room for disagreement.

Since Hart's OI program ingests numerical forecast data as well as numerical analysis data, it can easily be used to forecast specific ET start and stop times, an option not possible with the subjective satellite analysis of the conceptual model. Therefore, the overall conclusion of this thesis is that JTWC forecasters should employ Hart's OI program to differentiate between the stages of ET (of both past and future TCs). Hart's OI program not only gives them the capability of providing a forecast time for the completion of ET (which would help them coordinate the hand off of forecasting, tracking, and warning responsibilities), but also gives them a specific synoptic time of ET completion once it has occurred.

It should be noted, however, that even though Hart's OIs are so advantageous, Klein's conceptual model still has an enormous amount of merit. It is extremely helpful in understanding the three-dimensional characteristics of ET and very useful in verifying and/or validating the models used to produce Hart's OIs.

b. Recommendations

ET is truly an interesting and important topic, but the meteorological community still has a long way to go before ET is fully understood. To further improve the forecasting and global understanding of ET, the following recommendations are offered for JTWC (and other interested meteorologists):

1. When using Hart's OIs, utilize the now available six hourly numerical data increments (instead of the 12 hourly data increments used in this research) thereby providing better OI resolution and forecast accuracy.
2. When using Hart's OIs, utilize the "consensus mean and forecast envelope" phase space diagram (comprised of three models) instead of focusing on output from just one specific model (Hart 2003b).
3. When using Hart's OIs, utilize Klein's conceptual model and satellite imagery to validate the accuracy of the model(s) being employed.
4. Define ET universally so that meteorologists around the world can compare ETTCs using the same "foundation" or "starting point." The following definition is recommended for adoption by the American Meteorological Society and the World Meteorological Organization:

"Extratropical transition (ET) occurs when a tropical cyclone (TC) changes from a warm-core vortex to a cold-core vortex which typically happens when a TC encounters a synoptic disturbance in the mid-latitudes and then transitions into an extratropical cyclone. Objective tools which describe the thermal parameters of the atmosphere can be used to define the beginning and end of ET. Satellite analysis can also be used to ascertain the beginning and end of ET as the TC's cloud shape becomes more and more asymmetrical."

Appendix A: Acronyms

| | |
|--------|---|
| AFCCC | Air Force Combat Climatology Center |
| CISK | Convective Instability of the Second Kind |
| COAMPS | Coupled Ocean-Atmospheric Mesoscale Prediction System |
| ECMWF | European Centre for Medium-Range Weather Forecasts |
| ET | Extratropical Transition |
| ETC | Extratropical cyclogenesis |
| ETTC | Tropical cyclone that has undergone extratropical transition. |
| FNMOD | Fleet Numerical Meteorology and Oceanography Detachment |
| GrADS | Grid Analysis and Display System |
| GRIB | GRIdded Binary |
| GTCCA | Global Tropical Cyclone Climatic Atlas |
| IR | Infrared (as in satellite imagery) |
| ITCZ | Intertropical Convergence Zone |
| ITWC-V | Fifth WMO International Workshop on Tropical Cyclones |
| JTWC | Joint Typhoon Warning Center |
| NOGAPS | Navy Operational Global Atmospheric Prediction System |
| NOTC | A tropical cyclone that has had its remnants removed. |
| OI | Objective indicator |
| SLP | Sea level pressure |
| SSM/I | Special Sensor Microwave/Imager |
| TC | Tropical Cyclone |
| TUTT | Tropical Upper Tropospheric Trough |
| WISHE | Wind Induced Surface Heat Exchange |
| WMO | World Meteorological Organization |

Appendix B: Conceptual Model Analysis of Typhoon Halong

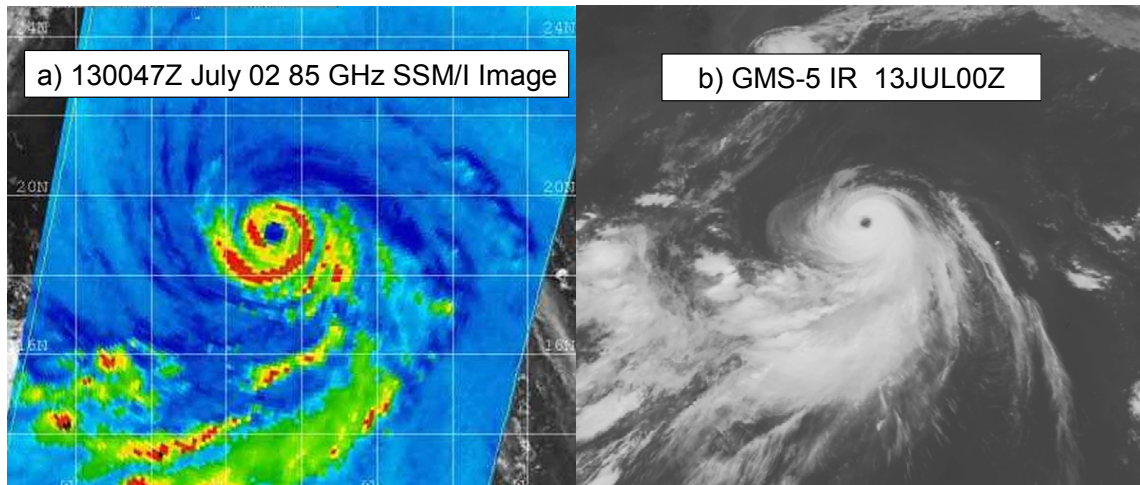


FIG. B1. a) SSM/I satellite image of Typhoon Halong at 0000 UTC on 13 July 2002 (USNPMOC/JTWC 2002) and b) high-resolution IR satellite imagery at the same time (UW-Madison 2003).

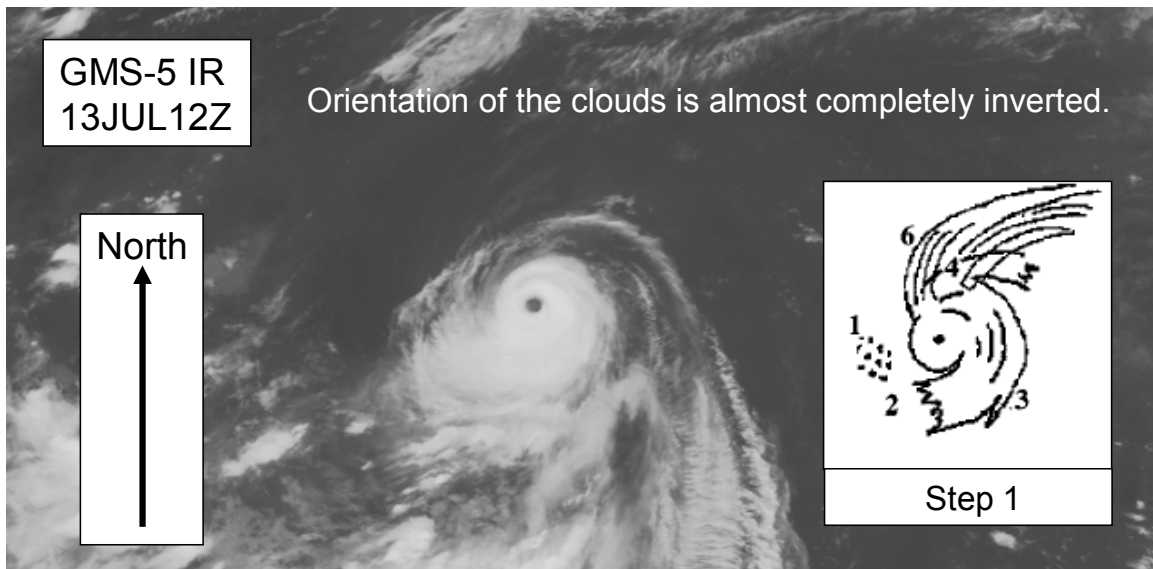


FIG. B2. High-resolution IR satellite image of Typhoon Halong at 1200 UTC on 13 July 2002 (UW-Madison 2003). Step 1 (inset) of the conceptual model of Klein et al. (2000).

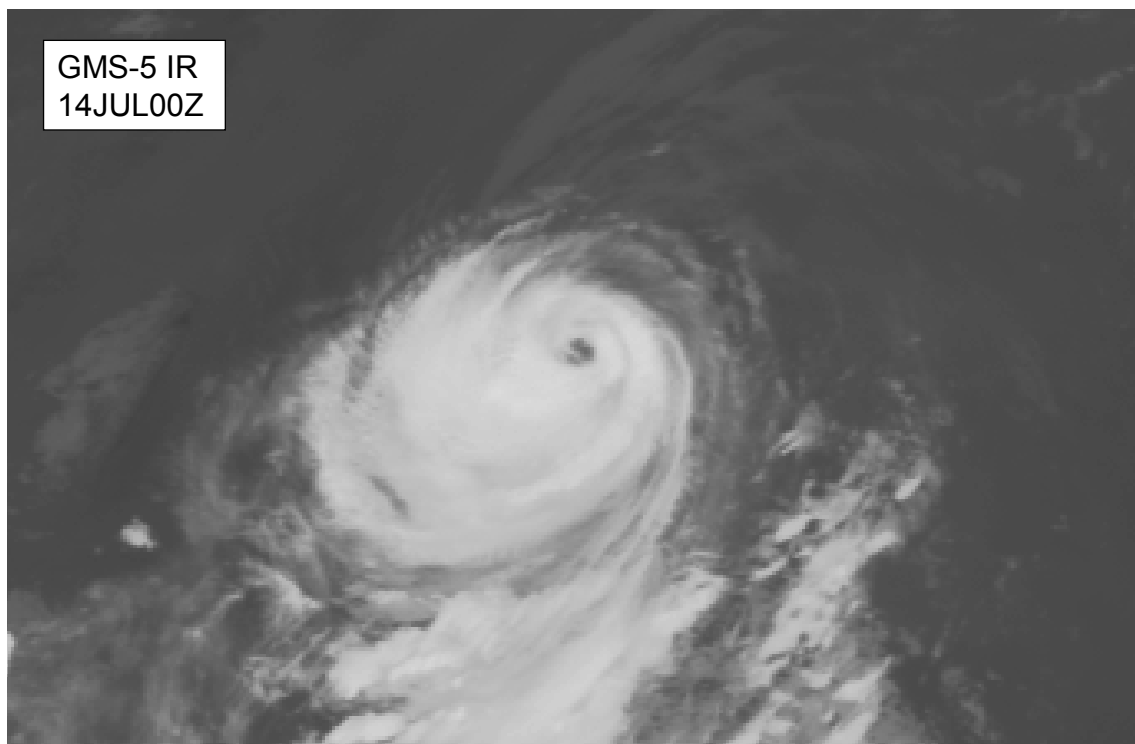


FIG. B3. High-resolution IR satellite image of Typhoon Halong at 0000 UTC on 14 July 2002 (UW-Madison 2003).

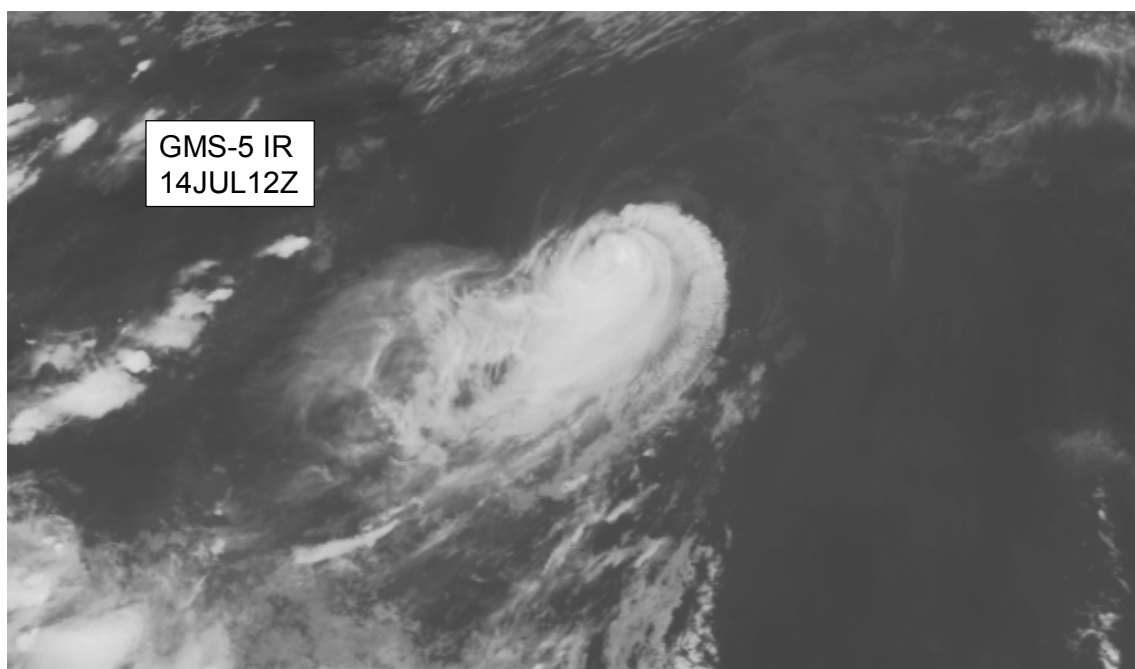


FIG. B4. High-resolution IR satellite image of Typhoon Halong at 1200 UTC on 14 July 2002 (UW-Madison 2003).

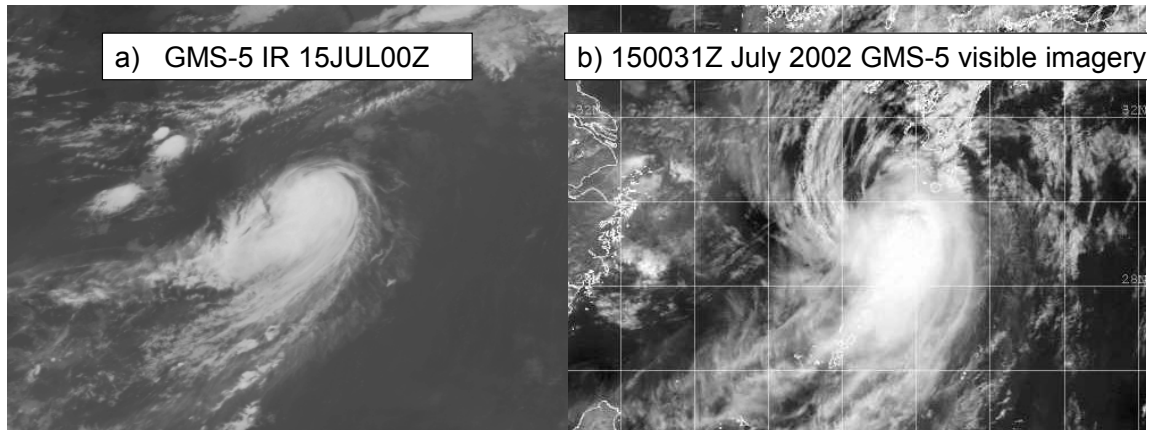


FIG. B5. a) High-resolution IR satellite image of Typhoon Halong at 0000 UTC on 15 July 2002 (UW-Madison 2003) and b) visible satellite imagery at the same time (USNPMOC/JTWC 2002).

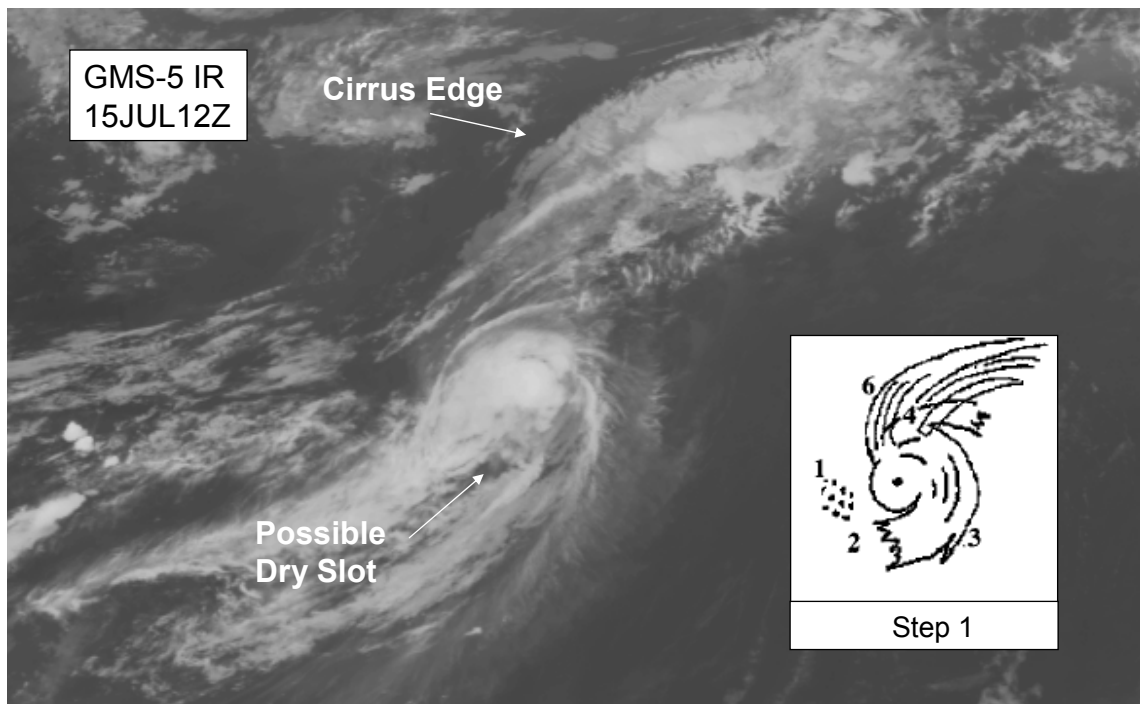


FIG. B6. High-resolution IR satellite image of Typhoon Halong at 1200 UTC on 15 July 2002 (UW-Madison 2003). Step 1 of the conceptual model of Klein et al. (2000) inset.

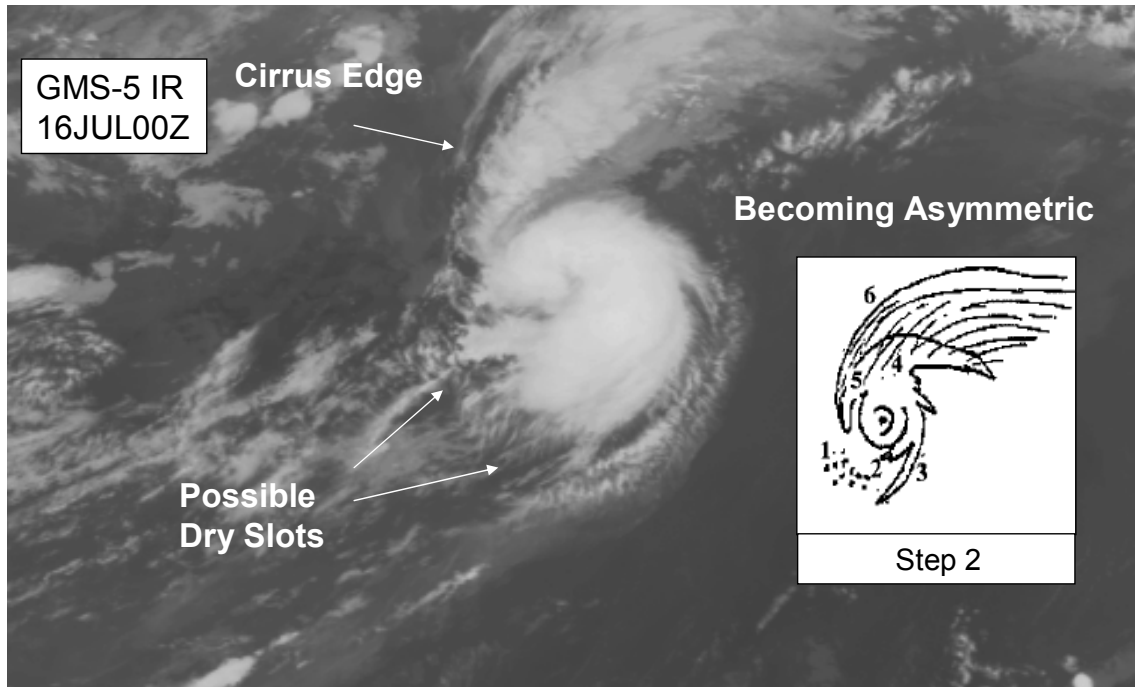


FIG. B7. High-resolution IR satellite image of Typhoon Halong at 0000 UTC on 16 July 2002 (UW-Madison 2003). Step 2 of the conceptual model of Klein et al. (2000) inset.

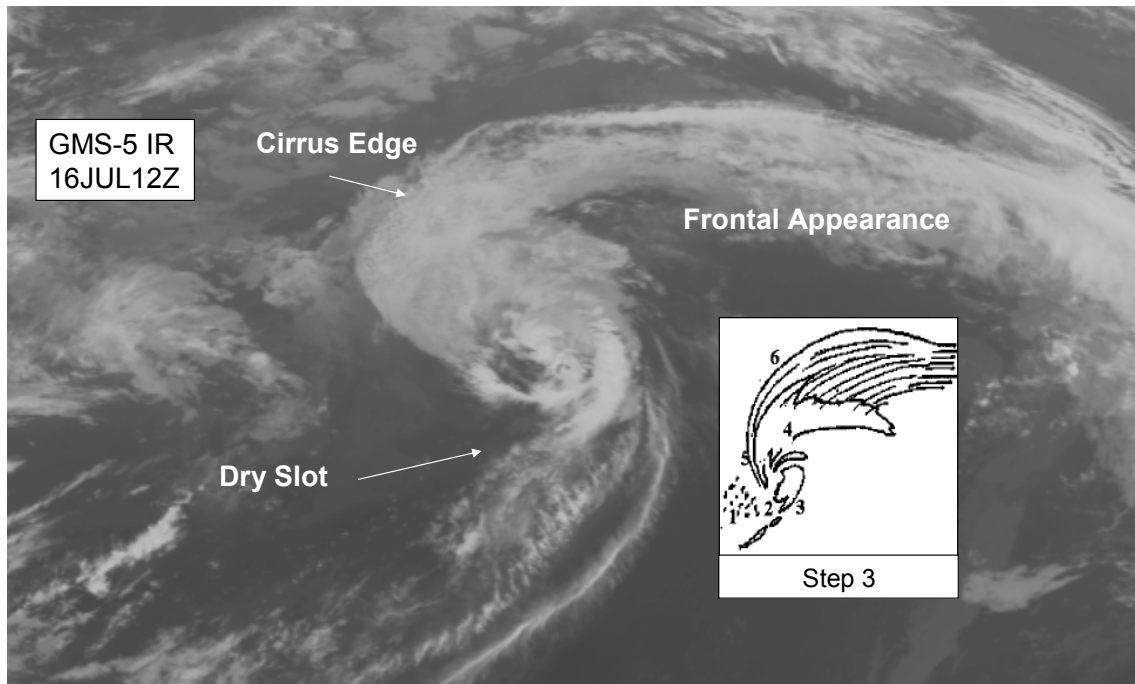


FIG. B8. High-resolution IR satellite image of Typhoon Halong at 1200 UTC on 16 July 2002 (UW-Madison 2003). Step 3 of the conceptual model of Klein et al. (2000) inset.

Bibliography

- AMS, 2002: *A Brief Guide for Authors*. American Meteorological Society (AMS), Boston, Massachusetts.
- Atkinson, G. D., and C. R. Holliday, 1977: Tropical cyclone minimum sea-level pressure and maximum sustained wind relationship for the western North Pacific. *Mon. Wea. Rev.*, **105**, No. 4, pp 421-427
- Browning, K. A., G. Vaughan, and P. Panagi, 1998: Analysis of an ex-tropical cyclone after reintensifying as a warm-core extratropical cyclone. *Quart. J. Roy Meteor. Soc.*, **124**, 2329-2356.
- Burpee, R. W., 1986: Mesoscale Structure of Hurricanes. *Mesoscale Meteorology and Forecasting*, P.S. Ray, Ed., Amer. Meteor. Soc., 311-330.
- Commonwealth of Australia (C of A) Bureau of Meteorology Geostationary Satellite Data Archive, 2003. [On-line at http://www.bom.gov.au/sat/archive_new/gms/.]
- Doty, B. E. and J. L. Kinter III, 1995: Geophysical Data Analysis and Visualization using GrADS. *Visualization Techniques in Space and Atmospheric Sciences*, eds. E.P. Szuszczewicz and J.H. Bredekamp, NASA, Washington, D.C., 209-219.
- Evans, J. L. and R. E. Hart, 2003: Objective Indicators of the Life Cycle Evolution of Extratropical Transition for Atlantic Tropical Cyclones. *Mon. Wea. Rev.*, **131**, 909-925.
- Fleet Numerical METOC Detachment (FNMOD) NOGAPS Climatology, 2003: Fleet Numerical Meteorology and Oceanography Detachment, Asheville, NC. [On-line at <http://navy.ncdc.noaa.gov/gradsmap/indexcustomfhf.html>.]
- Fogarty, C., 2002: Operational Forecasting of Extratropical Transition. Preprints, 25th Amer. Meteor. Soc. Hurricane Conf., San Diego, CA.
- Glickman, T., Ed., 2000: *Glossary of Meteorology*. 2d ed., Amer. Meteor. Soc., 855 pp.
- Global Tropical Cyclone Climatic Atlas (GTCCA), Version 1.0, 2003: Fleet Numerical Meteorology and Oceanography Detachment, Asheville, NC. [On-line at <http://navy.ncdc.noaa.gov/products/gtcca/gtccamain.html>.]

- Gray, W. M., 1979: Hurricanes: Their formation, structure, and likely role in the tropical circulation. *Meteorology Over the Tropical Oceans*, D. B. Shaw, Ed., Roy. Meteor. Soc., 155-218.
- Harr, P. A. and R. L. Elsberry, 2000: Extratropical Transition of Tropical Cyclones over the Western North Pacific. Part I: Evolution of Structural Characteristics during the Transition Process. *Mon. Wea. Rev.*, **128**, 2613-2633.
- Harr, P. A. and R. L. Elsberry, 2000: Extratropical Transition of Tropical Cyclones over the Western North Pacific. Part II: The Impact of Midlatitude Circulation Characteristics. *Mon. Wea. Rev.*, **128**, 2634-2653.
- Hart, R. E., 2003a: A Cyclone Phase Space Derived from Thermal Wind and Thermal Asymmetry. *Mon. Wea. Rev.*, **131**, 585-616.
- Hart, R. E., 2003b: Cyclone Phase Analysis and Forecast Help Page. [On-line at <http://moe.met.fsu.edu/cyclonephase/help.html>.]
- Hart, R. E. and J. L. Evans, 2001: A Climatology of the Extratropical Transition of Atlantic Tropical Cyclones. *J. of Climate*, **14**, 546-564.
- Hodur, R. M., 1997: The Naval Research Laboratory's Coupled Ocean/Atmosphere Mesoscale Prediction System (COAMPS). *Mon. Wea. Rev.*, **125**, 1414-1430.
- Jones, S. C., and Coauthors, 2003: The extratropical transition of tropical cyclones: Forecast challenges, current understanding and future directions. *Wea. Forecasting accepted*.
- Klein, P. M., P. A. Harr, and R. L. Elsberry, 2002: Extratropical Transition of Western North Pacific Tropical Cyclones: Midlatitude and Tropical Cyclone Contributions to Reintensification. *Mon. Wea. Rev.*, **130**, 2240-2259.
- Klein, P. M., P. A. Harr, and R. L. Elsberry, 2000: Extratropical Transition of Western North Pacific Tropical Cyclones: An Overview and Conceptual Model of the Transformation Stage. *Wea. Forecasting*, **15**, 373-395.
- Montgomery, D. C., and Runger, G. C., 2003: *Applied Statistics and Probability for Engineers*. John Wiley & Sons, Inc, 572-585.
- Petterssen, S. and S. J. Smebye, 1971: On the development of extratropical cyclones. *Quart. J. Roy. Meteor. Soc.*, **97**, 457-482.

- Rauber, R. M., J. E. Walsh, and D. J. Charlevoix, 2002: *Severe and Hazardous Weather*. Kendall/Hunt Publishing Company, 616pp.
- Ramage, C. S., 1995: *Forecasters Guide to Tropical Meteorology*. AWS/TR-95/001, Air Weather Service, Scott AFB, IL, 241-263.
- Rosmond, T.E., 1992: The design and testing of the Navy Operation Global Atmospheric Prediction System. *Wea. Forecasting*, **7**, 262-272.
- Stackpole, J. D., 1989: GRIB and BUFR: The only codes you will ever need. European Centre for Medium-Range Weather Forecasts, Second Workshop on Meteorological Operational Systems, 4-8 December 1989, Reading, UK. 44-67.
- Staudenmaier, M., 1997: The Navy Operational Global Atmospheric Prediction System (NOGAPS), Western Region Technical Attachment No. 97-09.
- USNPMOC/JTWC, 2002: 2002 Annual Tropical Cyclone Report, United States Naval Pacific Meteorology and Oceanography Center/Joint Typhoon Warning Center, Pearl Harbor, Hawaii. [On-line at <https://metoc.npmoc.navy.mil/jtwc/atcr/2002atcr/index.html>.]
- University of Illinois Urbana-Champaign (UIUC) Weather World 2010 (WW2010) Project, 2003: Hurricanes Online Meteorology Guide. [On-line at [http://ww2010.atmos.uiuc.edu/\(Gh\)/guides/mtr/hurr/home.rxml](http://ww2010.atmos.uiuc.edu/(Gh)/guides/mtr/hurr/home.rxml).]
- University of Wisconsin-Madison (UW-Madison) Space Science and Engineering Center (SSEC) Data Center Archive, 2003. [High resolution GMS-5 satellite imagery requested on-line at <http://dcarchive.ssec.wisc.edu/data/>.]
- Wakeham, D., 2001: Extratropical transition training for Typhoon Duty Officers. Joint Typhoon Warning Center (JTWC), Pearl Harbor, Hawaii.
- WMO, 1998: Topic chairman and rapporteur reports of the fourth WMO International Workshop on tropical cyclones (IWTC-IV), Haikou, China, 21-30 April 1998. Tropical Meteorology Research Programme Report No. 59, WMO, Geneva Switzerland.
- WMO, 2002: Final report on the proceedings of the fifth WMO International Workshop on tropical cyclones (ITWC-V), Cairns, Queensland, Australia, 3-12 December 2002. WMO, Geneva, Switzerland.

Vita

Captain Gregory D. Fox graduated from Natrona County High School in Casper, WY. He then attended Dixie College in St. George, UT where he graduated with an Associate of Arts degree in Pre-Med. Capt Fox enlisted in the United States Air Force and worked as a Communications-Computer Specialist for the 2163d Communications Group at Peterson AFB in Colorado Springs, CO. He was selected to participate in the Airmen's Education and Commissioning Program and entered undergraduate studies at the University of Arizona in Tucson, AZ where he graduated with a Bachelor of Science degree in Meteorology.

Capt Fox was then commissioned through the Officers Training School at Maxwell AFB in Montgomery, AL. His first assignment as an officer was to attend the Weather Officers Course at Keesler AFB in Biloxi, MS. He returned to Peterson AFB, CO where he served as the Weather Briefer for the Commander of Air Force Space Command. While stationed at Peterson, he deployed numerous times in support of the Mobile Consolidated Command and Control mission.

His next assignment was at Vandenberg AFB, CA as a Launch Weather Officer and Commander of the Training and Stan/Eval Flight for the 30th Weather Squadron. Capt Fox then entered the Graduate School of Engineering and Management, Air Force Institute of Technology. Upon graduation, he will be assigned to the Air Force Operational Testing and Evaluation Center at Kirtland AFB in Albuquerque, NM.

| REPORT DOCUMENTATION PAGE | | | | Form Approved OMB No. 074-0188 | |
|--|----------------------|-----------------------------------|---|---|---|
| <p>The public reporting burden for this collection of information is estimated to average 1 hour per response, including the time for reviewing instructions, searching existing data sources, gathering and maintaining the data needed, and completing and reviewing the collection of information. Send comments regarding this burden estimate or any other aspect of the collection of information, including suggestions for reducing this burden to Department of Defense, Washington Headquarters Services, Directorate for Information Operations and Reports (0704-0188), 1215 Jefferson Davis Highway, Suite 1204, Arlington, VA 22202-4302. Respondents should be aware that notwithstanding any other provision of law, no person shall be subject to a penalty for failing to comply with a collection of information if it does not display a currently valid OMB control number.</p> <p>PLEASE DO NOT RETURN YOUR FORM TO THE ABOVE ADDRESS.</p> | | | | | |
| 1. REPORT DATE (DD-MM-YYYY) March-2004 | | 2. REPORT TYPE Master's Thesis | | 3. DATES COVERED (From – To) Jun 2003 – Mar 2004 | |
| 4. TITLE AND SUBTITLE COMPARISON OF A CONCEPTUAL MODEL AND OBJECTIVE INDICATORS OF EXTRATROPICAL TRANSITION IN THE WESTERN NORTH PACIFIC | | | 5a. CONTRACT NUMBER | | |
| | | | 5b. GRANT NUMBER | | |
| | | | 5c. PROGRAM ELEMENT NUMBER | | |
| 6. AUTHOR(S) Fox, Gregory, D., Captain, USAF | | | 5d. PROJECT NUMBER | | |
| | | | 5e. TASK NUMBER | | |
| | | | 5f. WORK UNIT NUMBER | | |
| 7. PERFORMING ORGANIZATION NAMES(S) AND ADDRESS(S) Air Force Institute of Technology Graduate School of Engineering and Management (AFIT/EN) 2950 P Street, Building 640 WPAFB OH 45433-7765 | | | 8. PERFORMING ORGANIZATION REPORT NUMBER AFIT/GM/ENP/04M-06 | | |
| 9. SPONSORING/MONITORING AGENCY NAME(S) AND ADDRESS(ES) JTWC Attn: Mr. Ed Fukada 425 Luapele Road Pearl Harbor, HI 96860-3103 e-mail: jtwcta@nrmoc.navy.mil | | | 10. SPONSOR/MONITOR'S ACRONYM(S) | | |
| | | | 11. SPONSOR/MONITOR'S REPORT NUMBER(S) | | |
| 12. DISTRIBUTION/AVAILABILITY STATEMENT APPROVED FOR PUBLIC RELEASE; DISTRIBUTION UNLIMITED. | | | | | |
| 13. SUPPLEMENTARY NOTES | | | | | |
| 14. ABSTRACT The primary purpose of this research is to provide guidance to forecasters from the Joint Typhoon Warning Center (JTWC) to use in differentiating between the stages of extratropical transition (ET) of tropical cyclones (TCs). Not only is ET relevant to the Department of Defense, since JTWC stops providing TC warnings once they have undergone ET, but it is also applicable to the meteorological community since there currently “is no commonly accepted definition of ET” (Jones et al. 2003). This research compares the results of a conceptual model of ET using subjective satellite analysis with the results of objective indicators based on Navy Operational Global Atmospheric Prediction System (NOGAPS) model analyses. Recent studies provide a conceptual model of ET with definitions of two stages and ways to use satellite analysis to identify them (Klein et al. 2000). While this conceptual model was being analyzed with data from the western North Pacific Ocean, TCs were also being analyzed using data from the Atlantic Ocean (Hart and Evans 2001). The research from the Atlantic led to the exploitation of objective indicators in a hodograph-like display (Evans and Hart 2003). This thesis statistically compares the results of the conceptual model on 12 TCs in the western North Pacific with the results of the objective indicators on the same 12 TCs. Additionally, three specific case study comparisons are performed: 1) a “classic” TC that had undergone ET (Typhoon David in September 1997), 2) a TC whose output from the two methods matched each other almost perfectly (Super Typhoon Joan in October 1997), and 3) a TC whose stages of ET were difficult to forecast using the conceptual model alone (Typhoon Halong in July 2002). The overall findings demonstrate that the objective indicators are easier to utilize, more definitive, and less subjective than the results achieved through the use of the conceptual model method. This study strongly encourages the use of objective indicators by JTWC forecasters (and others) in defining the beginning and end of ET. Additionally, this thesis provides recommendations for improvements in ET forecasting and a definition of ET for adoption by the American Meteorological Society and the World Meteorological Organization. | | | | | |
| 15. SUBJECT TERMS Extratropical Transition, Tropical Cyclones, Objective Indicators, Conceptual Model, Western North Pacific | | | | | |
| 16. SECURITY CLASSIFICATION OF: | | | 17. LIMITATION OF ABSTRACT UU | 18. NUMBER OF PAGES 98 | 19a. NAME OF RESPONSIBLE PERSON Ronald P. Lowther, Lt Col, USAF (ENP) |
| a. REPORT U | b. ABSTRACT U | c. THIS PAGE U | | | 19b. TELEPHONE NUMBER (Include area code) (937) 255-3636, ext 4645; e-mail: Ronald.Lowther@afit.edu |